To the Graduate Council:

I am submitting herewith a thesis written by Donald V. Crider entitled "Structural and Stratigraphic Effects on Geomorphology and Groundwater Movement in Knox Dolostone Terrane." I recommend that it be accepted in partial fulfillment of the requirements for the degree of Master of Science, with a major in Geology.

Don W. Byerly, Major Professor

We have read this thesis and recommend its acceptance:

Accepted for the Council:

Vice Chancellor
Graduate Studies and Research

STRUCTURAL AND STRATIGRAPHIC EFFECTS ON GEOMORPHOLOGY AND GROUNDWATER MOVEMENT IN KNOX DOLOSTONE TERRANE

A Thesis

Presented for the

Master of Science

Degree

The University of Tennessee, Knoxville

Donald V. Crider

March 1981

3049615

ACKNOWLEDGMENTS

The author is indebted to Dr. Don W. Byerly for suggesting this topic and his guidance throughout the course of research. He also wishes to express his gratitude to Drs. Michael G. Clark, Fred B. Keller, and Steve Haase for their critique of the manuscript.

Research performed at the Oak Ridge National Laboratory was sponsored by the U.S. Department of Energy under contract W-7405-eng-26 with Union Carbide Corporation.

ABSTRACT

The relationship of joints and fractures, geomorphology, and geohydrology, in terrain underlain by carbonate rocks of the Cambro-Ordovician Knox Group has been investigated. Detailed field data and fracture traces for a 241 acre ecology study area, entitled the Walker Branch Watershed, located at the Oak Ridge National Laboratory were compared with sinkhole morphometry data and fracture traces observable on maps and imagery for nearby areas underlain by the same rock units.

Detailed studies of the watershed included:

1. Measurement of bedrock joint and fracture orientations.
2. Fracture trace analysis.
3. Sinkhole morphometry and orientation and alignment of geohydrologic feature analyses.
4. Mapping of stratigraphy, geomorphology (karst), and geohydrologic features (i.e., springs, potholes, stream-sinks) with construction of a detailed areal geohydrologic map.

Comparison of the directional histograms prepared from the above data collected for Walker Branch Watershed and surrounding areas underlain by Knox dolostone reveals a close parallelism between the various studies, indicating

each separate analysis is a viable method for predicting areas of more intense fracturing of bedrock, thus preferred groundwater movement directions. The results of this study also indicate that at least in part groundwater movement in the Knox Group is stratigraphically controlled.

Although the Knox in general is not ideally suited for waste storage/disposal, because of the abundant jointing which results in the formation of solution cavities and creates a highly variable groundwater regime with respect to space and time, the upper Mascot Formation after a site-specific study could have some utility for such purposes.

TABLE OF CONTENTS

CHAPTER		PAGE
I.	INTRODUCTION	1
	Purpose of the Investigation	1
	Site Selection, Location and Description	3
	Previous Investigations on WBW	7
	Methodology	9
	General research procedures	9
	Evaluation of precision levels in the analyses	10
	Photogeohydrologic fracture trace analyses	11
II.	GEOLOGY	12
	Regional Geology	12
	Stratigraphy of the Knox Group	14
	Copper Ridge Dolomite	15
	Chepultepec Dolomite	17
	Longview Dolomite	18
	Kingsport Formation	20
	Mascot Dolomite	20
	Structural Geology	22
	Outcrop structure analysis	23
	Geomorphology	28
	Doline subsidence	30
	Headward sapping at springs	34
	Speleological analysis of Harris Cave	36
	Potholes	41
	Slump	45
	Dry valleys and hanging dry valleys	48
	Rockfall	51
	Rockslide	52
	Bedrock pinnacles and cutters	54
	Gully erosion	56
III.	GEOHYDROLOGY	59
	General Carbonate Aquifer Characteristics	59
	Porosity and permeability of carbonate rocks	59
	Recharge to dolomite aquifers	60
	Carbonate aquifer flow types	63
	Aquifer Flow Types and Recharge Sources for the East and West Subbasins	64

CHAPTER PAGE

Groundwater Discharge and Recharge Features . 70
Springs and seeps 70
Swallets, semiblind valleys, and resurgences 79
Surface Geohydrology 83
Drainage basin analysis 83
Differences in processes and features of channel morphology between the East Fork and the West Fork 88

IV. PHOTOINTERPRETATIONS 96

Terminology 96
Procedures 97
Imagery Analyzed 97

V. ANALYSES OF OBSERVED ORIENTED FEATURES 102

Field Measured Joint Orientations 102
Orientations Derived from Imagery 103
Geohydrologic Feature Alignment and Sinkhole Morphometry Analyses 104
Alignment of geohydrologic features 104
Sinkhole (doline) elongation and alignment analysis 106
Comparison of Orientation Analyses 107
Procedure 107
General results 112
Comparison of WBW analysis with General Knox Terrane analysis 113
Applicability of alignment of geohydrologic features and sinkhole morphometry analyses to the prediction of groundwater movement in Knox Dolostone Terrane 114
Significance of the geohydrologic fracture trace and feature alignment analyses . 115

VI. EVALUATION OF THE KNOX DOLOSTONE TERRANE FOR WASTE STORAGE/DISPOSAL 117

Knox Group in General 117
Potential of the Upper Mascot Dolomite Formation of the Knox Group as a Repository for Wastes 119

VII. CONCLUSIONS 121

CHAPTER PAGE

BIBLIOGRAPHY 123

APPENDICES 130

A. GEOHYDROLOGIC MAP OF WALKER BRANCH WATERSHED . . 131
B. GEOHYDROLOGIC FEATURE LOCATION AND JOINT ACQUISITION SITE MAP 133
C. MAP AND HISTOGRAMS OF PHOTOGEOHYDROLOGIC LINEAR FEATURE ORIENTATIONS AND SINKHOLE ELONGATION OBSERVED IN WALKER BRANCH WATERSHED 135
D. MAP AND HISTOGRAMS OF PHOTOGEOHYDROLOGIC LINEAR FEATURES AND SINKHOLE ELONGATIONS AND ALIGNMENTS (FOR AREA 1) ON COPPER RIDGE 140
E. MAP AND HISTOGRAMS OF PHOTOGEOHYDROLOGIC LINEAR FEATURE ORIENTATIONS OBSERVED FOR CHESTNUT RIDGE 143
F. MAPS AND HISTOGRAMS OF ALIGNMENT OF GEOHYDROLOGIC FEATURES AND SINKHOLE ALIGNMENTS IN WBW 147
G. STATISTICAL EVALUATION OF ORIENTATION DATA . . . 152

VITA 162

LIST OF FIGURES

FIGURE		PAGE
1.	Location of Walker Branch Watershed Project . . .	4
2.	Photomap of Walker Branch Watershed Showing Monitoring Equipment and Facilities	6
3.	Horizontal Traverse of Walker Branch	7
4.	Generalized Structural and Stratigraphic Section of the Regional Geology of the Oak Ridge Reservation	13
5.	Classification of Knox Stratigraphy in the Western Part of the Valley and Ridge in Tennessee	16
6.	Large, Angular, Chert Blocks of the Longview Dolomite Near the Longview-Chepultepec Dolomite Contact	19
7.	Concentrically Banded Chert Nodules Occurring in Particular Horizons in the Mascot Dolomite . .	21
8.	Solutionally Widened Major and Minor Joints of the Closed and Open Types	24
9.	Specific Example Two of Outcrop Structure Analysis	25
10.	Isometric Diagram of Walker Branch Watershed Showing Landscape of Alternating Broad Ridges and Narrow Incipient Valleys	29
11.	Conical-Shaped Solutional Doline L Formed in a Midslope Valley in the Chert Zone Near the Longview-Chepultepec Contact	33
12.	Swallow Hole Located Above Harris Cave Into Which It Still Actively Transports Debris	37
13.	Main Passage of Harris Cave Formed by Solution between Bedding Planes and Along the N55°-60°E Joint Direction	37
14.	Pothole Area PA_2	42

FIGURE PAGE

15. Pothole Breaching 45

16. Pothole Area PA_3 46

17. Recent Slump Formed After a Storm Event Increased Soil Saturation in the Area 47

18. Dry Valley Section at the Lower Reaches of the N48°E Oriented Valley Coalescing at Stream Level at Spring S3W on the West Fork . . . 49

19. Rockslide 53

20. Bedrock Pinnacle of the Kingsport Formation . . . 56

21. Solutional Widening Along Bedding Planes and N35°W Joints 61

22. Springs S5W and S6W Joining Walker Branch West Fork as Tributaries 74

23. Detection of Spring or Seep by Change in Color of the Bed Load 74

24. Estavelle Showing Turbulent Flow 76

25. Lateral Residuum Conduits 77

26. Profile of East Fork Subwatershed and Tributaries 80

27. Massive Chert Blocks at the Longview-Kingsport Boundary 81

28. East Fork Stream Diversion Into a Swallet 83

29. Profile of West Fork Subwatershed and Tributaries 91

30. Histogram of Bedrock Fracture Orientations Based Upon 210 Observations Within Walker Branch Watershed 102

31. Joint, Fracture Trace, and Alignment of Geohydrologic Features for WBW, Chestnut Ridge, and Copper Ridge (Based on 799 Observations) 108

FIGURE PAGE

32. Preferred Groundwater Movement Histogram for WBW Derived from Analyses in Figure 31 and Based on 124 Quality Points 110

33. Preferred Groundwater Movement Histogram for General Knox Terrane Derived from Analyses in Figure 31 and Based on 220 Quality Points . . 110

A.1. Geohydrologic Map of Walker Branch Watershed . . 132

B.1. Geohydrologic Feature Location and Joint Acquisition Site Map 134

C.1. Histogram of Fracture Traces As Observed from Soil Tonal Variations and Tree Alignments in WBW, Based on 178 Observations 136

C.2. Sinkhole Elongation and Fracture Trace Map . . . 137

C.3. Histogram of Fracture Traces As Observed from Straight Stream Segments in WBW Based on 53 Observations 138

C.4. Histogram of Fracture Traces As Observed from Topographic Alignments in WBW and Based on 51 Observations 139

D.1. Histogram of Fracture Traces Observed for That Part of Copper Ridge Encompassed in TVA's Lovell, Bethel Valley, and Elverton 7.5 Minute Quadrangle Maps Based on 61 Observations 141

D.2. Map and Histograms of Fracture Traces and Sinkhole Elongations and Alignments Observed in Area 1 on Copper Ridge Located Northeast of Whiteoak Lake on Bethel Valley Quadrangle 142

E.1. Histogram of Fracture Traces Observed for That Part of Chestnut Ridge Encompassed in TVA's Lovell, Bethel Valley, and Elverton 7.5 Minute Quadrangle Maps, Based on 103 Observations 144

FIGURE PAGE

E.2. Map and Histogram of Fracture Traces Observed for Area 2 on Chestnut Ridge Located Northwest of ORNL Plant X-10 on Bethel Valley Quadrangle . 145

E.3. Map and Histogram of Fracture Traces Observed for Area 3 in Chestnut Ridge Encompassing WBW and the Immediate Area Northeast and Southwest on Bethel Valley Quadrangle 146

F.1 Map of Alignment of Geohydrologic Features and Sinkhole Alignments 148

F.2. Histogram of Orientation of Hypothetical Lines Adjoining Aligned Sinkholes in WBW Based on 7 Observations 149

F.3. Histogram of Orientations of Sinkhole Elongations Observed for WBW and Based on 18 Observations 150

F.4. Histogram of Orientations of Hypothetical Lines Adjoining Concentrations of Geohydrologic Features Across WBW Based on 10 Observations 151

G.1. Histogram of Fracture Traces As Observed from Topographic Alignments in WBW and Based on 51 Observations 155

G.2. Histogram of Bedrock Fracture Orientations Based upon 210 Observations within Walker Branch Watershed 158

CHAPTER I

INTRODUCTION

I. PURPOSE OF THE INVESTIGATION

This investigation is a detailed examination of the geohydrology of a watershed to determine what influence structure and stratigraphy in a terrain underlain by carbonate rock of the Knox Group may have on geomorphology and groundwater movement. The Cambro-Ordovician Knox Group crops out extensively in the Southeastern United States and geomorphologically usually forms karst topography due to solutional processes.

The Knox Group is economically important for crushed rock products as well as being the host rock for zinc, barite, fluorite, and some iron deposits in East Tennessee. Also, because of its areal distribution, it frequently is the bedrock foundation for commercial and domestic structures. Two of Knoxville's main sanitary landfills are located in a Knox dolostone terrane, and many areas are dependent on it for domestic, commercial, and municipal water sources.

The purpose of this study is to define the main contributory parameters for developing karstification in Knox dolostone. These parameters include:

1. Stratigraphy—Variance in resistance to chemical and physical erosional processes between strata.

2. Structure—Variations in spacial distribution and density of bedrock fractures.

3. Nature of groundwater recharge system and aquifer flow types.

Walker Branch Experimental Watershed (WBW) at Oak Ridge National Laboratory (operated by the Nuclear Division of Union Carbide Corporation under contract W-7405-eng-26 for the U.S. Department of Energy) was the focus of the investigation.

Along with establishing the extent and direction these features have proceeded, an extensive review of mass movement features and their process origins was evaluated. A photogeohydrologic fracture trace analysis was prepared for WBW, as well as for surrounding areas underlain by the Knox Group. Using WBW as the base line or control study, an attempt is made to determine what effects fractures exert on the groundwater regime and geomorphic processes.

Two analyses, alignment of geohydrologic features and sinkhole morphometry, were also conducted as a major part of this study to determine the validity of such analyses on predicting preferred groundwater movement directions in the Knox dolostone terrane.

There are relatively few geohydrologic studies of karstified dolostone terranes in comparison to karstified

limestone regions. This situation is perhaps due to the fact that dolostone terranes which, compared to limestone areas in the United States and the world, are less extensive and less karstified and therefore studied less intensively.

Through the efforts of this paper and others like it, a better understanding of the parameters leading to karstification of the Knox may hopefully be obtained and applied to not only waste disposal but also groundwater resources, structural stability, and other uses of the Knox dolostone.

II. SITE SELECTION, LOCATION AND DESCRIPTION

The Oak Ridge area was first considered as a potential study area because of the opportunity Oak Ridge National Laboratory (ORNL) presented through a cooperative research agreement with The University of Tennessee, Knoxville, Department of Geological Sciences. Also, there is need for the assessment of all terrains on the ORNL reservation for their utility in the disposal of wastes in environmentally safe methods.

The area chosen for this karst geohydrologic study is Walker Branch Watershed (Figure 1). It is located on the federally owned Oak Ridge Reservation in Anderson County, Tennessee approximately 1.6 km east of Union Carbide's Oak Ridge National Laboratory (Plant X-10) and 0.3 km north of Bethel Valley Road. The area is represented on the

Tennessee Valley Authority's (TVA) Bethel Valley 7.5 minute quadrangle. The confluence of the two main tributaries of Walker Branch is located at 35°57'30"N latitude and 84°16'45"W longitude. From this confluence, Walker Branch flows in a southeasterly direction for about 0.3 km into the Melton Hill Reservoir of the Clinch River.

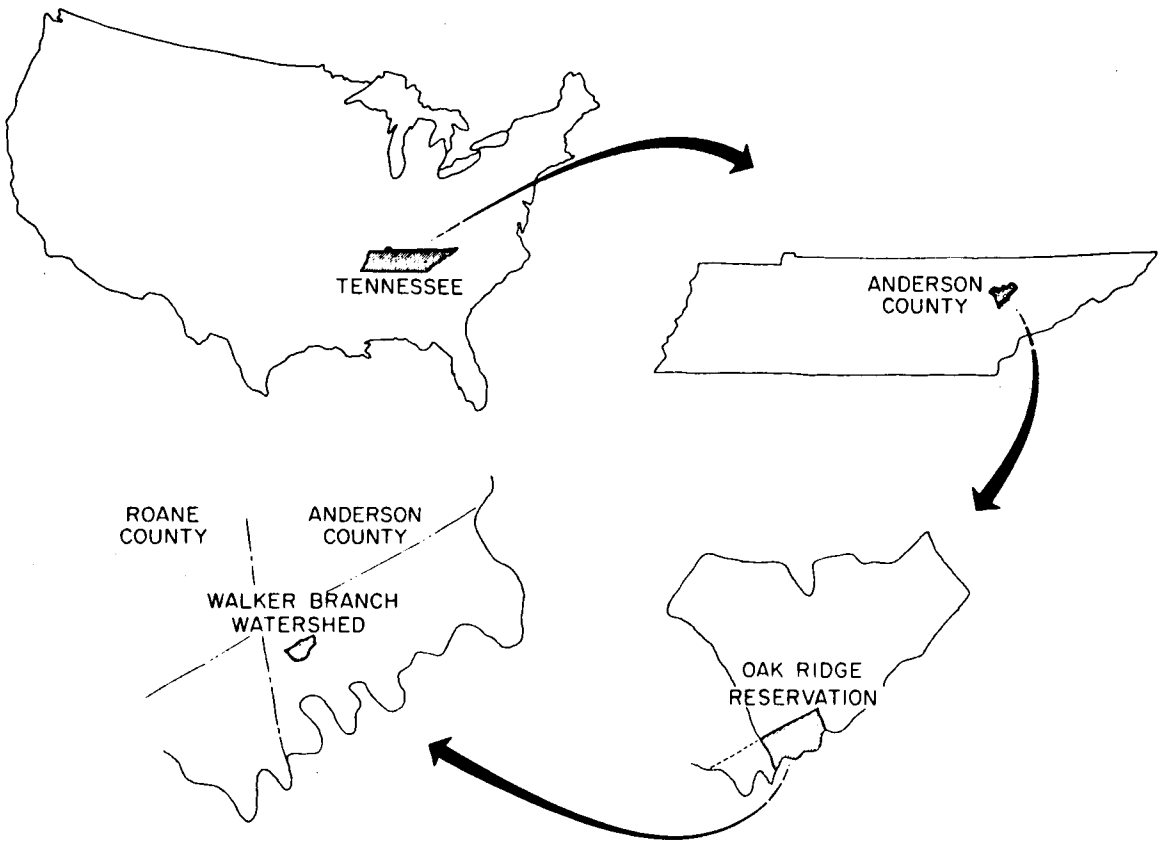


Figure 1. Location of Walker Branch Watershed project (after Curlin and Nelson, 1968).

The Walker Branch Watershed ecological project was conceived by the Environmental Sciences Division of ORNL in

the late 1960's to quantify element cycles and relate them to biological and physical processes of terrestrial and aquatic components of the watershed ecosystem (Curlin and Nelson, 1968). The size of the watershed and corresponding project area is 97.5 HA (241 acres). It is divided into two subwatersheds by a surface drainage divide located in approximately the center of the watershed on a north-northwest trending spur of Chestnut Ridge. The West Fork subwatershed is 38.4 HA (95 acres) in area, and the East Fork subwatershed occupies 59.1 HA (146 acres). Chestnut Ridge bounds the catchment basin to the north with a maximum elevation of 351 m. and slopes rapidly to the south to a low elevation of 265 m. at the confluence of the two forks. Some monitoring equipment and facilities used in the original ecology study include: five precipitation and dry fall collectors and gages, spring gages, lysimeters, litter fall baskets, and 120° V-notch weirs and automatic water samplers on the East Fork and West Fork (Figure 2).

A high density grid system prepared for the ecology project enhanced accuracy in plotting geohydrologic data gathered in this study. The grid interval is 80.47 m. and is located in the field by aluminum stakes numbered with East and North coordinate numbers. Both forks were surveyed and marked at 100 foot intervals starting from their V-notch weirs and ending at their respective limits of perennial

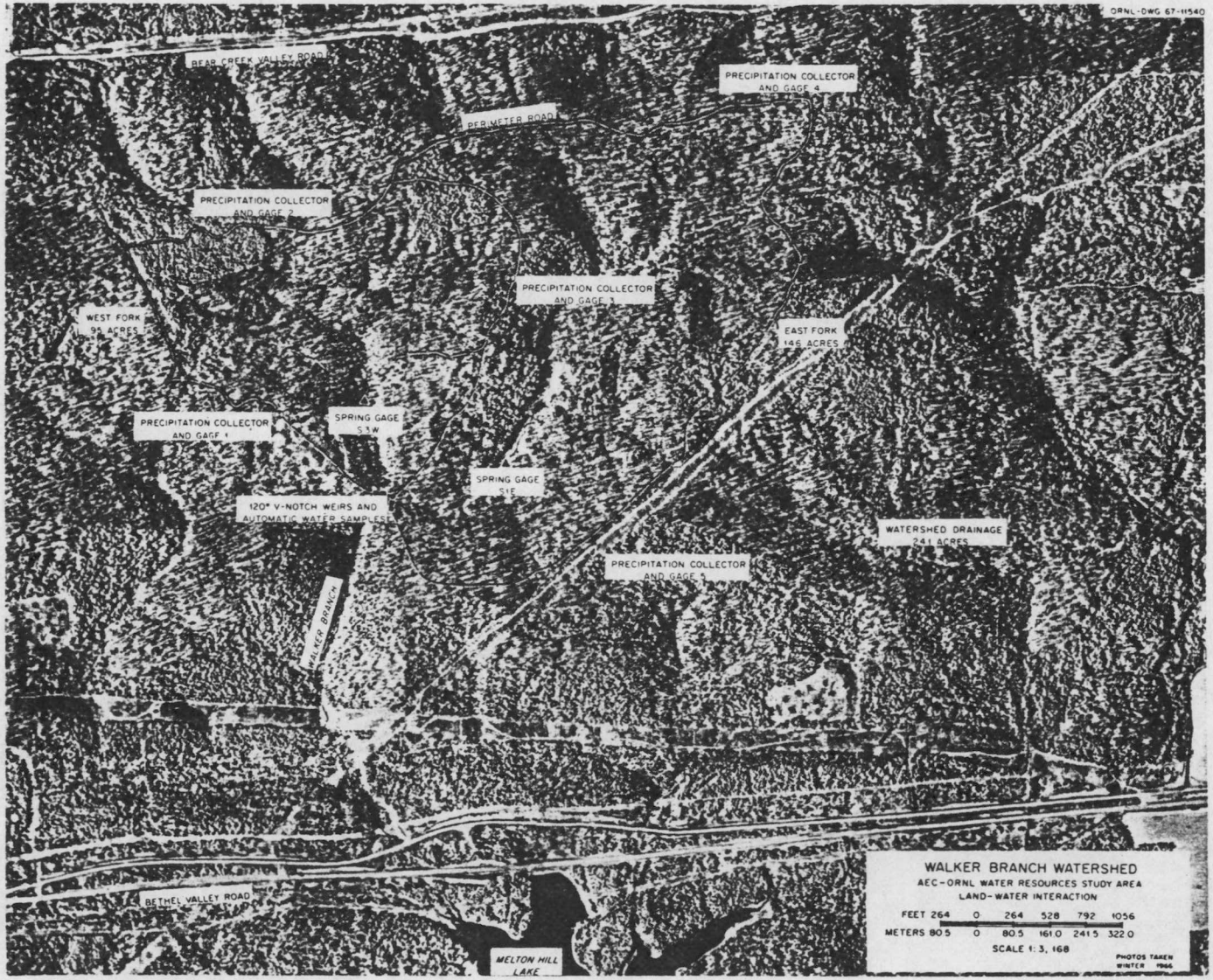


Figure 2. Photomap of Walker Branch Watershed showing monitoring equipment and facilities (after Curlin and Nelson, 1968).

flow (Figure 3). The watershed is almost completely encircled by a tertiary road system which coincides with surface drainage divides and allows easy access to the area.

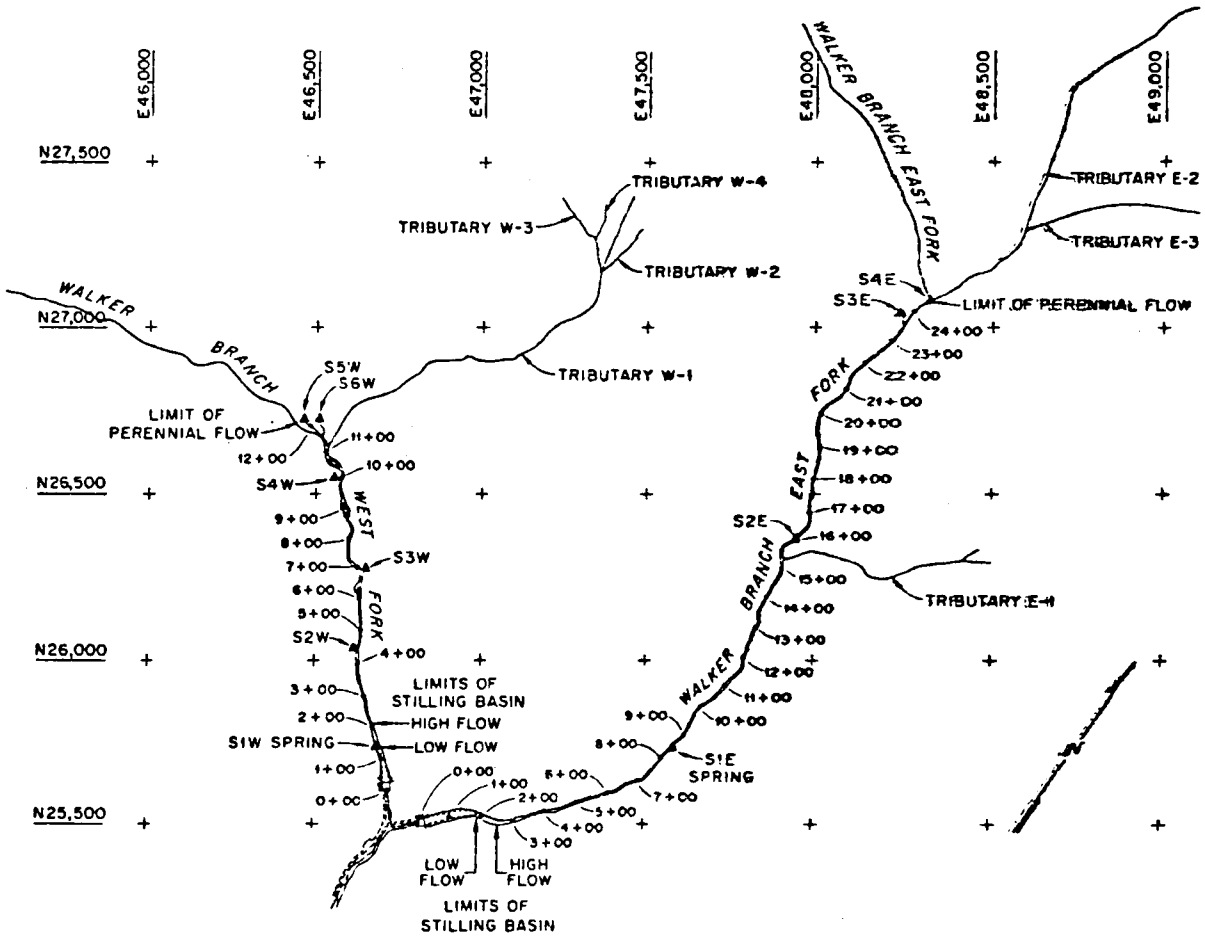


Figure 3. Horizontal traverse of Walker Branch (Curlin and Nelson, 1968).

III. PREVIOUS INVESTIGATIONS ON WBW

In September 1968, J. W. Curlin and D. J. Nelson reported on research to that date in WBW, including: aquatic, terrestrial, geological, and hydrological studies. This

report contains a detailed table of the organization of research activities defining instrumentation, data to be collected, and resulting analyses to be executed.

In April 1971, results of a preliminary hydrogeologic report and a structural and stratigraphic geologic map of the watershed compiled by William M. McMaster was submitted to the Environmental Sciences Division of Oak Ridge National Laboratory (ORNL). Geomorphology, structure, and stratigraphy are discussed, especially to the extent they influence storage and movement of groundwater through the watershed.

J. D. Sheppard (1971) reported on variations of water quality with flow rates and seasonal variations.

Another report relates annual precipitation over a six year period, 1970-76, to water balance for the watershed in forms of streamflow, evaporation, deep seepage loss, and transpiration (Henderson, Huff, and Grizzard, 1977).

Other research in WBW has centered around soil characteristics, organic matter transport, trace element analyses, nutrient influx and discharge, and various modeling systems.

By combining geologic and hydrologic data for the watershed contained in these reports and others with the writer's observations, analyses, and research of the karst literature, it is hoped that a useful quantitative and qualitative report on the utility of terrain underlain by strata of the Knox Group can be produced.

IV. METHODOLOGY

General Research Procedures

For the present study, reconnaissance mapping and aerial photo analysis of the terrain was conducted for the entire Chestnut Ridge area from Walker Branch on the east to the Watt's Bar Reservoir—ORNL (X-10) boundary on the west. Walker Branch was eventually delineated as the study area because of greater number of springs and outcrops, accessibility of the site, and available data on spring discharge, chemical compositions of the spring water, soils, etc. McMaster's (1971) geologic map (scale = 1:3,168) was used as a base for more detailed field mapping of WBW.

A black and white photomosaic with a scale of 1:3,168 was prepared for terrain and fracture trace analysis for the watershed. Two hundred and ten joint orientations were measured from outcrops using a Brunton compass and plotted on directional histograms. Previously unplotted geological and hydrological features, such as a cave, chert variations, mass subsidence features, some springs, etc., were mapped, and the base map was checked for accuracy.

Changing geohydrologic conditions in the watershed, such as apparent spring and stream discharge variation, effects of increased precipitation on erosion processes and resulting features formed, etc., were continually monitored and mapped from the Fall of 1979 to the Summer of 1980.

Geohydrologic feature alignments and sinkhole alignments and elongations were visually inspected from geohydrologic and geologic base maps for suggesting preferred groundwater movements.

For WBW and surrounding areas underlain by the Knox, all main, secondary, and tertiary maxima derived from geohydrologic feature alignment (WBW only) and sinkhole morphometry analyses, as well as bedrock fractures (WBW only), and fracture trace data were tabulated and used in the preparation of preferred groundwater movement histograms for WBW and Knox dolostone terrane in general.

Evaluation of Precision Levels in the Analyses

Field mapping and analyses. The high density grid system (Curlin or Nelson, 1968) allowed precise plotting of the field observed geohydrologic features on the WBW base map. This accuracy was further enhanced by the division of the East and West forks into 100 foot intervals (Figure 3) and the 10 foot contour interval of the WBW base map.

Bedrock fracture and geohydrologic feature orientations were precise to 1.0 degree using the Brunton Compass.

Distances of less than a few meters were precisely determined by tape measure or ruler, and longer distances were less precisely determined by pacing.

Photogeohydrologic Fracture Trace Analyses

Different levels of precision in these analyses were determined by various resolutions and types of imagery. In general, higher resolution afforded more detail in features, which enabled better recognition and more precise plotting of those features when observed in the field. Some imagery types enhanced spectral characteristics (signatures) and contrasts between particular features, thereby aiding in precise delineation. For example, the Color Infrared and Multispectral Scanner (MSS) data enhanced detection of water, which increased precision in the straight stream segment analysis.

Distortion in imagery by crabbing, pitching, or rolling of the aircraft, errors made in printing, etc., were negligible except in Color Infrared and MSS imagery of WBW. Corrections for this were made by comparing orientations of, and distances between, the same features on distortion-free imagery.

CHAPTER II

GEOLOGY

The stratigraphy, structure (particularly bedrock fractures and joints), and geomorphology of WBW were evaluated in detail for determining:

1. Effects structure and stratigraphy have on groundwater characteristics in Knox dolostone.

2. The influence of structure and stratigraphy, groundwater, and surface hydrology on geomorphology, thereby determining cause and effect relationships between geomorphological features.

3. The utility of Knox dolostone terrane for safe disposal of potentially hazardous wastes.

I. REGIONAL GEOLOGY

Walker Branch Watershed is located in the Valley and Ridge physiographic province of East Tennessee. This province is structurally characterized by subparallel northeast trending ridges upheld by strata dipping gently in a southeasterly direction. All rock units are consolidated Paleozoic marine sediments (Figure 4). The traces of two major thrust faults exist near the WBW. Northwest of the area is Whiteoak Mountain fault, and

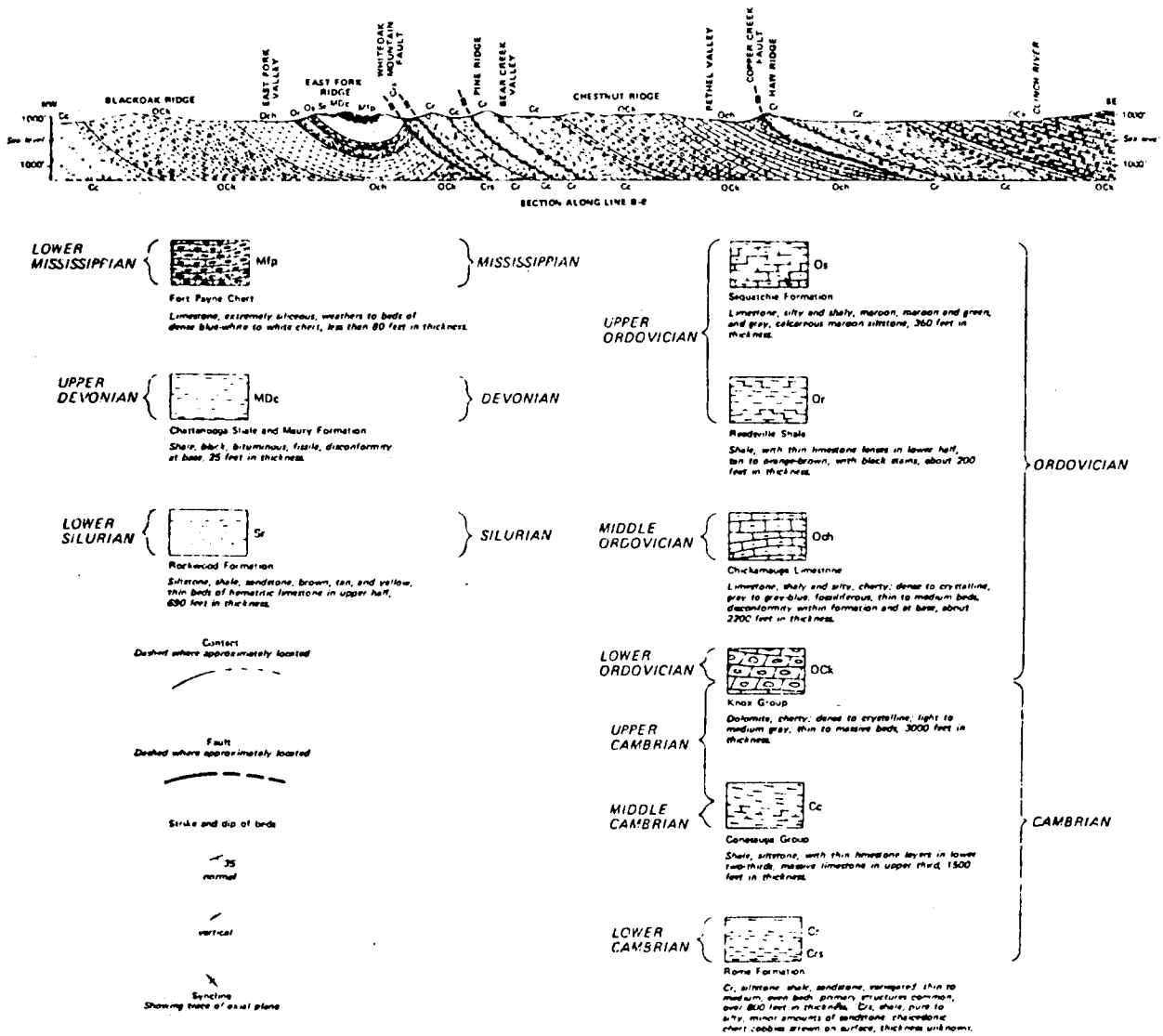


Figure 4. Generalized structural and stratigraphic section of the regional geology of the Oak Ridge Reservation (Oak Ridge Operations, 1975).

southeast of the area is Copper Creek fault. Both strike northeastward and dip southeastward.

II. STRATIGRAPHY OF THE KNOX GROUP

Walker Branch Basin is underlain entirely by the Cambro-Ordovician Knox Group. Throughout most of East Tennessee, this group exceeds 610 m. in thickness and consists primarily of siliceous dolostone with some limestone and sandstone. On a regional scale, the Knox Group has been reported to be dolomite (dolostone) to the west and limestone to the east of Knox County (Milici, 1973).

Generally, the Knox Group weathers to a deep cherty residuum locally greater than 30 m. thick in WBW. The paucity of outcrops makes mapping and subdividing the group into its formations a difficult task because of buried contacts. The writer used variations in chert types and amounts, presence of sandstone float, and lithologic characteristics of bedrock where exposed in an attempt to subdivide the Knox in WBW. Topographic expression was also used to a limited extent. In some localities, the Knox has been mapped and subdivided on a paleontological basis, but no fossils were found in WBW.

The Knox dolostone was named by Safford in 1869. In 1911, Ulrich first proposed subdivisions of the Knox Group and Oder (1934), Hall and Amick (1934), Rodgers (1953), and

Bridge (1956) have brought the classification of the Knox in the Western Valley and Ridge in Tennessee to that shown in Figure 5. Harris (1969) suggested extending the Kingsport Formation to include the Longview Dolomite. The writer has used the classification of Rodgers and Bridge (1956) in mapping the stratigraphy of WBW. The formations are, in ascending order, Copper Ridge Dolomite of Late Cambrian age, and the Chepultepec, Longview, Kingsport, and Mascot formations of Early Ordovician age.

Copper Ridge Dolomite

Cherty residuum of the Copper Ridge Dolomite is exposed mostly on the East subbasin of WBW (see geohydrologic map; Appendix A). Although no bedrock of the Copper Ridge Dolomite is exposed in the watershed, residual chert float is significant in recognizing this formation in the field. The very abundant cherts are characteristically variable, being light colored, concentrically banded, or oölitic. Haney (1966) reports that much of the chert occurs as replacement structures such as siliceous oölites and silicified cryptozoans which were probably composed of calcium carbonate when deposited.

Outside the watershed abundant outcrops of lower strata of the formation were found on the northwest face of Chestnut Ridge near the contact between the Conasauga Group and Copper Ridge Dolomite. There the formation is composed of medium

<table>
<tr><th>Safford (1869)</th><th>Ulrich (1911)</th><th>Butts (1926)</th><th>Hall and Amick (1934)</th><th>Oder (1934)</th><th>Bridge (1956)</th></tr>
<tr><td rowspan="6">Knox Dolomite</td><td rowspan="2">Upper Knox</td><td rowspan="2">Newala Limestone</td><td>Thorn Hill</td><td>Cotter-
Powell
Beds</td><td>Mascot
Dolomite</td></tr>
<tr><td>Forked Deer</td><td>Jefferson
City</td><td>Kingsport
Formation</td></tr>
<tr><td rowspan="4">Copper Ridge</td><td>Longview
Dolomite</td><td rowspan="3">Nittany</td><td>Nittany</td><td>Longview
Dolomite</td></tr>
<tr><td rowspan="2">Chepultepec</td><td>Stonehenge</td><td rowspan="2">Chepultepec
Dolomite</td></tr>
<tr><td>Chepultepec</td></tr>
<tr><td>Copper Ridge</td><td>Copper Ridge</td><td>Conococheague-
Copper Ridge</td><td>Copper Ridge
Dolomite</td></tr>
</table>

Figure 5. Classification of Knox stratigraphy in the Western part of the Valley and Ridge in Tennessee.

to dark gray, coarse grained dolostone with some chert and is generally thick-bedded.

Because of its chert, the Copper Ridge Dolomite occupies persistant broad ridges which are slightly asymmetrical, the steeper side next to the Conasauga and the more gentle side forming a dip slope (see under Copper Ridge Dolomite, Appendix B). These broad ridges, such as at WBW and on Copper Ridge to the southeast, contain abundant sinkholes which are probably a direct influence of variations in the chert content. The Copper Ridge Dolomite is approximately 305 m. thick in the area of WBW.

Chepultepec Dolomite

The Chepultepec Dolomite is reported to conformably overlie the Copper Ridge (Cummings, 1960, p. 228). The boundary between these two units is generally considered to mark the Cambro-Ordovician boundary. The basal contact of the Chepultepec could not be precisely located due to poor outcrops. The contact was drawn between oölitic and banded chert float of the Copper Ridge and sandstone float derived from basal sandstones of the Chepultepec. Sandstone occurs as eight to ten centimeter thick brown to light tan colored slabs with siliceous cement instead of calcareous cement as reported from other locations (Smith, 1968).

Chepultepec cherts are lighter colored than the Copper Ridge in general and commonly lack the oölitic and banded

nature of the latter. They vary in color from white, yellowish gray or yellowish brown and are distinctly lightweight and porous. The Chepultepec occurs in broad, shallow swales bounded by a ridge capped by Copper Ridge Dolomite on the northwest and a ridge of the Longview on the southeast.

Delineation of the contact between Chepultepec and the next higher stratigraphic unit, Longview Dolomite, was determined by the presence of large chert boulders located approximately 76 m. northwest of a cave formed in the Longview.

A thickness of 152 m. was estimated for the Chepultepec Dolomite at WBW.

Longview Dolomite

The Longview Dolomite crops out sparingly at stream level in WBW and is typically thin to thick-bedded, fine-grained, light to medium gray dolostone. In some areas, the fine grained texture is replaced by a coarser grained gray dolostone. Only one thin continuous chert layer was seen in outcrop, but the residuum contains abundant large white angular chert blocks as evidence of the very siliceous nature of this formation (Figure 6). The chert blocks have distinctive parallel sets of gashes intersecting at various angles to give a cross hatched or grid-iron appearance, as is described from other areas (Haney, 1966), and are massive near the Chepultepec-Longview boundary. Even more massive

chert blocks over 2 m. in diameter occur in upper Longview at the Longview-Kingsport contact and can be seen cropping out in relief at the weir on the west branch of Walker Branch and on top of the ridge to the northwest.

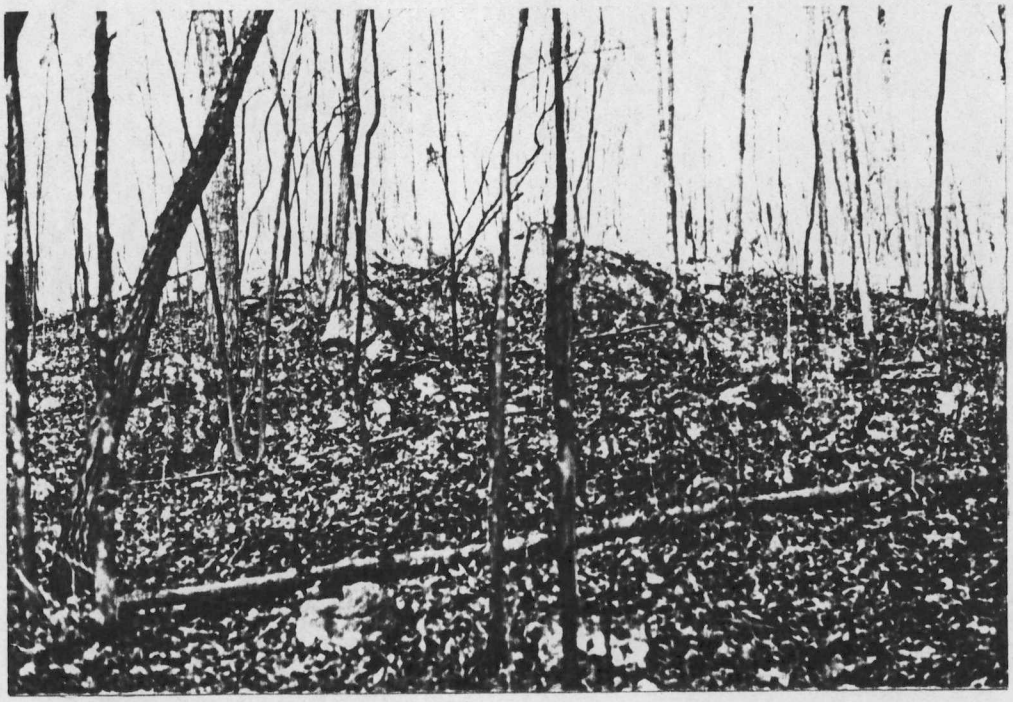


Figure 6. Large, angular, chert blocks of the Longview Dolomite near the Longview-Chepultepec Dolomite contact. Scale 1" = 8'.

A distinctive characteristic of the Longview is that it typically underlies symmetrical ridges, such as the north trending spur dividing the East and West Subwatershed. In WBW, the Longview is estimated to be 183 m. thick.

Kingsport Formation

Regionally, in other areas of East Tennessee, the Kingsport Formation is economically important as the host rock for ore mineralization.

The Kingsport is typically dark gray, coarse grained, medium to thick-bedded dolostone with chert that occurs sparingly as interbedded layers and nodules in outcrop or small pieces of float in the overlying residuum. The sequence of basal limestones reported to occur in other areas (Haney, 1966; Smith, 1968) was not found in WBW. The upper boundary was determined in the field by a change in lithology from the coarse grained dolostones of the Kingsport to the fine grained gray dolostones of the Mascot. The Mascot also contains much chert. The Kingsport Formation is 76 m. thick at WBW.

Mascot Dolomite

Although the Mascot is mostly dolostone, it does contain some thin interbedded shaley limestone in the upper part, so it may be more correct to refer to this unit in WBW as the Mascot Formation. Chert is more abundant than in the Kingsport and occurs mostly as two distinctive types. Most characteristic of the two types is concentrically banded chert as nodules up to ten or thirteen centimeters in laterally continuous horizons in the bedrock (Figure 7). The second type occurs in beds approximately fifteen

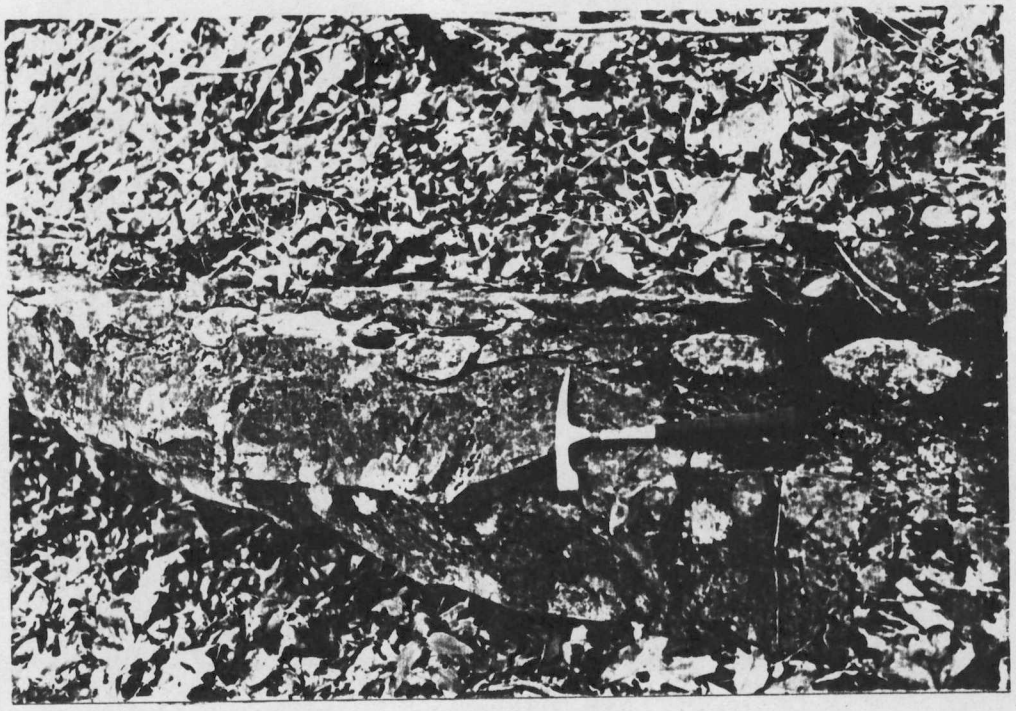


Figure 7. Concentrically banded chert nodules occurring in particular horizons in the Mascot Dolomite.

centimeters thick as small, blue white, angular pieces of chert in a dolostone matrix. The thickness of the Mascot averages 213 m. for WBW, but it varies laterally due to the erosional unconformity at the top of the Knox. This erosional unconformity of regional extent marks the boundary between the Knox Group and the Middle Ordovician Chickamauga Group. The Chickamauga limestone is recognized by thick, light colored limestones with thin bedded, dark, nodular chert. It underlies the Bethel Valley directly southeast of Walker Branch Watershed.

III. STRUCTURAL GEOLOGY

The rocks in WBW strike N55°-60°E and dip from 30°-40° southeast. Due to fairly consistent strike and dip readings throughout the watershed, minor faults and folds are not thought to exist, although if any do, they might be obscured by thick soil mantle (McMaster, 1971). Because of apparent absence of faults and folds, research on the structure involved a detailed examination of bedrock fractures and joints as main avenues of groundwater movement.

Seven areas (Appendix B) were designated as joint acquisition sites (includes bedrock fractures) on the basis of greater abundance of outcrops. For each area, every joint on selected outcrops at different stratigraphic intervals was recorded and marked to assure that no joints were measured twice.

Utilizing Jennings' classification (1971), joints in WBW are of three morphological types:

1. Latent—Narrow and hairlike; rock has to be broken to see; only minor joints.

2. Closed—Visible and allowing descent of small amounts of water; major and minor joints.

3. Open—Allowing free water movement; major joints and minor joints.

To accurately determine the relationship between groundwater storage and movement with bedrock fractures and

joints, a detailed outcrop structure analysis was conducted for two selected outcrops; specific example one and specific example two, described below. These outcrops were selected for study because both contain abundant joints, joint sets, fractures, well-defined enlargement of certain joints by solution, and some important geohydrologic features not found or less predominant in other outcrops.

Outcrop Structure Analysis

Specific example one. Figure 8 (Location: see Appendix B) shows solutionally widened major and minor joints of the closed and open types occurring in strata of the Longview Dolomite. The following is a list of orientations and the average amounts of enlargement by solution recorded for these joints:

1. N25°W – 7 cm.
2. N35°W – 18 cm.
3. N55°-60°E – 5 cm.

There is also solutional widening between bedding planes averaging 10 centimeters. At the bottom of the outcrop is a conduit (diameter = 0.3 m.) oriented in the bedrock strike direction and formed at the intersection of a N55°-60°E joint with the bedding plane.

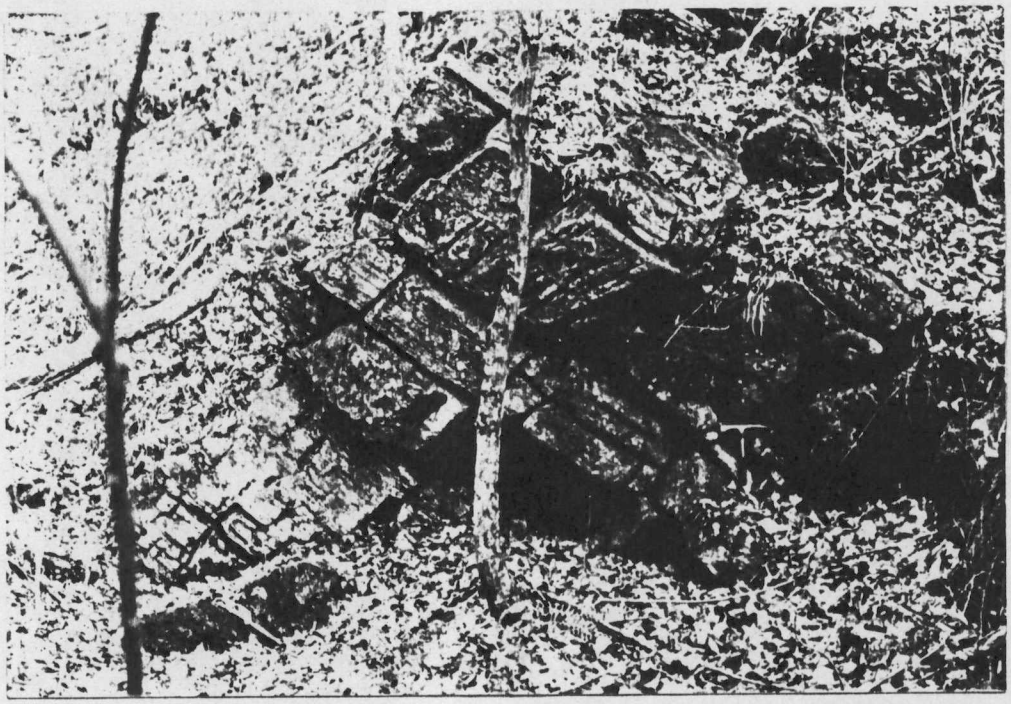


Figure 8. Solutionally widened major and minor joints of the closed and open types. Photograph taken in N55°E direction parallel to bedrock strike.

Specific example two. This outcrop is located approximately 20 m. southeast of the confluence of the East and West Forks. This outcrop, illustrated in Figure 9, reveals many clues to the geohydrology of WBW. The Kingsport Formation at this locality is composed of dolostone with two thin lenses of chert. The upper chert lens occurs as red nodules approximately 8 cm. in length and the lower chert lens is characterized by small, irregular, angular masses of chert. Joint sets in the outcrop have been solutionally enlarged along two preferred directions, N55°-60°E and N35°W. A vertical conduit and a horizontal conduit have developed along joints oriented in the latter direction.

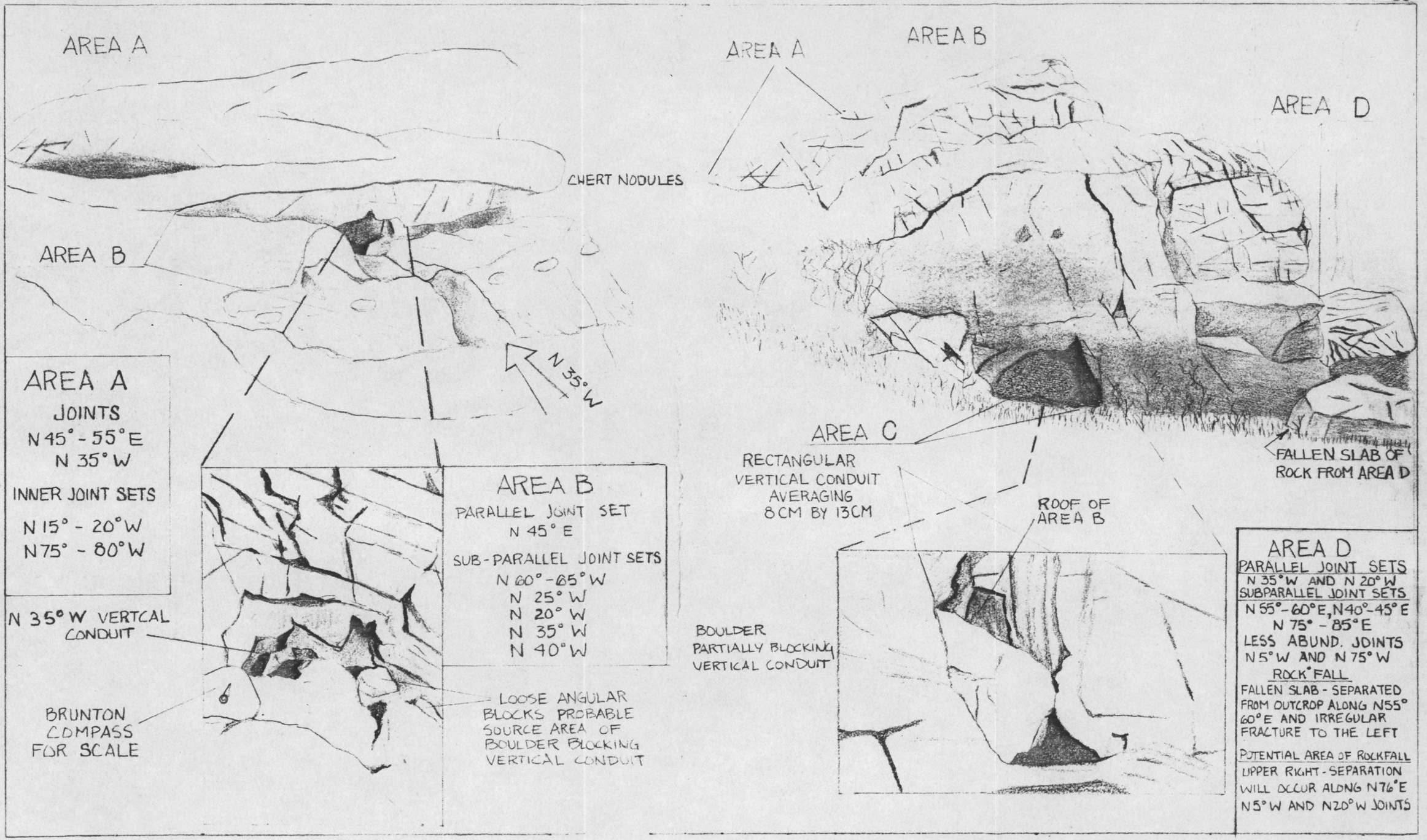


Figure 9. Specific example two of outcrop structure analysis.

To facilitate the analysis, the outcrop was divided into four sections on the basis of joint characteristics, areas of solutional enlargement, and physical erosional features.

Area A has been solutionally enlarged between bedding planes to an oval-shaped cavity measuring 8 cm. wide, 61 cm. long and 15 cm. deep. The long axis of the cavity is oriented N55°-60°E. The roof of this cavity contains two intersecting joint sets, N15°-20°W and N75°-80°W, with fewer joints oriented along N45°-55°E and N35°W.

Area B contains a larger oval-shaped cavity measuring 1.2 m. long by 25 cm. wide, also developed by solution between bedding planes. A parallel joint set oriented N45°E occurs in this area. Subparallel joint sets are oriented N60°-65°W and N25°W, N30°W, N35°W, and N40°W. The N35°W joint set is solutionally enlarged along one bedding plane to a width averaging 9 cm. and extends from the front of area B to almost the back of the cavity where a vertical conduit has developed along the same joint set. Stringfield and Legrand (1971) state that vertical conduits are formed by solution in the zone of aeration, and horizontal channels and cavities form in the upper part of the zone of saturation. Since the outcrop could only be in a zone of aeration after the zone of saturation had lowered with the incision of Walker Branch, the formation of this horizontal cavity must have preceded that of the vertical conduit.

This vertical conduit, with a rectangular opening that averages 8 cm. by 13 cm., begins as a swallow hole (groundwater recharge feature) at the top of the outcrop and terminates into an opening (Area C) measuring 50 cm. in width at bottom. A N45°W joint surface is visible as an inflection point on the otherwise rounded terminus of the conduit. In viewing this vertical cavity from the larger opening, a boulder almost completely blocking the lower cavity area can be observed. This boulder probably originated from Area B, where loose angular blocks may currently be observed. If more material is transported through the swallow hole, this partial blockage may be the first stage leading to eventual complete clogging of the conduit and termination of the swallow hole as a medium for transporting debris from the surface.

Area D is dissected by parallel joint sets that strike N55°-60°E, N20°W, and N35°W. Subparallel joint sets also strike N40°-45°E and N75°-85°E, and less abundant joints were oriented along N5°W and N75°W directions. This area is unique in that joints are involved in the physical weathering (disintegration and mass wasting) process of rock fall as opposed to chemical weathering by solution evident throughout the rest of the outcrop.

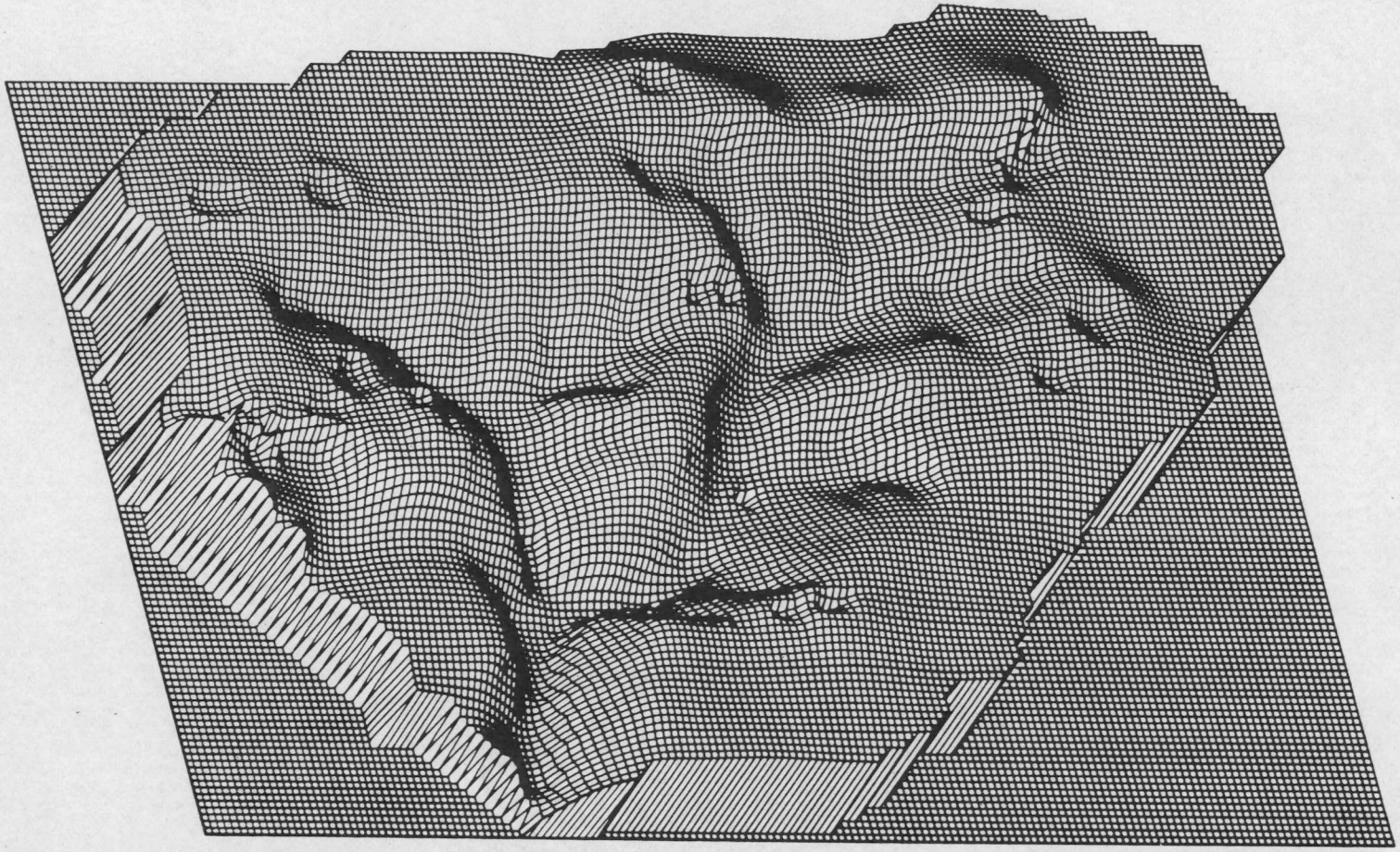
IV. GEOMORPHOLOGY

Geomorphologically, Walker Branch Watershed forms karst terrain. Defined by Jennings (1971), karst terrain is terrain with distinctive characteristics of relief and drainage arising primarily from a higher degree of rock solubility in natural water than is found elsewhere. The degree of karstification in WBW has not yet approached the classical "Karst" defined by S. Mandel (1965):

> With further karstic erosion by groundwater, a few channels will become progressively larger while the rest will become clogged by calcitic deposits and by silt. An aquifer will be replaced by a few large solution channels in an almost impermeable rock.

WBW is probably in an immature Karst stage because in a less than one square kilometer area, the writer mapped over forty springs and seeps and was able to find only a few large conduits.

Erosion of the Knox Group generally results in a landscape of alternating broad ridges and narrow incipient valleys (Figure 10). This is due to varying siliceous content in the formations. The Copper Ridge Dolomite, Longview Dolomite, and Mascot Dolomite are more siliceous than the Lower Kingsport Formation and the Chepultepec Dolomite (except for thick basal sandstone in some areas), so that they underlie ridges between incipient valleys occupied by the latter.



Scale: 1" = 100'

View Angle: 75° from horizontal

Figure 10. Isometric diagram of Walker Branch Watershed showing landscape of alternating broad ridges and narrow incipient valleys (note abundant sinkholes on ridgetops).

Many features formed by chemical and physical erosional processes (mostly solution, abrasion, and mass wasting) were observed in WBW. Prominent features include: sinkholes, subsidence at spring heads, a cave, slumps, potholes, pinnacles, rockfall, rockslide, and gully development. Each is discussed separately with an interpretation as to their formative processes and the effects that structure, stratigraphy, and hydrology have on their formation.

Doline Subsidence

There are a variety of morphological types of dolines (sinkholes) found in karst terrain, including solutional dolines, collapse dolines, alluvial dolines, and solution subsidence (Cramer, 1941). The largest and most abundant dolines of WBW appear to be of the solutional variety and discussion here will be limited to arguments supporting this interpretation. The less abundant and smaller alluvial dolines found in upper reaches of the forks are discussed in the chapter on hydrology.

According to Malott (1939), most dolines in the United States were formed beneath a residual soil called terra rossa and were developed as symmetrical depressions with flat bottoms and gentle slopes. This shape which resembles a bowl is characterized by a diameter to depth ratio of approximately 10:1, the slope angle ranges from 10 to 12 degrees. Accumulation of sediment at the base of the

opening often ponds water and allows the bottom to spread laterally as is the case in Doline G (Appendix B).

Where there is one central solutionally widened plane kept essentially open, the doline will develop a conical shape. The diameter is two to three times the depth and slopes are inclined at 30 to 40 degrees. This type of solutional doline was displayed best by Doline A (Appendix B) where the actual central shaft can be detected.

In the formation of the solutional doline, the surface is depressed by solutional enlargement of bedrock at joint intersections and/or along weaker stratigraphic beds. Once formed, internal drainage continues the process by delivering concentrated amounts of solutionally agressive soil percolation water. The frequency of solutional dolines is inversely proportional to surface gradient, since ponding or retardation of flow accelerates infiltration needed to initiate the solvent process. At Walker Branch Watershed, 80% of solutional dolines are found on broad gently sloping to essentially horizontal ridgetops (Figure 10).

Descriptions and formative processes of selected dolines.*

1. Conical or Funnel-Shaped: Dolines A, L, P.

Doline A: Structural alignment is due west. Major joint

---

*Refer to Appendix B for location of particular dolines described.

orientations and fracture traces were found to be abundant along this direction. Alignment might be explained by (1) development of central solution shaft along joint intersections or intersection of Mascot Dolomite bedding plane and joints or (2) erosion upslope delivering material to the cavity through mechanical slope wash and mass movement.

The inner doline or area where overland flow is concentrated and funneled downward through the shaft is essentially circular, 1.2 m. in diameter, and 0.3 m. deep (topographic sag of residuum).

Dolines L and P: Of these two, Doline L shows the most characteristic funnel shape. Both, however, are located in the same cherty interval of the Longview Dolomite. Their difference in degree of development may be accounted for by Doline L being positioned in a midslope valley (Figure 11). There concentrated surface runoff would deliver larger amounts of water which would quickly infiltrate through chert blocks and enhance solutional erosion of bedrock.

In all three dolines, there is pronounced asymmetry in their slope as viewed in cross-section. Jennings (1971) states that if the bedrock has a substantial dip, the dip-slope side of the doline is likely to be less steep than the undip side due to stronger influence exerted by bedding planes on the one and joints on the other.

Asymmetry in Doline L is oriented at an angle to dip due to control exerted over it by the midslope valley and



Figure 11. Conical-shaped solutional Doline L formed in a midslope valley in the chert zone near the Longview-Chepultepec contact. Scale-chert blocks center left are approximately 0.3 meters in diameter.

the asymmetry in Doline P is oriented along strike. The asymmetry of Doline A is oriented in the same bearing as bedrock dip; however, the less steep slope of Doline A is on the updip side which is in disagreement with the findings of Jennings (1971). This anomaly may be accounted for if solution and mass wasting processes have been more prevalent along the N55°-60°E joint direction. Joints oriented in this direction were observed to be solutionally widened over the entire watershed, which suggests they are major conduit routes in transportation of groundwater. Also, a N55°-60°E joint face forms a plane for an area of prominent

rocksliding located on the East Fork 200 meters to the northwest of Doline A. This rockslide is discussed in more detail later in this section.

2. Bowl-Shaped: Dolines B, C, D, E, F, G, H, I, J, M, N, O, Q, R, and S. All of these dolines are essentially symmetrical in cross-sectional slope. In addition to being more numerous at WBW, the bowl-shaped dolines on the average are shallower, areally larger, and contain more swallow holes than the conical doline type.

Standing water was observed only in Doline G, but evidence of ponding at times was detected in Dolines H and I by matted down leaves and contrasting soil color in the center of the dolines. Also, it is probable that Doline D retains more soil moisture than the surrounding area because of overabundant bush and small plant vegetation it supports.

Headward Sapping at Springs

Another form of subsidence observed at WBW and common to Karst terrains is headward sapping at spring heads. This process begins as a spring undermines the slope or cliff above it, and rock and soil gravitate into the spring. This material is then removed in solution or as clastic load, and there is a headward recession of the valley.

Spring S1WB (Appendix B) is a perennial spring which displays two levels of headward sapping. The upper level contains a dry conduit which was the former spring outlet

and former site of active undermining of the slope by solution. The current spring outlet located a few meters downslope is now the active site of solutional undermining as shown by the depression formed immediately above it. Although this area is a classic example of spring sapping, it also carries the morphological trait of a dry valley and is discussed in more detail under that heading later in this chapter.

Several gullies located on the same ridge slope and to the immediate south of spring S1WB may have been formed in part by headward sapping. Evidence for this is supported by spring MDS1 (Appendix B) which flows after extended precipitation and is located at the end of one of these gullies. The bottoms of these gullies are very uneven with chert blocks and large slabs of rock out of place due to support removal by undermining.

Another example of extensive spring sapping is spring S1E on the East Subwatershed (Appendix B). Although this spring is probably fed by several conduits, the presence of a large main conduit or direction of most intense fracturing and solutional enlargement may be inferred by the directional subsidence caused by spring sapping. Here, headward recession is oriented in a North 20° East direction from S1E for a distance of approximately 4.6 m.

Recognition of valleys formed by spring sapping will help in defining areas of more intense fracturing and former

spring outlets which usually are a manifestation of a former stream level at that height for an extended length of time.

Speleological Analysis of Harris Cave

Geomorphological aspects. During field reconnaissance, a large swallow hole (Figure 12) was found in the Longview Dolomite and while traversing from it toward the west fork of Walker Branch a previously unplotted cave was discovered.

Harris Cave (after Frank Harris, past Director of WBW Project) has essentially two passageways. The main channel (Figure 13) is approximately 3.6 m. long, 2.1 m. wide, and 1.2 m. high. At its fartherest end, it connects with the previously mentioned swallow hole. It has an orientation of N55°-60°E, which is a major joint set and the bedding strike direction. This is good evidence for solution preference along bedding planes at least in this area. The subsidiary channel strikes in a direction N35°W and then takes a sharp turn toward the stream in a direction close to the strike of the bedding. Its length is not known because its diameter decreased to a size too small to explore farther. The floor of the cave did not have standing water but some small droplets were noted on the roof and sides. This shows that local stream level and thus groundwater table has lowered to a degree that the cave which was initially formed below or at the water table is now located in the vadose zone.



Figure 12. Swallow hole located above Harris Cave into which it still actively transports debris. Boot at bottom center for scale.

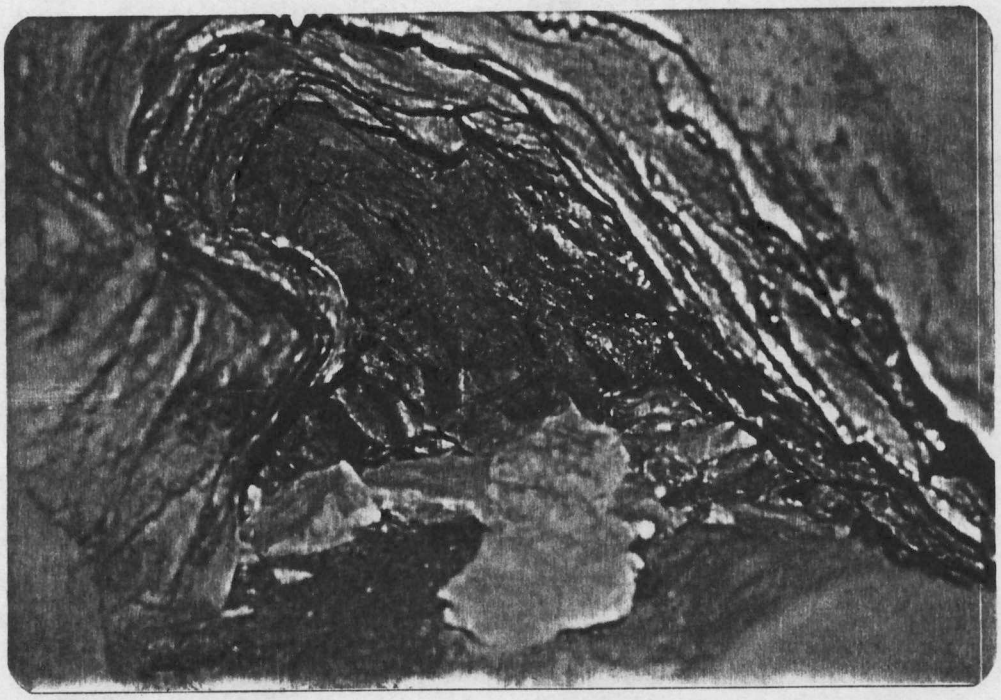


Figure 13. Main passage of Harris Cave formed by solution between bedding planes and along the N55°-60°E joint direction. Scale: Boulder in foreground = 50 cm. high.

Rockfall resulting from collapse of passage ceilings cover the floor in one area. Davies (1960) has classified these falls, which are generally controlled by joint patterns and bedding planes as slab breakdown, plate breakdown, and block breakdown. Walker Branch's cave exhibits the latter two. Plate breakdown is small scale slab breakdown in which a single bed falls as a result of solution along bedding planes. Where several beds fall as a result of solution along joints and bedding planes, block breakdown is exhibited. Main joints (as noted in the ceiling) exerting control on this phenomenon are N55°E, N10°W, N45°W, and N35°W. All of these directions were also found to be main orientations on joint and fracture trace histograms.

Relation of Harris Cave to the groundwater regime. The entrance to the cave is just large enough for an average size person to enter and is oddly positioned at roof level. This was probably an ancient spring outlet according to Jakus (1977, p. 241). In caves, due to secondary dissolution in the phreatic zone (or lowering of base level) Jakus states:

> The entry to the cave (the former spring outlet) is higher than the rest of the cave passages, and access to more or less horizontal passagees requires climbing down the ancient spring tunnel.

The cave is divided into three distinct morphological areas on the basis of prevailing groundwater regime during

the period of its formation and directions of solutional enlargement. Passage one begins 2 m. from the entrance along strike direction and terminates at the end of the cave in a distance of 2.4 m. It then turns in a N75°E direction for 0.6 to 0.9 m. In the upper northwest corner there is a swallow hole that still remains open and transports material from the surface as shown by dirt and leaf mound buildup on the cave floor below it. The passage is horizontal and elliptical in shape, which further proves structural control according to Jennings (1971, p. 160). The floor has no breakdown blocks and slope of the channel floor is essentially horizontal.

Passage two leads from passage one to the entrance. It is the largest in cross section due to ceiling breakdown and development along bedrock dip. The passage is not only enlarged along strike direction but also down-dip for approximately 0.9 m.

Passage three is strike and joint-controlled but does not appear to be influenced by dip because the dip of the channel floor is approximately 20-30 degrees and is in the opposite direction of the dip of the bedding.

The first and second passages were formed in the shallow phreatic zone when the west fork channel was topographically higher and thus had a higher groundwater table than at present. If the bedrock strike passage and channel floor

are manifestations of the piezometric surface, and if this surface was nearly horizontal, as is typical of karst terrains, then there is good evidence that these near horizontal passages were formed at local base level conditions.

The horizontal elliptical cross-section also agrees with excavation in the phreatic zone (Jennings, 1971).

As there was a lowering of stream level with incision of the West Fork, passage three, which was probably being solutionally enlarged along joints and bedrock strike before stream level change, became the conduit route to the new stream level. A free surface cave stream resulted and followed a steeper piezometric surface as shown by the average 20 to 30 degree channel bed slope. The N35°W joint and bedrock strike direction of the passage floor were parallel to the maximum slope of the piezometric surface of the dry valley to the northwest and the West Fork, respectively.

The third stage in the cavern's development is a process continuing to a minor extent today. After the drop in stream level, Harris Cave (at least passages one and two) was located entirely in the vadose zone and all flow was governed by only gravitational force and by differences in hydrostatic pressures. According to Palmer (1974), since water pressure in the vadose zone does not exceed one atmosphere, water

movement will be essentially independent of pressure differences and will flow down-dip in inclined strata due to influence by gravity alone. This development is located only in area two, but the floor of all three channels is covered with a clay residuum. This clay infilling may be due to the transition from a past active cave to the present condition of relative inactivity in which now it becomes a settling tank for fine-grained sediment.

Potholes

Figure 14 shows erosion features called potholes that are limited to the West Fork and Walker Branch below the weirs. Formed in channel bedrock, they are not only the result of downward corrasion but also corrosion in carbonate terranes. Morphologically, potholes at WBW are round vertical shafts ranging in width from 12.7 cm. to 43 cm. and from 7.6 cm. to 36 cm. in depth.

Potholes in varying types of rocks are formed by abrasion resulting from the whirling of pebbles by a turbulent eddy in a crevice in the rock. They are common in steep channels carrying large volumes of water where their development is closely related to joints (Douglas, 1977, p. 125). Ford (1965) further explains they are best developed in harder rock types and in limestones, where the roles of the pebbles (grinders) may be played by swirling solvent water. Since the shape formed in both processes is

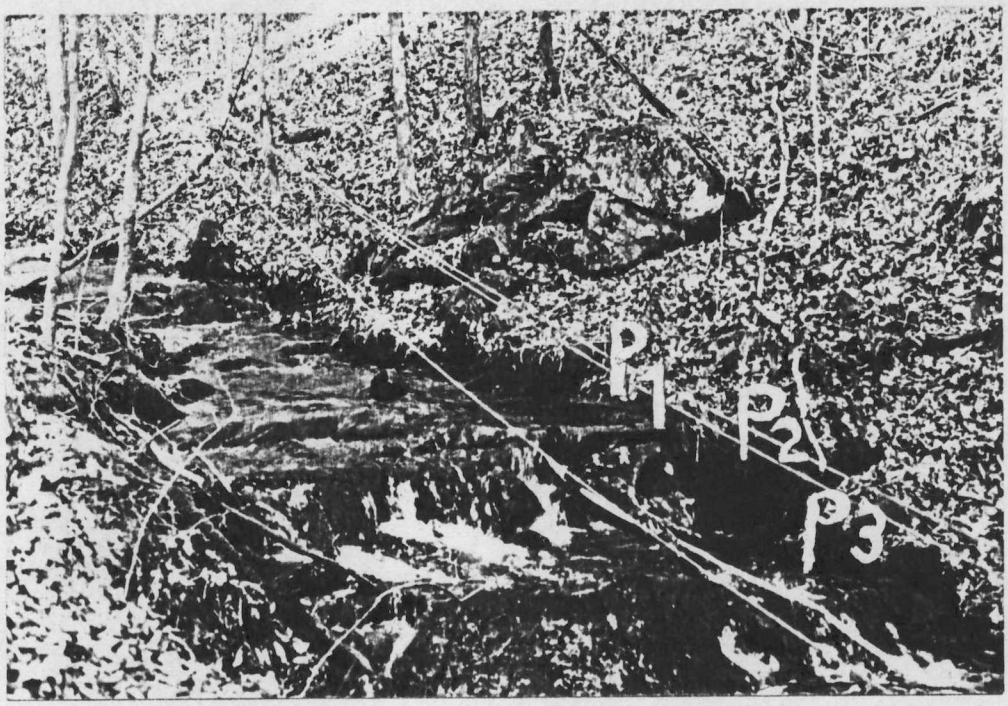


Figure 14. Pothole Area PA_2. White water showing turbulence in the potholes. Note solutionally enlarged N55°-60°E joints in background outcrop. Camera case on outcrop for scale.

P_1 = Large (0.3 m. diameter) shallow pothole on horizontal reach.

P_2, P_3 = Area of pothole breaching. P_2 has undergone two sculpturing phases.

the same, the latter can only be postulated when no grinders are observed in the potholes.

In WBW, both mechanical and chemical erosion are probably at work creating the potholes. Although a layer of particles completely covering the floor of some of the deeper and larger potholes was seen, many contained no abrading particles. With the exception of a scattered few, the potholes occurred in three concentrated locations

(Appendix B—PA_1, PA_2, PA_3) ranging from the upper 61 m. of the Longview on the West Fork to the Upper Mascot Dolomite on Walker Branch. Thus, there appears to be a strong lithologic control to their location.

Pothole Area PA1 is essentially on a near horizontal reach of the West Fork approximately 107 m. from the West Fork stilling basin. They are very shallow, generally less than 7.6 to 10 cm. deep and average about 12.7 cm. in diameter. The potholes are aligned along runnels which are solutionally enlarged joints striking N55°E, N75°W, and N15°-20°W. Either water force is not turbulent enough, the potholes are very young, or lithology there does not lend itself to the formation of larger and deeper potholes.

Pothole Area PA_2 (Figure 14) is located a few meters upstream from the West Fork stilling basin and contains very large and well developed potholes. This area appears to be undergoing erosion as shown by the sculpturing of some potholes and the destruction of others. P1 is a particularly large shallow pothole (approximately 0.3 m. in diameter) which is located on a horizontal reach. It may represent the floor of a large pothole whose walls have been eroded away as the stream incised downward.

This particular area has been subject to potholing for some time, as shown by a pothole found on the upper part (approximately 1 meter above stream level) of the outcrop in the background (Figure 14).

Along dip of the bedding just below P1, there is a concentration of potholes. At the top, some elongate potholes have been sculptured in the N55°E joint direction. This joint can also be seen solutionally enlarged in the background outcrop. Potholes along the bedrock dip surface that are currently being abraded can be detected by turbulent white water. All of these contain grinders, and they are formed at the intersection of joints striking N35°W, due North, N10°-15°W, N10°-15°E, and N55°E. The N35°W joint direction is the same bearing as the bedrock dip direction, and it is the only other solutionally enlarged joint direction in the background outcrop.

The largest pothole found, P2, measures 35.6 cm. deep by 43.2 cm. wide at top and narrows down to less than 0.3 m. at bottom. Its upper walls slope outward as if it was being destroyed during a period of lower stream flow and was headed towards the fate of P1. Before it was destroyed completely, however, renewed incision occurred creating a sudden break in slope to the now vertical walls below. Directly in front of P2 is a pothole (P3) whose evolution and correlation with P2 is shown in Figure 15. This condition, described by Ford (1965), is called pothole breaching, and it occurred under constant flow conditions when P2 was in the second sculpturing phase.

PA_3 contains the most potholes probably caused by a combination of lithology and channel bed slope. They are

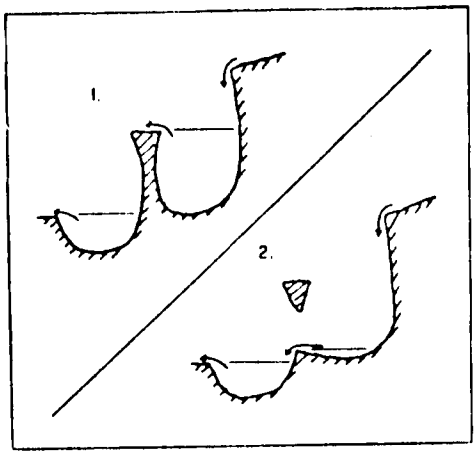


Figure 15. Pothole breaching (after Ford, 1965).

preferentially sculptured out of a light gray to tan colored dolostone of the upper Mascot Dolomite. The channel bed consists of a series of graded reaches and nickpoints but has an overall gentler slope than PA2. The upstream limit of the area is characterized by partially destroyed potholes aligned along runnels which have been created by enlargement of N20°-35°W joints. Only 4.6 meters downstream from this area is a bed dissected by an almost completely different set of joints with development of potholes preferred along certain joints (Figure 16).

Slump

Slumping may be initiated in a variety of ways but usually it results from a lowering of the internal resistance of debris by water.

Slumps (now slump scars) in upper channel reaches (first and second order tributaries) of the East Fork may

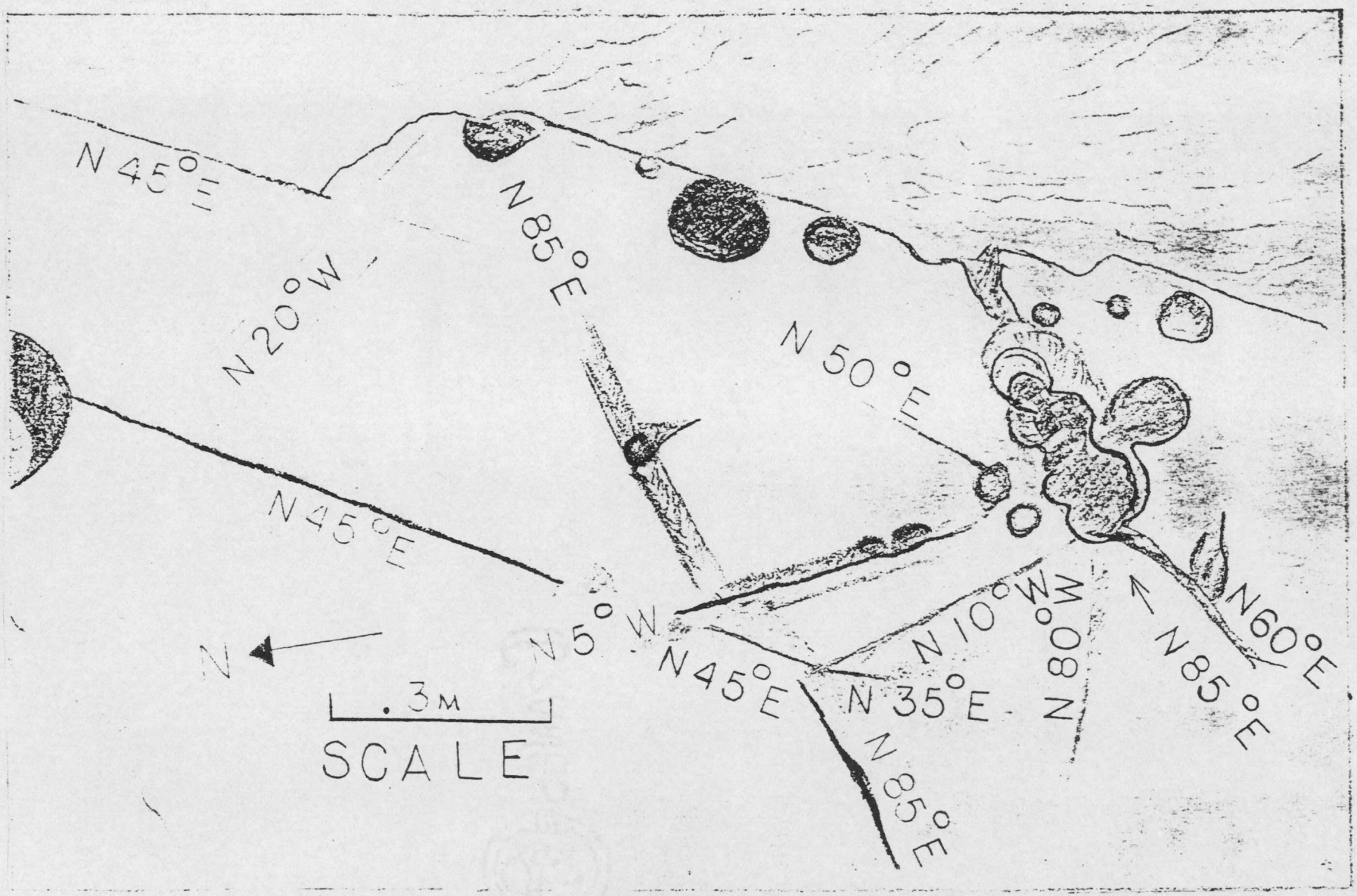


Figure 16. Pothole Area PA_3.

be the result of the fluctuating groundwater table that prevails here. This is indicated by the occurrence of wet season springs that appear after storm events and disappear rapidly in a downstream direction as the groundwater table declines.

The recent slump in Figure 17 occurred after a particularly heavy storm in early Spring of 1980. Although the main factor for its formation may be attributed to removal of underlying support with construction of the road, it was probably triggered by a sudden increase in soil saturation by percolation.

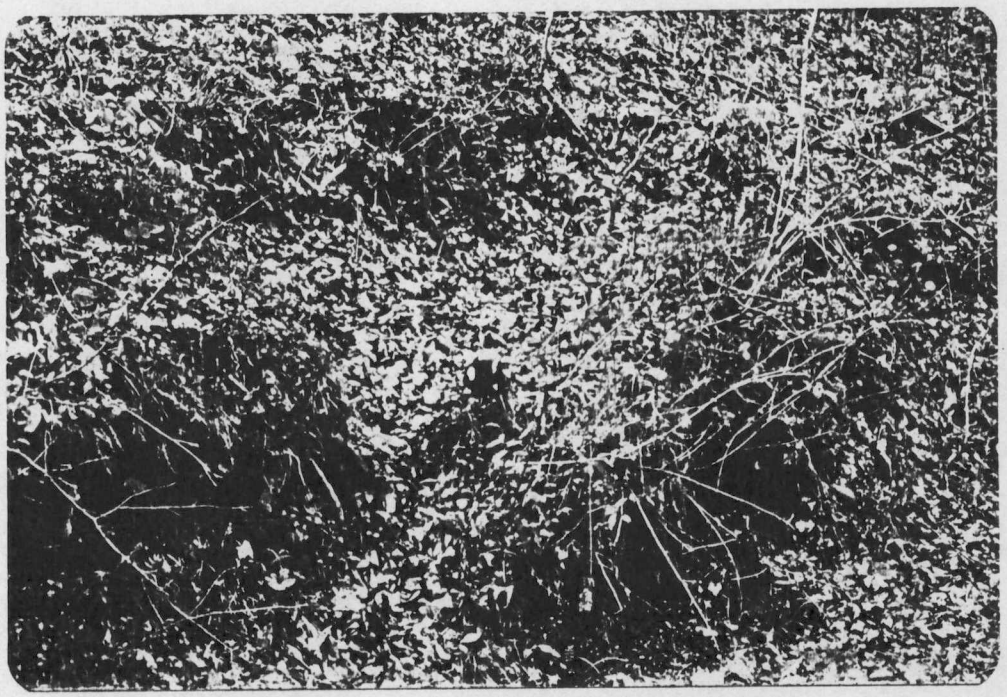


Figure 17. Recent slump formed after a storm event increased soil saturation in the area. Note: Support had been previously undermined in road construction.

All the old slumps average around 4.6 m. to 6.1 m. in scarp length and 3 m. in scarp height. In some areas, although no definite slump is observed, evidence of rotational mass movement may be deduced by a concave bend in tree trunks in a downslope direction.

Dry Valleys and Hanging Dry Valleys

Dry valleys, considered typical of karst terrains, are valleys that have no stream channels in their floors (Jennings, 1971, p. 114). They form at the heads of valleys subject to throughflow, and many of the first order tributaries across the watershed display them in certain sections along their lengths.

An example of a valley containing a dry valley section is the valley oriented N48°E and located forty meters southeast of the end of Rain Gage 3 road (Appendix B). A very shallow, temporary channel formed at the lower reaches of this valley following a very intense storm event which created surface flow due to gathering of overland flow (Figure 18).

One particular dry valley at WBW is of a special morphologic type called a hanging dry valley. The hanging condition has been described by Jennings (1971, p. 118) as a product of the main valley continuing to cut down after tributaries ceased to have a surface flow. This hanging dry valley (Appendix B) at WBW does not coalesce at stream level



Figure 18. Dry valley section at the lower reaches of the N48°E oriented valley coalescing at stream level at spring S3W on the West Fork. Coat upper left for scale.

with the West Fork. Its occurrence here is puzzling though because it is only approximately 20 m. from the N48°E valley which coalesces at stream level with the West Fork at spring S3W. One possible explanation might be found in a correlation of the hanging dry valley with the main bedrock strike passage in Harris Cave. They are located adjacent to each other and the morphogenesis of both features may be closely related.

Probable steps leading to the formation of this hanging dry valley at this location follow:

1. The original valley before becoming dry was formed in an area of relatively more intense fracturing.

2. Overland flow concentrated in the valley but infiltrated quickly due to high chert content.

3. Selective bedrock fractures became solutionally enlarged (correlation with passages in Harris Cave).

4. Conduits (enlarged bedrock fractures) increased to a size capable of accepting all throughflow thereby ceasing almost all surface flow.

5. As surface flow diminishes so does the relative erosion on the channel.

6. Valley becomes "dry" and is unable to keep up with the incision pace of the West Fork.

7. As the West Fork continues to cut down, it leaves the valley above in a hanging dry condition.

Pinchenel (1954) suggests that headward sapping consequent on a fall of base stream level would dry out higher reaches of valleys. He also believes valley deepening over a long period of time would dry out tributary valleys and springs would shift down subsidiary valleys as each incision in major valleys lowered the watertable.

This condition was displayed by spring SWB1 (Appendix B). The valley formed is less than 4.6 m. long, but the formative

process is still the same as one that is tens of meters long with several former spring outlets. As stream level lowered, the water table lowered and the original spring dried up, with a new one appearing further down the valley segment. The former spring outlet and the current spring align in a N55°E direction. So it appears that water movement is through a solutionally enlarged, less resistent to corrosion bed and/or the N55°E oriented joints dipping greater than 90 degrees opposite bedrock dip direction. Both directions are seen solutionally enlarged across the watershed and, as can be noted from the conduit at the bottom of Figure 8 (page 24), the conduit at spring SWB1 may be the result of solution at the intersection of the two directions.

Rockfall

Although rockfall is certainly taking place in many localities within the watershed where bedrock is exposed, one area where it is observed to be most prominent is illustrated in Area D of Figure 9 (page 25; see Appendix B for location). The fallen slab (bottom right) is a 25 cm. thick bed of the Kingsport Formation. It was separated from the rest of the outcrop by an irregular fracture and along the N55°-60°E joint face. Note that the area on the outcrop above the fallen slab contains a potential area of slab failure (upper right) in which rockfall will occur

along a N76°E joint face, with separation also occurring along N5°W and N20°W joint directions.

Rockslide

A mass movement process responsible in part for disintegration of bedrock at WBW is rockslide. Rockslides that occur along dip slopes are controlled by bedding planes and those that occur along a scarp face are controlled by joints (Ritter, 1978, p. 149). At WBW, no evidence for dip slope rocksliding was found, although specific examples of dip slopes formed by extensive solution along bedding planes are given later in this thesis.

Figure 19 is a sketch of a feature resulting from a rockslide along a scarp face where only material outside the outermost continuous joint was involved in sliding.

The slab failure in Figure 19 is located approximately twelve meters upstream from the farthest limits of the East Fork stilling basin and six meters up the ridge underlain by the Kingsport Formation. Also characterized by a slide plane oriented N55°-60°E and dipping 45°NW, the slabs involved in sliding belong to a bed measuring 1.2 meters thick. The lengths along strike and thicknesses of individual slabs vary due to control by different joints. Slab A measures 15 cm. thick and 1.5 meters long. Separation of Slab A from the missing segment to the left appears to have been along a joint face oriented in a N35°W direction. Close observation,

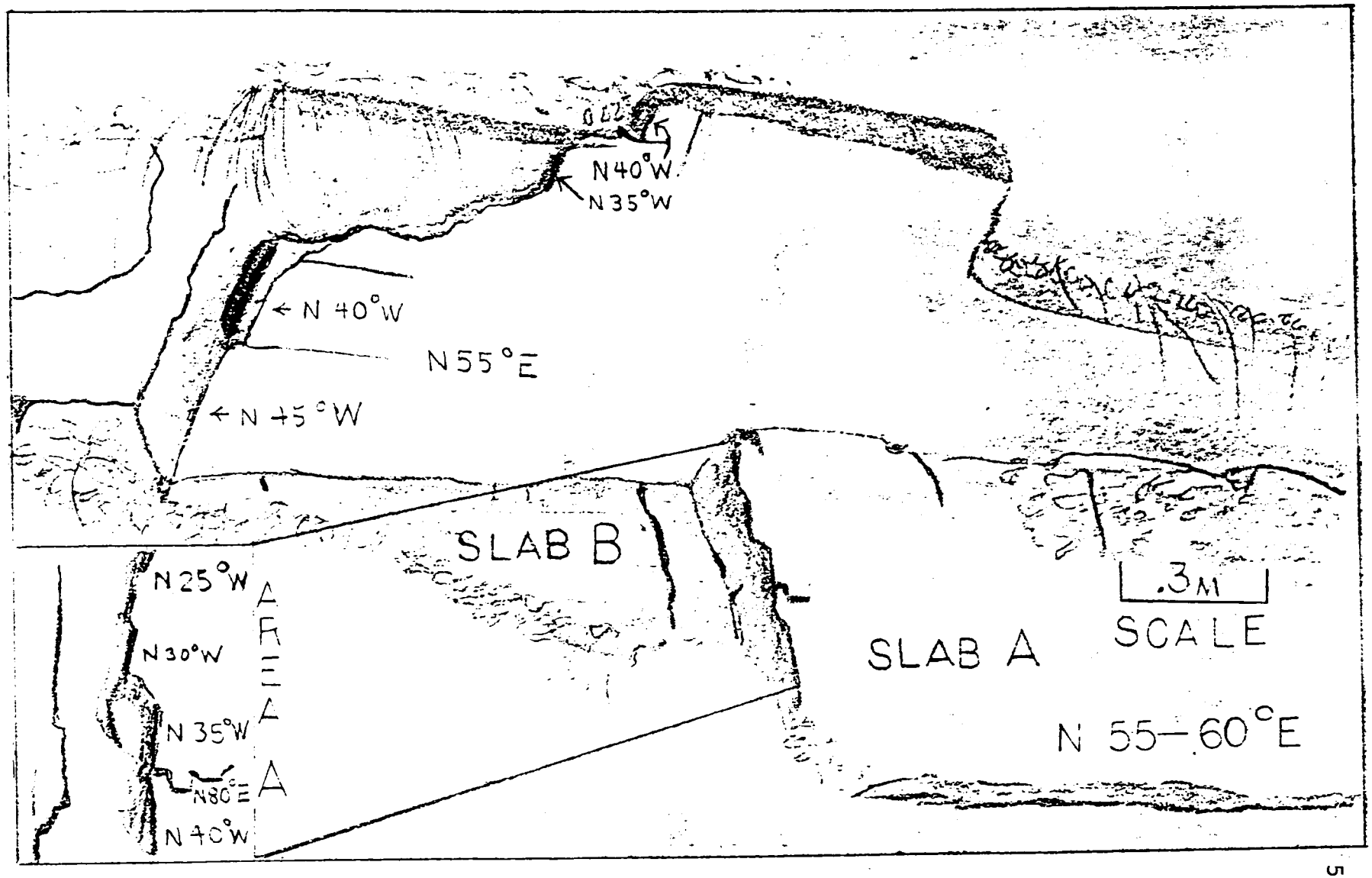


Figure 19. Rockslide.

however, reveals the joint face is actually composed of four different joints ranging from N40°W to N25°W. Beginning with the N40°W joint at the bottom, the four joints develop an unusual pattern in which they increase in five degree increments toward north at even intervals as they appear stratigraphically higher in the bed (Slab A).

No joints outside of a N25°W to N45°W range other than the N55°-60°E slide plane were observed in outcrop. Talus accumulated at the base of the slope and the general area shows evidence of creep on both sides of the outcrop.

Bedrock Pinnacles and Cutters

The underground topography is characterized by an undulating bedrock-regolith interface where projecting masses (pinnacles) of bedrock are separated by areas of residuum (cutters) formed by dissolution of bedrock. The selective dissolution of bedrock forming the cutters may be a result of preferred groundwater movement along high density fracture zones in the bedrock. If sufficient data on the bedrock-regolith interface was obtainable for an area, a correlation between cutter development and fracture traces observed on imagery might be observed for that area.

Bedrock pinnacle and cutter topography is usually hard to detect because it is masked by a deep regolith formed over the Knox in many places, such as WBW. Two methods used to obtain this information are by geophysical (essentially

seismic, although gravity has been used) and borehole drilling.

A seismic survey was conducted during 1969 to obtain information on the bedrock-soil interface and groundwater table height (Tom Grizzard, personal communication). The success of that survey was limited due to scatter produced by the residual chert blocks. A seismic reflection survey was considered for this project; however, it was abandoned due to expense, interpretation problems related to terrain, and the potential effect of blasting on instrumentation of other WBW projects.

For the ecological project, ORNL contracted (1977) two observation wells to be drilled close to surface divides on the West subwatershed. A depth of approximately thirty meters was drilled at each site before reaching bedrock (Frank Harris, personal communication).

Surface mapping yielded little information on the bedrock-regolith interface. Regolith tends to be comparatively thin everywhere on side slopes over the Kingsport Formation and the Mascot Dolomite as noted by McMaster (1971). A bedrock pinnacle of the Mascot Dolomite—located adjacent to Sinkhole A (Figure 20)—was the only direct evidence noted by the writer for pinnacle and cutter topography found at WBW.

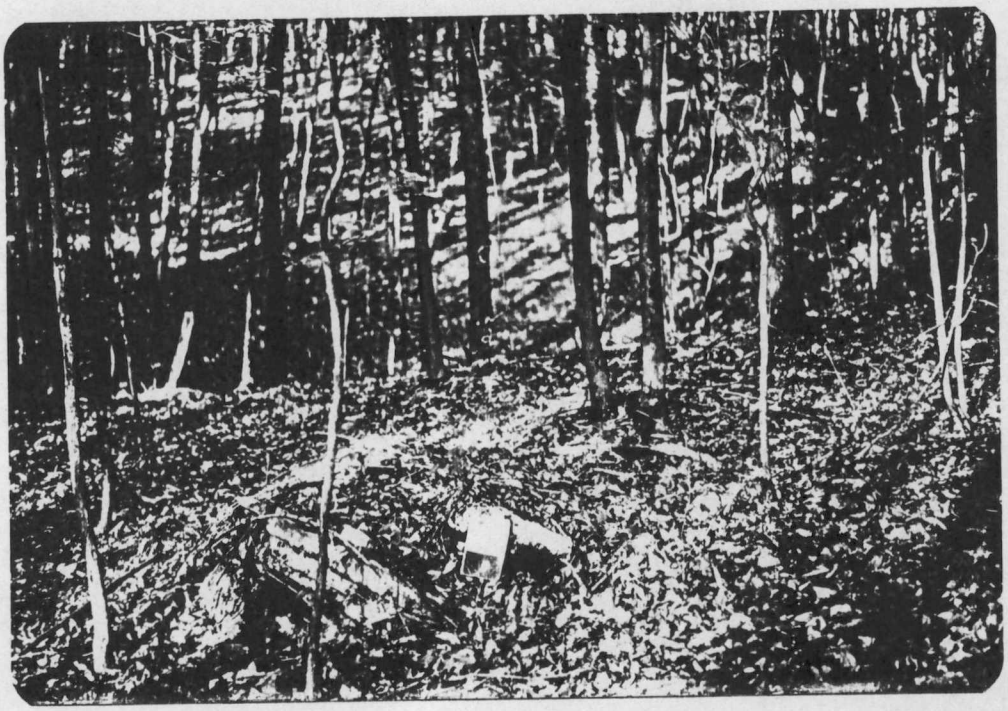


Figure 20. Bedrock pinnacle of the Kingsport Formation. Sinkhole A with a depth of over 6 meters in the immediate background.

Gully Erosion

Gully development at WBW appears to be localized in two areas. The major area is along the east flank of that part of Chestnut Ridge which bounds Walker Branch and the west prong of Walker Branch. A second, but less gullied area is along the eastern flank of the spur dividing the East and West subwatersheds.

The difference in degree of gully development between the subwatersheds may be anthropogenic. Elwood and Henderson (1973) report that prior to 1942, 44% of the area within the West subwatershed was cleared for agriculture while only 13%

was cleared on the East subwatershed. Cleared land will contribute more surface runoff (thereby increasing gully erosion) than forested canopy since in the latter, some water is absorbed and transpired by trees.

Discussion of gully erosion here will be limited to vast gullies located immediately to the southeast of the West weir because their development must be attributed to more than just increased surface runoff. However, even these gullies have probably been enlarged by increased runoff resulting from the cleared area around Rain Gage Three during its construction. Arguments are presented here that suggest structural (bedrock fractures and joints) and stratigraphic control on their location and extensiveness. This area is characterized by six subparallel gullies trending approximately N50°W which intersect a main linear gully trending N70°E. The minor gullies average 1.5 meters in depth, 1.2 to 1.5 meters in width and 40 to 80 meters in length, and are positioned 4 to 8 meters apart. The main gully is up to 2.4 meters in depth and averages two meters wide. A small sinkhole measuring 1.5 meters in diameter and one meter deep was observed in the upslope reach of the main gully. Fracture traces detected on imagery occur in the form of straight tree alignments and are located immediately adjacent to and in the same orientation as the main gully. The soil tonal and tree alignment directional histogram

(Appendix C, Figure C.1) shows tertiary maxima in both N50°W and N70°E directions.

As a final argument for possible structural and stratigraphic control accounting for this extensive gully development, it should be noted that the gullies are located over the same general stratigraphic position as the lower reaches of the East Fork where a semiblind valley (karst geohydrologic feature) is developed due to increased permeability (probably by greater bedrock fracture and joint density). Also, one of the most densely fractured outcrops observed at Walker Branch Watershed can be correlated with this location (Figure 9, p. 25). If the gully area also lies along a more fractured zone, infiltration of runoff would further its development by increasing solutional processes on underlying bedrock and creating greater subsidence of residuum through enlarged fractures.

CHAPTER III

GEOHYDROLOGY

The geohydrology of WBW is analyzed to establish:

1. The influence imposed on groundwater and surface water movement and occurrence by structure and stratigraphy.

2. Geohydrologic features (sinkhole, semiblind valleys, etc.) formed as a result of solution of bedrock by acidic waters.

3. Linkages between areas of groundwater recharge and discharge.

4. Variances in groundwater characteristics caused by seasonal precipitation fluctuations.

An understanding of the above characteristics and relationships is important when evaluating an area for waste disposal because groundwater is the main transporting medium of contaminants to the biosphere, and surface water is the predominent surface erosion agent in temperate climates.

The following section is an introduction to principles that govern the groundwater regime in carbonate aquifers.

I. GENERAL CARBONATE AQUIFER CHARACTERISTICS

Porosity and Permeability of Carbonate Rocks

In the groundwater regime, porosity and permeability decrease with depth. This is because void size and

interconnection of fractures decreases due to decreasing solutional activity. The most active zone of solution is formed where vadose water highly charged with free CO_2 intercepts the top of the groundwater table.

Primary porosity or intergranular void space in dolostones is practically nil. Instead, solution opens voids in the rocks and working along preexisting bedding planes and fractures forms secondary porosity (Ritter, 1978, p. 469). This allows the rocks to hold more water and promote circulation within the system. The permeability or the capacity to transmit water is determined by the interconnection of these voids (see Figure 8, page 24, and Figure 21).

Recharge to Dolomite Aquifers

Recharge is made up of two components, swallet or swallow hole water and percolation water. Swallet water consists of those streams which sink at a clearly defined point through several fractures or conduits (Jennings, 1971) while swallow holes are separate conduits usually situated in closed depressions such as dolines. Percolation water originates as precipitation falling directly onto either bedrock or regolith. This water then percolates by gravity down through the overburden in a more dispersed manner than the conduit components of flow. Since there are few outcrops in WBW, the percolation component of precipitation is mostly

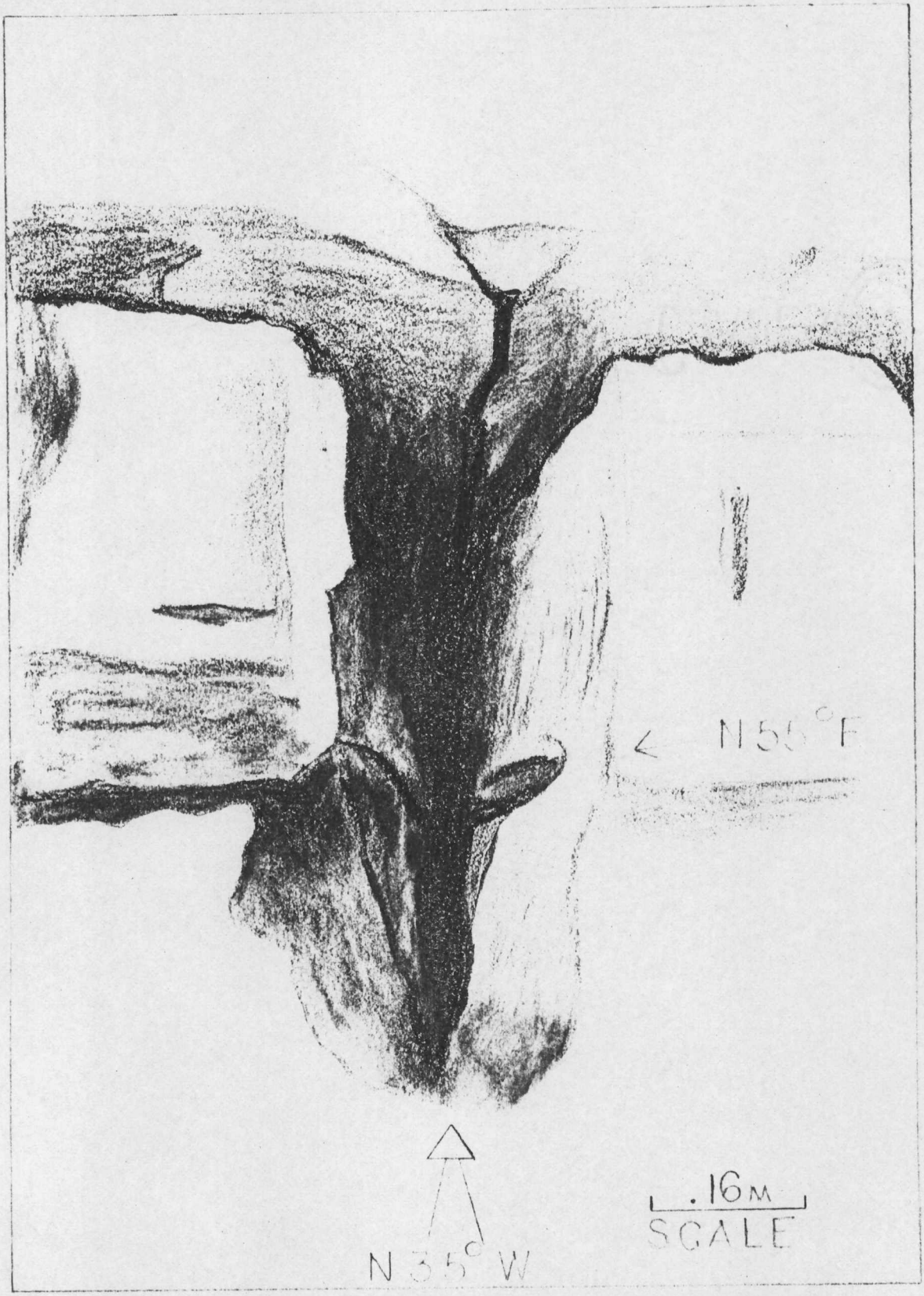


Figure 21. Solutional widening along bedding planes and N35°W joints.

through soil overburden. Percolation water may contribute more of the precipitation to the groundwater regime because of larger catchment area, but conduits will undoubtedly have more volume flow per unit area as well as higher velocities and more rapid travel times to groundwater outlets.

Swallets contribute surface stream water that is a mixture of direct precipitation, groundwater from nearby springs and seeps, and runoff from overland flow to the groundwater table which exists close to the surface in stream valleys. Detailed examinations of the swallet type recharge system can be found later in this report under "Differences in Aquifer Flow Types of the East and West Subbasins" and "Swallets, Semiblind Valleys, and Resurgences."

The swallow hole recharge system is characterized by a sinkhole catchment area which channels flow through one or more swallow holes to a groundwater discharge outlet located usually at stream level. It is not known how much mixing there is between preexisting groundwater and the precipitation water that is contributed by the sinkholes. By establishing the amount of mixing, flow velocity, linkages between recharge and discharge areas, etc., one can theorize whether the aquifer in that area is characterized by diffuse flow or free flow (conduit) conditions.

The best method to acquire this information is by tracer experiments. An experiment might consist of placing a

predetermined weighted amount of different tracers (to establish individual linkages) in the sinkholes prior to a major precipitation event. By obtaining the amount of rainfall from the nearby rain gauges and knowing the areal extent of the particular sinkholes, a concentration or dilution factor of that tracer without groundwater addition could be predicted and tested at the spring outlet. Sinkhole A (Appendix B) exhibits ideal conditions for this experiment since its aerial extent can be precisely measured and it contains one central swallow hole.

The writer was not able to conduct any tracer experiments to establish relations between the recharge systems and aquifer flow types, but he was able to hypothesize the aquifer flow types prevalent for each subbasin at WBW by differences in stream and spring discharge and chemical characteristics.

Carbonate Aquifer Flow Types

W. B. White (1969) classified carbonate aquifers according to their hydrogeologic properties as to diffuse flow, free flow, or confined flow.

A confined flow aquifer is a rock system that is confined to some degree by impervious beds and that allows water to move in response to pressure. No proof for existence of these conditions was found at WBW. However, WBW did exhibit diffuse flow and free flow aquifer conditions.

Shuster and White (1971) later divided the subterranean flow into conduit flow in place of free flow (White, 1969), and diffuse flow. In the diffuse flow aquifers, cavities are limited in size and numbers, caves are rare, and a well defined water table is present. The dispersed nature of flow in the diffuse system, together with its longer residence time, favors the solution reaction. Because of its lower flow velocity than that of conduit flow, diffuse flow is limited in the size and quantity of particulate load it can carry. Also, corrosion dominates over corrasion because the diffuse flow component passes through a soil cover where it derives increased acidity for dissolution of bedrock by addition of CO_2. Conversely, conduit flow favors more rapid flow with a load of clastic material mineralogically harder than calcite, for example, chert. The conduit component of flow when directly connected to surface stream sinks will show more variability in discharge with individual storm events. In this type of flow regime, corrasion or erosion by abrasion is the more dominant erosion agent.

II. AQUIFER FLOW TYPES AND RECHARGE SOURCES FOR THE EAST AND WEST SUBBASINS

The purpose of this analysis is to determine aquifer flow types and recharge sources for the East and West subbasin. This is done by correlating characteristics of particular variables (groundwater flow rates, groundwater

storage or residence, amounts and composition of inorganic particulate matter in suspension, etc.) in conduit flow versus diffuse flow common to carbonate aquifers (preceding section) with spring and stream discharge and chemical data collected for these same variables at WBW.

In the Environmental Sciences Division's technical progress report on WBW (ORNL, 1975), an experiment was mentioned in which concentration of fine suspended particulates were compared over a discharge range for each subwatershed. Concentrated flows of less than 400 $m.^3$/day on the East Fork contained more than 1 mg/L of fine suspended particulates, but five times this discharge value was needed on the West Fork before particulate concentrations significantly greater were reached. Because suspended particulates in the East Fork had a slightly higher average inorganic content, it was suggested that there may be more soil erosion on the East Fork. This anomaly may also be explained by increased conduit flow, which favors abrasion and more concentrated transport of suspended clastic material on the East Fork. The West Subbasin may favor diffuse flow until the groundwater table increases sufficiently to create turbulent erosive flow in sediment laden conduits above the limit of perennial flow.

By simply comparing between each subwatershed the development of diversion of surface streams to underground

and their reappearance as springs, it may be surmised why greater discharge is needed on the West Fork to reach significantly greater concentrations of fine suspended (inorganic) particulate matter. On the East Fork, stream water sinks into gravel (swallets) and flows through large conduits for almost half the distance covered between the weir and the limit of perennial flow before emerging as a spring (resurgence). On the West Fork, there are only minor underground streams and resurgences created during higher groundwater conditions when new springs appear at higher reaches in the valley. Therefore, greater amounts of inorganic particulate matter would be expected on the East Subbasin since the predominant conduit flow type there favors corrasion over corrosion which prevails in the diffuse flow system of the West Subbasin. Because the stream water travels such a short distance before disappearing into gravel, and the phenomenon fluctuated in its positioning so much, no attempt was made to plot these underground streams and resurgences of the West Fork on the geohydrologic map.

There is also an anomaly in the amount of discharge variance in each fork. Sheppard (1971) found that at East Fork and West Fork stream flow greater than 0.3 CFS, the relationship between discharge at the two weirs was approximately linear and flows were essentially equal. However, he

found that when the East Fork flow was less than 0.1 CFS, the West Fork stream flow fluctuated from only 0.15 to 0.21 CFS while the East Fork stream flow ranged a much larger order of magnitude, 0.01 to 0.1 CFS. Sheppard then compared discharge values for the largest spring on each fork, S3W (West Fork) and S1E (East Fork) and saw the same pattern. Clearly, there is a direct relationship on each fork between the largest spring discharge and discharge at the weir. It was also suggested that the relatively high and constant West Fork stream flow probably reflected the influence of the spring S3W which might be fed from outside the West Fork subwatershed.

The difference in spring and weir discharge variances between the two forks may also be explained by considering the aquifer flow types and recharge sources. To explain this difference, an analysis was conducted using available chemical and discharge data on each spring for a particular week encompassing a storm event. Springs fed by percolation water (diffuse flow) show little variation in hardness when plotted against discharge, but hardness does vary in conduit fed springs. Table I (Bonner, 1968) shows that the calcium and magnesium content of S1E vary by a factor of almost two in the time period of one week while values for S3W differ only by a few tenths. The difference in discharge response of the two springs at low and high flows also gives a clue

TABLE I

SOME CHEMICAL CONSTITUENTS AND STREAM FLOW DATA OF BONNER (ORNL) FOR THE WALKER BRANCH WATER SHED (MARCH 1968)

	Calcium (ppm)		Magnesium (ppm)		Nitrate (ppm)		Stream Flow (CFS)	
	3/11/68[a]	3/18/68[b]	3/11/68	3/18/68	3/11/68	3/18/68	3/11/68	3/18/68
East Fork Weir	22.0	13.2	10.0	0.2	0.155	0.151	0.38	[c]
Spring S1E	14.0	8.8	6.8	3.7	0.151	0.124	0.20	0.33
Above S1E	14.0	8.8	7.3	3.4	0.173	0.138	[c]	[c]
West Fork Weir	29.2	19.2	14.6	7.3	0.078	0.204	[c]	[c]
Spring S3W	28.6	28.8	16.8	15.1	0.484	0.346	0.073	0.075
Above S3W	21.6	8.6	12.2	4.0	0.097	0.124	[c]	[c]

[a] Sampled after 0.75-in. rain on March 11.

[b] Three-inch rain on week preceding sample.

[c] Not available.

to their origin with respect to recharge. Springs respond very rapidly to an increase in precipitation when fed by percolation and rain water but springs fed by groundwater in storage have a more even discharge. S1E varied in discharge from 0.20 CFS to 0.33 CFS in the week encompassing March 11, 1968 to March 18, 1968 but spring S3W only varied from 0.073 CFS to 0.075 CFS in the same time period.

This would suggest that S3W is an outlet for groundwater (probably in storage) of the diffuse flow type (small fissures and fractures) while S1E is fed by the larger conduit or free flow type aquifer with discharge fluctuating proportional to precipitation.

Water from S1E and the area above it gave the same calcium hardness values and close to the same magnesium hardness values suggesting that the conduit system feeding spring S1E is extensive, interconnected, and partially fed by percolation water. Also, bedrock and regolith in this area do not possess good storage capacity. The area above S3W shows an immediate response to rainfall (hardness varies inversely to discharge) while spring S3W remains unchanged. This suggests that there is little or no mixing of groundwater with percolation water in the source area of spring S3W.

III. GROUNDWATER DISCHARGE AND RECHARGE FEATURES

Springs and Seeps

Springs and seeps are localized areas of groundwater discharge and although they are not limited to karst, they are probably most characteristic of this type of terrain. Not including lateral residuum pipes in alluvial dolines, 46 springs and seeps were observed at WBW (Appendix A). Groundwater discharge outlets were classified on a topographical basis as: (1) midslope springs and seeps, and (2) stream bed springs and seeps. They were further divided on the watershed as to perennial versus wet season springs. "Wet season" is used in the context of intermittent and is not limited to those months in Winter and Spring of increased precipitation when discharge is maximum. This is because major storm events during the dry season will also cause the appearance of new springs with a sudden rise in the groundwater table.

Midslope springs and seeps. A midslope spring or seep is one that occurs some distance up the valley side slope from stream level. Only three midslope springs were observed on Walker Branch and these are located below the weirs. Their locations with respect to formations of the Knox can be seen in Appendix B where MDS1 and MDS2 are below the confluence of East and West Forks and MDS3 is immediately downstream from the East Fork weir.

MDS3 is on the stream bank approximately 1 m. from the stream and discharges during the wet and dry season. MDS3 continues seepage even when there is no flow over the east weir. Since the seep is located topographically lower than the water level in the East Fork weir stilling basin, this seep may result from leakage through the East Fork weir dam. However, MDS3 is located approximately 15 m. downstream from the stilling basin dam and no seepage occurs between. Therefore, it is possible that if leakage is occurring, the transporting medium may be a conduit(s) which confines the water until it emerges as spring/seep MDS3.

MDS1 was observed to flow only after a heavy rain, and it is therefore concluded that it is definitely percolation fed. Located highest up the slope of all the midslope springs (approximately 6.1 m.), it discharges from a gully possibly having its origin in spring sapping and flows through a drainage pipe in the road to Walker Branch below.

Midslope spring, MDS2 (4.6 m. upslope from Walker Branch) ceases flow only during the summer season. Water can be seen emerging from a distinct channel in residuum which has an elliptical opening in a horizontal direction approximately 5.1 cm. wide and 2.54 cm. high. It essentially maintained an even discharge from fall through spring which indicates its source is probably from storage in a perched water table. If this channel is in the vadose zone and the dry outcrops

immediately adjacent to it indicate this is to be the case, the ability of the karst channel to maintain this flow may be accounted for by the possible clogging of its floor with fine clays and silts. Upon encountering one of these clay aquicludes, descending infiltration water would change flow directions from vertical to near horizontal and be expelled at midslope instead of stream bed level.

Stream bed springs and seeps. Stream bed springs and seeps are groundwater discharge areas occurring at the level of the stream. Of the 43 stream bed springs and seeps at WBW, 24 are located on the East Fork subbasin, 15 on the West Fork subbasin, and 4 below the weirs on Walker Branch. Besides being either perennial or wet season, stream bed springs are classified on the nature of their recharge source (Jennings, 1971, p. 74). Springs and seeps fed by groundwater percolation are called exsurgences while those supplied by the sinking of surface streams are referred to as resurgences. A resurgent spring is nearly always fed in part by seepage so there is no sharp distinction between the two. Resurgences and their upstream counterparts, semiblind valleys, are elaborated on further in the following section, since they are a special type of stream bed spring and a groundwater recharge feature respectively. Discussion here is limited to different exsurgent stream bed bed springs.

The writer has divided stream bed springs and seeps of WBW into the following categories:

1. Median stream bed springs and seeps,
2. Estavelles,
3. Upwelling springs or risings,
4. Lateral residuum conduits in alluvial dolines, and
5. Saturated zone seeps.

Median stream bed springs and seeps. These types vary in their appearance depending on how and where they emerge, so an understanding of these characteristics can aid in their detection. Sometimes turbulent flow can be seen emerging from a conduit. In springs emerging from a circular pool filled with fine clays, silts, and sands, flow may be so low that it can only be detected by movement of floating particles on the surface. The springs may emerge directly within the confines of the stream channel or they may emerge some distance away in which the spring joins the main stream as a tributary. Figure 22 (see also Appendix B) shows circular pool springs S5W and S6W that contain water-loving plants called phreatophytes (another aid in spring detection). Both join the West Fork as tributaries. In some areas, the only way a spring or seep emerging under the stream's surface could be detected was by a change in color of fine particle deposits of the bed load (Figure 23).

S1WB (Appendix B) is a noninstrumented spring in which flow from an approximately 12 cm. side conduit is diverted

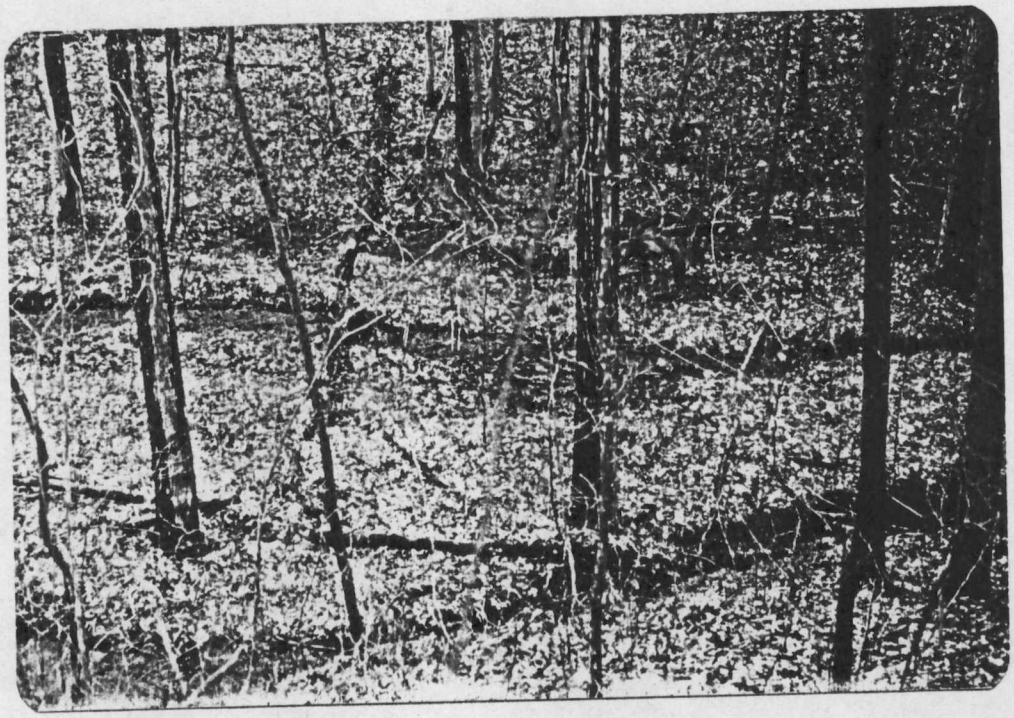


Figure 22. Springs S5W and S6W (note phreatophytes) joining Walker Branch West Fork as tributaries. Coat at center right for scale.

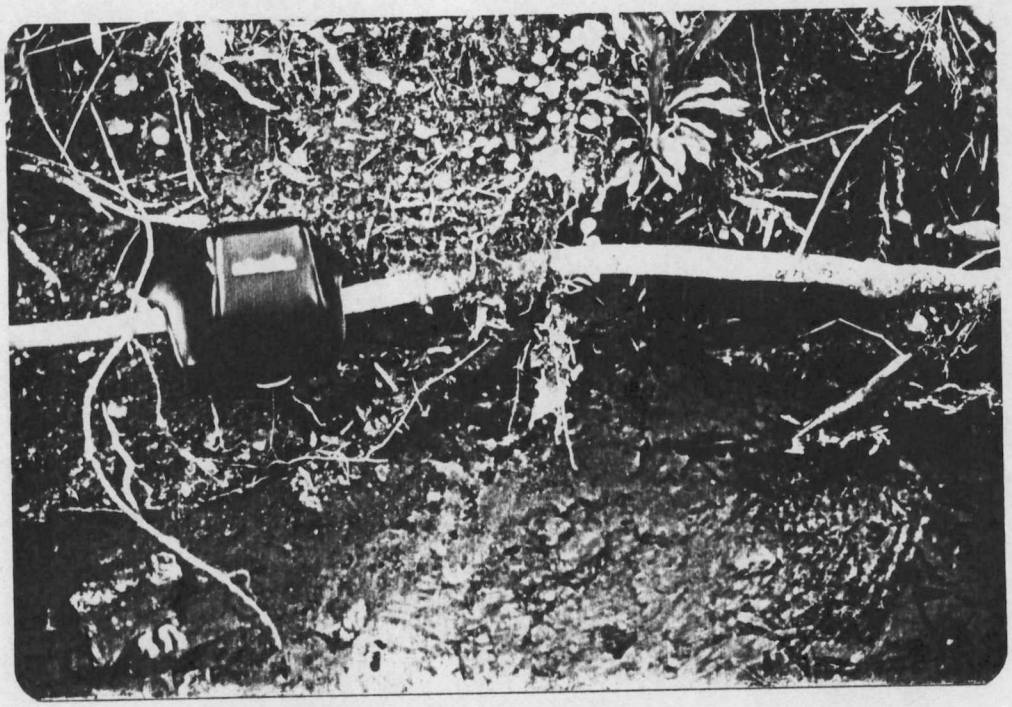


Figure 23. Detection of spring or seep by change in color of the bed load.

through the road into Walker Branch by a drainage pipe. Although discharge could not be quantitatively examined, this drainage pipe allowed the visual observation of incremental changes in flow with increasing monthly precipitation. This discharge varies more with seasonal precipitation conditions rather than individual precipitation events.

Estavelles. Some springs are actually streamsinks that have reversed their function in times of increased stream discharge. Estavelles are normally swallets or swallow holes that contribute to the groundwater recharge system, but following particular heavy precipitation events, the conduit system is fed by groundwater sources and the combined total will exceed the holding capacity of the conduit, resulting in an upsurging spring (Figure 24). This estavelle was observed after a major storm event to discharge as a spring with much turbulence; however, the conduit at this location functions as a swallow hole during low baseflow conditions.

Upwelling spring or rising. An upwelling spring or rising is one that issues with some turbulence into a surrounding body of calm water. Such a spring was detected in the upstream limits of the East Fork stilling basin. This upwelling spring ceases flow only during low baseflow conditions. Its origin is not positively known, but it could also be labelled as an estavelle if it serves the dual

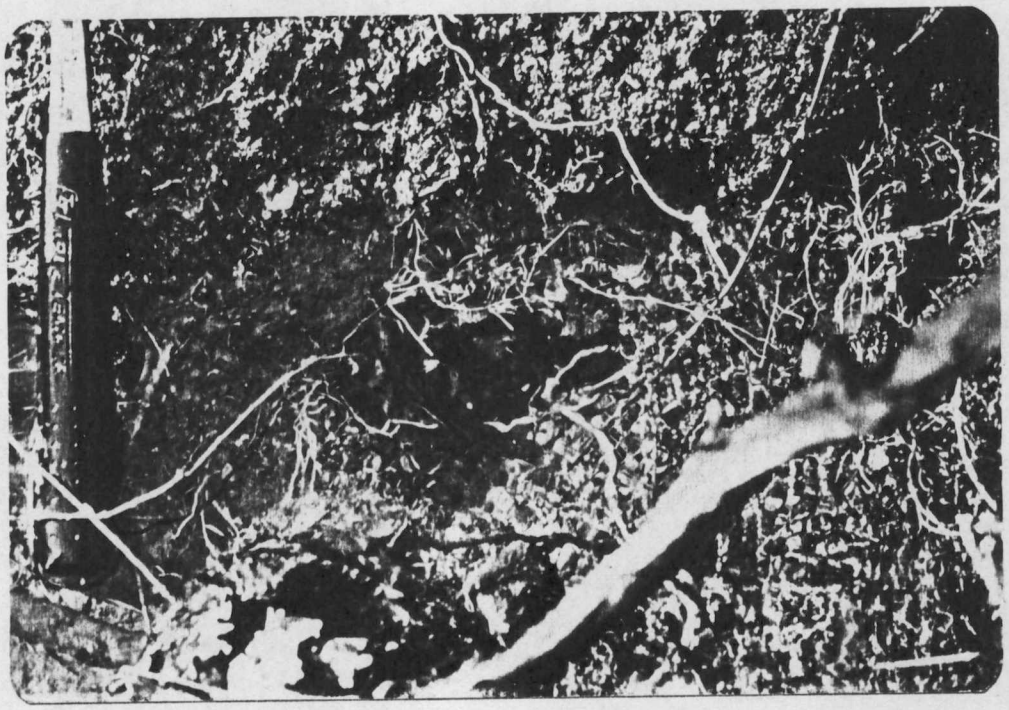


Figure 24. Estavelle showing turbulent flow. Conduit opening at center of photograph.

purpose of a swallet. Also, it might be a resurgence if it is the surface reappearance of the East Fork branch in semiblind valley conditions.

It was detected by a slight turbulence or rippling effect on the surface immediately above a small circular depression in the stilling basin floor. Several seeps emerge just below the water at the edge of the northwest facing bank adjacent to it. At times when there is no discharge over the East weir, the upwelling spring ceases flow and all bank seeps except one at the fartherest end of the stilling basin disappear.

Lateral residuum conduits in alluvial dolines. Lateral residuum conduits are small conduits having a horizontally elongate shape and occurring in a clay soil residuum in higher reaches of valleys (Figure 25). Most of them discharge only following precipitation events and thus are percolation fed. However, a few in higher reaches of the East and West Forks were observed to discharge even during times of lower flow conditions. This indicates that these particular conduits may be draining an area possessing good groundwater storage capacity.

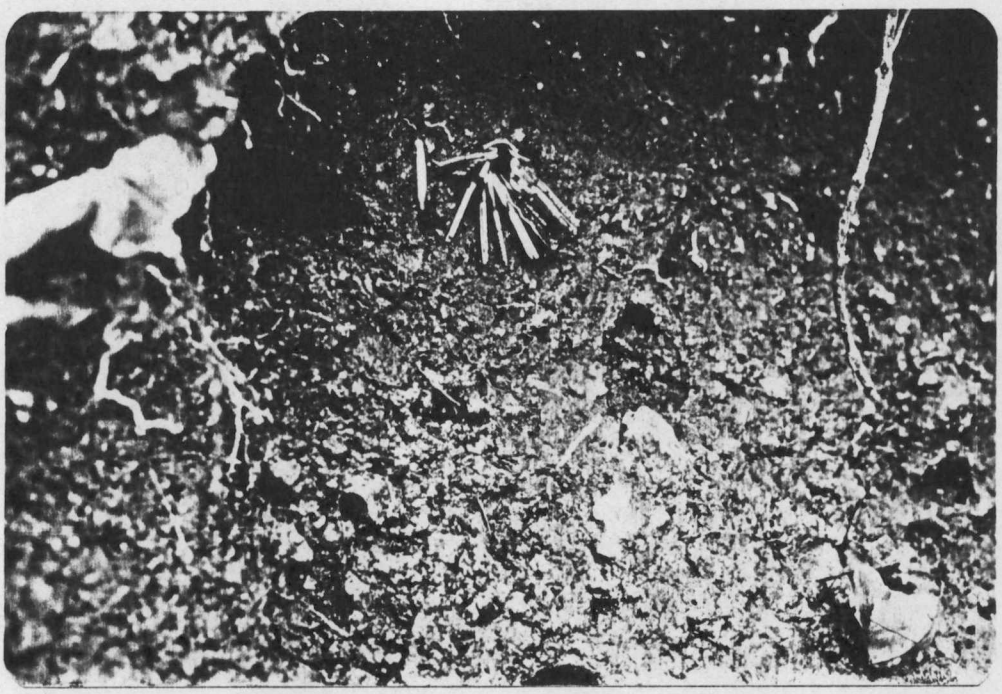


Figure 25. Lateral residuum conduits. Note larger five cm. conduit to the left of the keys.

There is some evidence that these may be linked to throughflow in first order tributary valleys. This idea was prompted by the observation of a small alluvial doline in upper reaches of the West Fork channel across from a N10°E oriented valley on the north face of a Longview Dolomite ridge.

Several lateral residuum conduits were observed in a subsidence feature called an alluvial doline. These dolines are usually less than 1.5 m. in diameter and anywhere from .61 to 1.2 m. deep. The initiation and further development of these subsidence features is probably enhanced solution of bedrock from carbon dioxide-enriched water issuing from these lateral residuum conduits.

Saturated zone seeps. At the onset of this research, a field reconnaissance of Chestnut Ridge revealed many areas at stream level in which the ground surface contained alternating saturated and nonsaturated zones. These saturated areas are interpreted to be the coincidence of the groundwater table with the surface. In nonkarst areas which contain rock types that lend themselves to a more even groundwater table than found in karstified carbonates, one would expect this saturated area to be continuous in a downstream direction once it appeared. This alternating saturated and nonsaturated zone in the Knox dolostone of WBW may be explained by the formation of a local groundwater

mound occurring in an area of low permeability or by an area of large discharge over relatively low permeable material.

Saturated zone seeps around S1E are caused by discharge over an area of relatively low permeability bounded on either side by semiblind valleys which are areas of high permeability. An examination of the East Fork Longitudinal Profile (Figure 26) shows this area emerges on top of a bench which should be massive chert blocks of the upper Longview. Normally, highly fractured chert blocks in residuum will cause greater permeability, but these are massive, dense chert blocks, as can be seen in Figure 27. Saturated zones around S5W and S6W on the West Fork and S3E and S4E on the East Fork are also due to large groundwater discharge over relatively impermeable materials. There are no visible concentrated seeps or springs in the saturated zone between S2E and S3E, however, and this saturation may be accounted for by the area possibly being over just the optimum permeability needed to allow the groundwater table to remain at stream level.

Swallets, Semiblind Valleys, and Resurgences

In karst terrains, many rivers and streams follow underground routes at least part way through their courses. The surface manifestation of this phenomena is referred to as the semiblind valley, if there is surface flow at times when the underground course cannot carry the total flow.

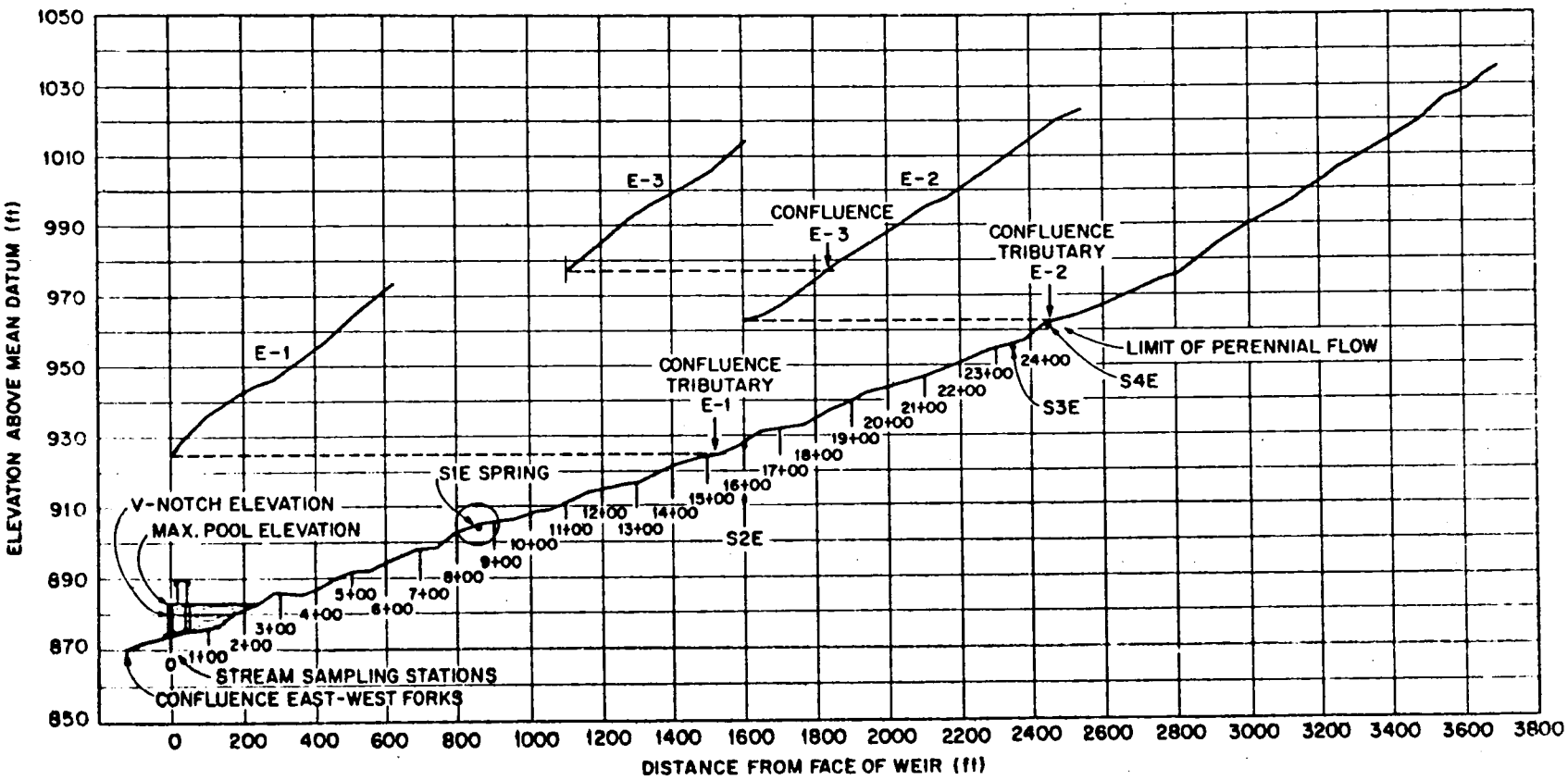


Figure 26. Profile of East Fork subwatershed and tributaries. The circled area is the location of groundwater seeps postulated to be caused by low permeability over massive chert blocks at the Longview-Kingsport boundary (after Curlin and Nelson, 1968).

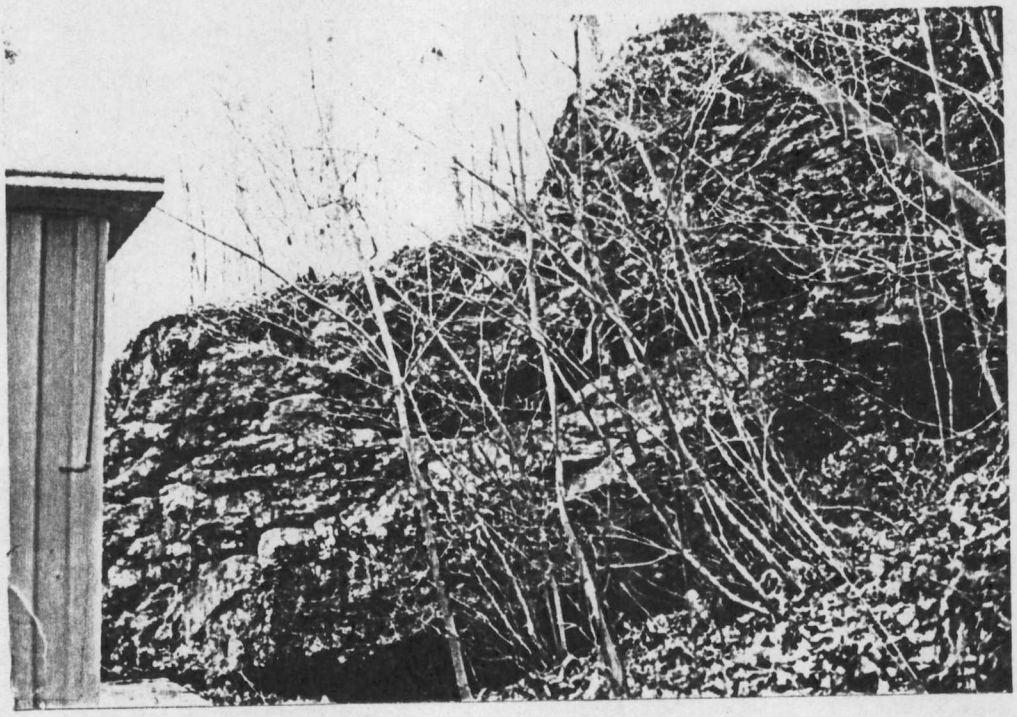


Figure 27. Massive chert blocks at the Longview-Kingsport boundary.

The point of sinking either through fractures beneath gravels in the stream bed or through a visible sink is called a swallet or streamsink. If the stream reappears at the surface further downstream, it does so as a resurgent spring.

Actually, the only valid way to link these features to each other is by tracer experiments. Although the writer was unable to perform these experiments, there is evidence in WBW that this process is prevalent especially on the East Fork. Legrand and Stringfield (1969) interpreted the underground and missing segment of a stream as being in a permeable zone and the segment of overland flow slightly upstream from the swallet or streamsink being impermeable.

This may not necessarily explain all semiblind valleys in the upper reaches of the East and West Forks. In the upper valley reaches, flow is generally very low and intermittent so that sinking of the streams occurs along several places in the alluvium. A stream's disappearance may also be considered a result of failing supply and/or evaporation.

Downstream from the limit of perennial flow on the East Fork, alternating permeable and relatively impermeable zones appear to influence groundwater movement and the creation of karst geohydrologic features under consideration. Sinkhole T (Appendix B) is formed adjacent to a semiblind valley segment, and since it is generally agreed that sinkholes are formed above the water table, this area must be permeable enough to depress the water table sufficiently for the formation of a sinkhole at stream level this far downstream. The permeability is most likely afforded by fracturing such as can be seen in Figure 8, page 24. As discussed previously, they have solutional widening along N35°W, N25°W, N55°E directions and between beds, as well as a large conduit oriented along strike. The stream sinks by infiltration into gravel (swallet) at the end of the semiblind segment at approximately spring S1E.

At 213 meters from the weir, the stream enters a swallet in gravel near the Kingsport-Longview contact (Figure 28).

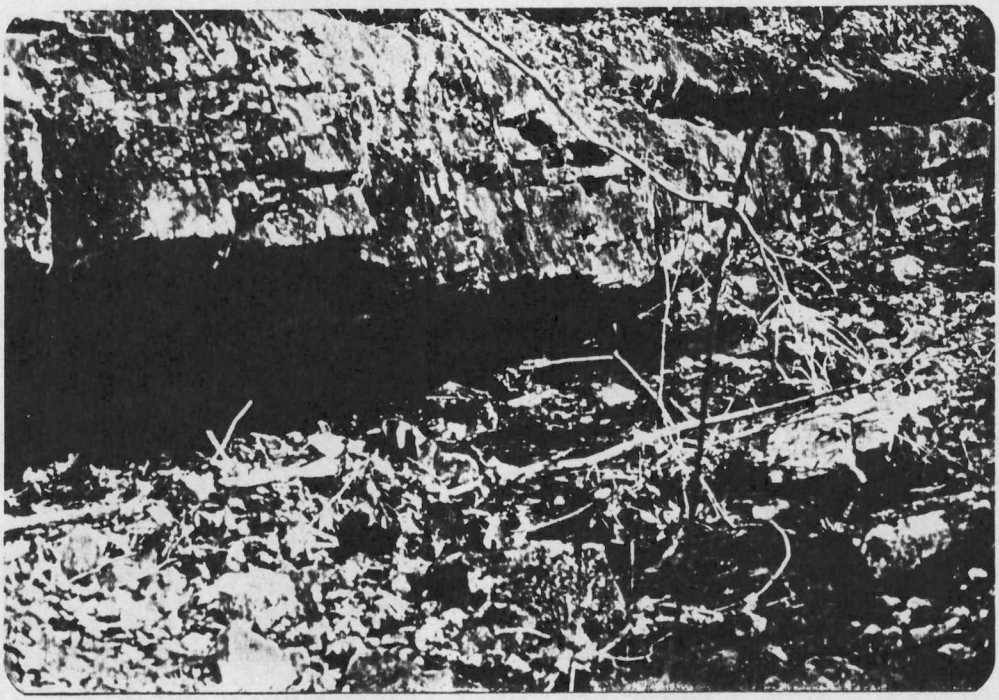


Figure 28. East Fork stream diversion (in part at high discharge) into a swallet. Camera case for scale at lower center. Note abundant N35°W oriented bedrock fractures under the lower bed far left.

A large conduit is inferred to be associated with this swallet because even during low flow conditions turbulent water can be heard rushing through what sounds like a short waterfall and large conduit.

The area of this stream's resurgence has still not been satisfactorily proven.

IV. SURFACE GEOHYDROLOGY

Drainage Basin Analysis

In the vicinity of WBW, the drainage pattern is characterized by development of elongate strike valleys

with various transverse valleys oriented along bedrock dip and several major fracture (joint and fracture trace) orientations. The NE-SW elongate strike valleys are monoclinical valleys as opposed to anticlinal or synclinal valleys.

The West Fork subbasin adheres closest to the characteristic trellis drainage pattern with two elongate strike valleys. One is the second order tributary W-1 (Figure 3, page 7) to the East which has its confluence with the West Fork just below the limit of perennial flow. The other strike valley, which is actually a part of the same longitudinal strike system is the West Fork above the limits of perennial flow. Both of these occur approximately along the same stratigraphic position in the Chepultepec Dolomite. The idea that these elongate strike valleys were formed by extensive solution along bedding planes (McMaster, 1971), which is common in tilted carbonate rocks, is supported by the occurrence of the dip slope in the Chepultepec Dolomite on the West Subbasin.

Several minor bedrock dip oriented transverse valley segments occur in first and second order tributaries adjoining the elongate streams, but there is a major dipslope valley where the West Fork flows through the Longview Dolomite. It is oriented generally in a N40°W direction which is close to the direction of dip of the

bedrock (S35°E). The West Fork channel is heavily fractured by several major joint and fracture trace directions of which N55°E, N35°-40°W, N10°-20°W, N10°-20°E, N75°-85°W, and N75°-85°E are in abundance. The N35°-40°W orientated joints are one of the major groups enlarged through solution to conduit proportions at WBW. The influence of this on the location of this dipslope transverse valley is supported by the following features:

1. N35°W oriented secondary passage in Harris Cave.

2. Development of abundant potholes along N35°-40°W solutional runnels and joints.

3. Large vertical solution pipe along N35°W joint formed in an outcrop of the Kingsport Formation just below the weirs (Figure 9, page 25).

4. Only joint solutionally enlarged to conduits in outcrops on the West Fork except for N55°E.

5. Alignment of the transverse West Fork valley with the straight valley segment oriented N35°W (Appendix C.2, above the words Chepultepec Dolomite). They are 152 m. apart from each other, being separated by the intervening elongate strike valley.

The following summarizes major influences which may account for positioning of this valley in the Longview Dolomite.

1. Massive chert block zones in upper and lower Longview which underlie the ridge, hindering major development of longitudinal strike valleys.

2. General slope of WBW in a southeastward direction.

3. Possible fractured and weathered zone.

4. Preferred solutional enhancement of N35°W and N40°W joint directions.

The 83 m. stratigraphic sequence between the two massive chert block zones of the Longview contains beds with low content siliceous material and areas of relatively small, very fractured, chert blocks. This zone is more susceptible to solution along bedding strike and forms two longitudinal strike valleys of limited extent, the hanging dry valley on the West Fork adjacent to Harris Cave and the valley to the east of Sinkhole T on the East Fork. Some other geohydrologic features resulting from solution along bedrock strike in this zone are:

1. The main passage of Harris Cave.

2. Sinkhole T—probability of its formation at the intersection of joints with bedrock strike.

3. Semiblind valley on the East Fork just below Sinkhole T.

4. Outcrop on the East Fork with large conduit along bedrock strike direction (Figure 8, page 24).

5. Alignment of potholes along and conduit development of the N55°E bedrock strike and joint intersection on the West Fork (Figure 13, page 37).

The East Fork and its tributaries do not seem to be as controlled by bedrock strike and dip in their overall drainage pattern as the West Fork. On the East Fork, there are many valley segments oriented along major joint directions. Although there are three strike valleys on the East Fork, no major dipslope valleys occur here other than the N35°W topographic sag and N30°30'W straight stream segment occurring in the massive chert block zone at the Chepultepec-Longview boundary (Appendix C, Figure C.2).

The longest strike valley (approximately 732 m. long) occurs in the Copper Ridge Dolomite. There is a dip slope due to solution between bedding planes (Appendix B) also located there. This elongate strike valley has a much different pattern than the slightly larger one of the West subbasin. The first order tributary E-2 to the east and the East Fork are strike oriented only in their highest reaches for approximately 152 m. before each diverts along one of the major fracture trace and joint orientations at WBW.

The upper reach of the East Fork is oriented N60°W, N62°W, and N65°W for close to 244 m. beginning at the downstream limit of its strike oriented channel and ending at its confluence with tributary E-2 at spring S4E, the

limit of perennial flow. From the end of its strike oriented segment, tributary E-2 continues in a N11°W and N15°W direction until it reaches its confluence with tributary E-3. Second order tributary E-3 is another strike oriented valley in the Chepultepec Dolomite. Along its strike oriented segment, tributary E-2 has discharge from six small wet season springs but becomes a semiblind valley from just above the N15°W segment to its confluence with tributary E-3. The elongate strike valley (tributary E-3) also has discharge from a group of four wet season springs issuing from the Chepultepec Dolomite.

These findings suggest that movement and discharge of groundwater in these locations is through conduits developed along bedrock strike.

The straight stream and valley fracture trace analysis (Appendix C, Figure C.3) revealed orientations coinciding closely to major joint and fracture traces in WBW. The preferred orientations in this analysis are N55°-60°E, N65°-70°W, N5°-10°E, and N75°-80°W. Secondary orientations are Due N-N5°E, N50°-55°E, N10°-40°W, and N70°-75°W.

Differences in Processes and Features of Channel Morphology between the East Fork and the West Fork

The East Fork and the West Fork of Walker Branch not only differ in their drainage patterns (see Drainage Basin Analysis) but also in their degree of incision, longitudinal

profile gradients, amounts of alluvium, their stream's competency and capacity, discharge characteristics, etc. The purpose of this analysis is to determine cause and effect relationships on channel morphology between geohydrologic processes and resulting features formed by contrasting the East Fork and West Fork stream channels.

Alluvium on the two forks consists mostly of chert and weathered dolomite. The East Fork stream flows almost entirely over alluvium except for random locations where it flows over bedrock for distances of only a few meters. On the West Fork, however, the stream flows over exposed bedrock with minor alluvium from the weir to almost the confluence of the West Fork with tributary W-1. Above this confluence the West Fork channel bed appears much like the East Fork.

The difference in amounts of alluvium between the East Fork and West Fork can be explained in their differing competency and capacity (and factors influecing this), channel shape, and amounts of chert available for erosion on each subbasin.

Competency is defined as the largest size of grain that a stream can move in traction as bed load. Morisawa (1968, p. 53) states that floods of great force occurring very infrequently may move large boulders in the stream channel because of a manyfold increase in the competence of the stream. Several large chert boulders too large for one

person to pick up were noted only in the West Fork channel. This may be accounted for if one of the rare floods that moved these boulders had more force in the West Subbasin than the East Subbasin. However, they may have just rolled into place along the steep gradient of the West Fork (Figure 29).

Capacity is the maximum amount of debris of a given size that a stream can carry in traction as bed load. Gilbert (1914) determined that a stream's capacity is dependent upon stream gradient, discharge, and caliber of load. Morisawa (1968) further explains that channel shape has an influence on capacity. These characteristics are vastly different between the two forks and greater capacity is favored on the East Fork over the West Fork.

In the experiments on stream capacity, Gilbert held all factors constant except for stream gradient and found that increasing slope resulted in increased capacity. Rate of fall of the primary channel of the West Fork exceeds the East Fork by 19.8 meters per kilometer while secondary channel rate of fall of the West Fork is 157 meters per kilometer greater than the East Fork (see Figure 26, page 80, and Figure 29).

By varying discharge and keeping other factors constant, Gilbert found that increased discharge resulted in increased capacity. Total amounts of water discharged out of each

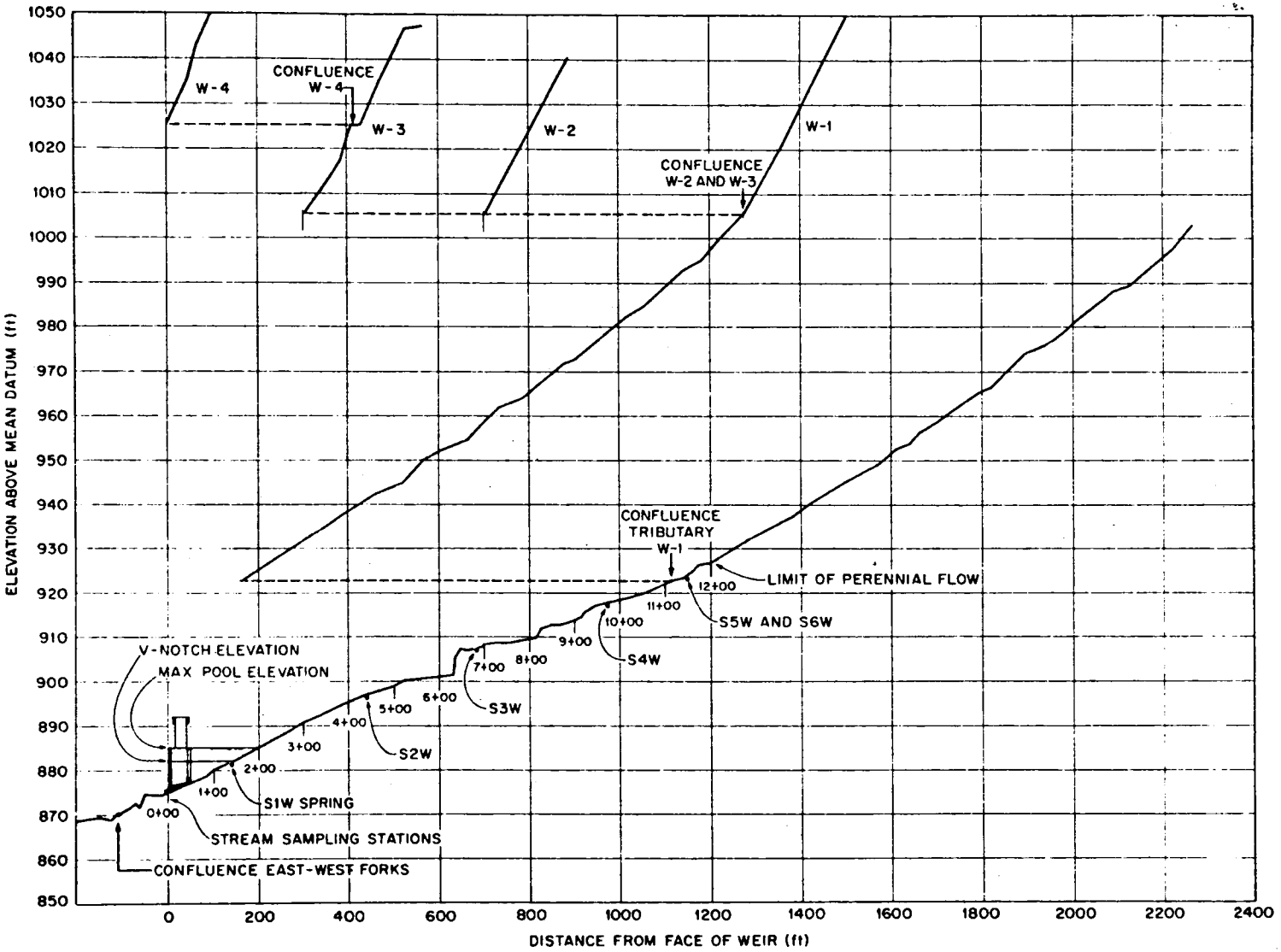


Figure 29. Profile of West Fork subwatershed and tributaries (Curlin and Nelson, 1968).

subbasin calculated from discharge values over the weir for the month of December 1969 (maximum discharge) were found (Intra-Laboratory Correspondence, August 2, 1972, Sheppard to Nelson) to be 533,374 m^3 for the East Fork and 475,465 m^3 for the West Fork. The total stream channel length from the limit of perennial flow to the weir on the West Fork is 336 m. while the distance between these features on the East Fork totals 732 m. The wetted perimeters of the two channels probably average out to close to the same so there is nearly twice the discharge value for the West Fork as opposed to the East Fork since the latter has twice the channel area.

The East Fork has a very seasonal discharge. Much sediment is transported during high discharge, but during low flow conditions the stream sinks underground at swallets thereby discarding its load downstream from the swallets. On July 20, 1980, the writer noted that flow had completely ceased over the East weir, while the West weir maintained a sizable discharge.

Gilbert found that with increasing grain size, capacity decreased. Although no analysis of differences in grain size between the forks was completed, it should be noted that pebble and cobble size material on the West Fork appeared more rounded and polished by abrasion than on the East Fork.

The transporting efficiency of a channel form depends, in part, on the distribution of shear and velocity distribution

(Morisawa, 1968). Both of these vary with channel shape. A wide, shallow channel such as the West Fork (within the area of perennial flow) has a higher velocity gradient and a greater rate of shear near the bed which aids in entrainment and transport. On the East Fork, however, the channel is more narrow and deeper on the average and the higher velocity lies closer to the walls. Therefore, bedload is more efficiently moved on the West Fork stream channel over that of the East Fork.

Another explanation in the difference in amounts of alluvium may be in the greater amount of easily transportable chert released on the East Subwatershed over the West Subwatershed. The Copper Ridge Dolomite contains the most chert of any stratigraphic unit of the Knox that will produce pebble and cobble size alluvium. Over 80% of total exposure of this formation on the watershed lies in the East subbasin (Appendix A).

Many characteristics which affect amounts of alluvium, such as discharge, capacity, etc., also influence how deeply incised the channel is into bedrock. Since these aspects have already been evaluated, discussion here will be limited to the effect solutional processes have on the greater degree of incision of the West Fork over the East Fork.

An explanation of why the West Fork below the limit of perennial flow is oriented close to the direction of bedrock

dip was given under Drainage Basin Analysis of this report. This evidently has a direct influence over how much more deeply incised the West Fork is over the East Fork. Elwood and Henderson (1973) suggest that this is a result of more extensive solution along bedding planes. Solution is not only extensive between bedding planes but also along the N55°E joint direction. The intersection of these two fractures is seen solutionally enlarged over the watershed and specific features are discussed in detail throughout this paper. For review of the solutional enlargement along joints and bedding planes on the two forks, the reader is referred to the discussions, Potholes and Drainage Basin Analysis.

The importance of the overall greater discharge of the West Fork over the East Fork has been discussed in terms of mechanical erosion. However, chemical erosion also increases proportionally with increasing discharge. Even though the amount of $CaCO_3$ content varies inversely with stream discharge, more limestone in total amount is dissolved under higher flow conditions, despite lower concentrations of $CaCO_3$ in ppm in the water.

The aggressiveness with which a stream corrodes its bedrock depends on the amount of free CO_2 it has to dissolve it. Accelerated corrosion (Gams, 1965) occurs when two waters of different hardness meet either on the surface or underground. Bögli (1964) explains that if two waters both

saturated with $CaCO_3$ but containing different concentrations of $CaCO_3$ mix, then active CO_2 is released and therefore available for further solution of limestone. CO_2 is released because mixed waters require less total CO_2 for equilibrium than the sum of the CO_2 required for the equilibrium of individual solutions. As may be noted from the Geohydrologic Map (Appendix A) below the limit of perennial flow on each branch, there are approximately 66% more springs on the West Fork than on the East Fork. Also because on this segment of the West Fork, channel length is only half that of the East Fork, springs are much more concentrated. Therefore, the chances of more solution of bedrock by accelerated corrosion are greater on the West Fork due to more areally concentrated spring waters at various saturation levels combining with the West Fork stream water.

CHAPTER IV

PHOTOINTERPRETATIONS

I. TERMINOLOGY

Fracture traces and lineaments are natural linear features consisting of topographic, vegetational, soil tonal and bedrock alignments which are visible or remotely sensed imagery (Slusarski, 1979). In compliance with definitions proposed by Lattman (1958), the differentiating factor between a fracture trace and a lineament is one of distance. A fracture trace is a natural linear feature expressed continuously for less than one mile and a lineament is a natural linear feature expressed continuously for at least one mile.

Many investigators (Blanchet, 1957; Lattman, 1958, Kaiser, 1960) have noted the relationship between linears expressed in residuum to joints and fractures in bedrock at depth. Parizek (1967) describes a relationship between groundwater movement through solution cavities and photogeologic fracture traces in a carbonate rock terrane in Pennsylvania.

To the writer's knowledge, no previous investigations have been performed relating photogeologic linears to groundwater movement in Knox dolostone terrane.

II. PROCEDURES

All imagery was viewed monoscopically and if stereo coverage was available, stereoscopically. All contact print stereopairs were viewed with a pocket stereoscope which produces a vertical exaggeration of 2.5 ×. However, film base positive transparencies were on flight roll sheets in which the amount of separation between individual photographs warranted the use of a mirror stereoscope (no vertical exaggeration).

Plotting of fracture traces and lineaments was conducted by three methods:

1. By visual inspection from the imagery and direct transfer to a topographic base map.

2. By annotation on stable, transparent, acetate overlays with later transference to a topographic base map for selected areas.

3. By annotating directly on contact prints with a grease pencil with later transference to a topographic base map for selected areas.

III. IMAGERY ANALYZED

Table II is a list of the imagery utilized in the fracture trace and lineament analysis with information as to source, dates of acquisition, scales, etc.

TABLE II

PHOTOGRAPHIC AND NONPHOTOGRAPHIC IMAGERY UTILIZED IN THE INTERPRETATIVE PHASE OF THE FRACTURE TRACE AND LINEAMENT ANALYSIS OF WBW, CHESTNUT RIDGE, AND COPPER RIDGE

Source	Imagery Type	Format	Image Size	Date of Imagery	Normal Scale	Area of Negative Coverage
*AIR NATIONAL GUARD (OHIO)	BLACK & WHITE PANCHROMATIC	CONTACT PRINT	9 in x 9 in 22.9 cm x 22.9 cm	*LATE 60'S TO EARLY 70'S (WINTER-EARLY SPRING	RF 1:3168 1:264'	.5 sq. mi
NATIONAL AERONAUTIC AND SPACE ADMINISTRATION (NASA) EROS DATA CENTER, SIOUX FALLS, SD	COLOR IR	FILM BASE POSITIVE TRANSPARENCY	9 in x 9 in 22.9 cm x 22.9 cm	APRIL 18, 1972	1:63,714 1"=5810	82.0 sq mi 211.0 sq km
CONTINENTAL AERIAL SURVEY, INC. (CAS) ALCOA, TN	BLACK & WHITE PANCHROMATIC	CONTACT PRINT	9 in x 9 in 22.9 cm x 22.9 cm	MARCH 8, 1977	1:7920 1"=660'	10.1 sq mi 26.2 sq km
ACCU-AIR SURVEYS INC. P. O. BOX 763 FREEMAN FIELD 1220 A Ave SEYMOUR, ID 47274	COLOR	CONTACT PRINT	9 in x 9 in 22.9 cm x 22.9 cm	MARCH 29, 1978	1:7920 1"=660'	10.1 sq mi 26.2 sq km

TABLE II (continued)

Source	Imagery Type	Format	Image Size	Date of Imagery	Normal Scale	Area of Negative Coverage
TENNESSEE VALLEY AUTHORITY (T.V.A.) MAPPING SERVICES BRANCH, KNOXVILLE TN	COLOR INFRARED	CONTACT PRINT	9 in x 9 in 22.9 cm x 22.9 cm	APRIL 7, 1979	1:8000 1"=667'	10.2 sq mi 26.5 sq km
TENNESSEE VALLEY AUTHORITY (T.V.A.) MAPPING SERVICES BRANCH, KNOXVILLE TN	COLOR INFRARED	CONTACT PRINT	9 in x 9 in 22.9 cm x 22.9 cm	APRIL 7, 1979	1:3000 1"=250'	3.8 sq mi 9.8 sq km
TENNESSEE VALLEY AUTHORITY (T.V.A.) MAPPING SERVICES BRANCH, KNOXVILLE TN	MULTISPECTRAL SCANNER (NEAR INFRARED AND THERMAL INFRARED	CONTACT PRINT	9 in x 9 in 22.9 cm x 22.9 cm	APRIL 7, 1979	1:8000 1"=667'	10.2 sq mi 26.5 sq km
**	BLACK & WHITE PANCHROMATIC	CONTACT PRINT	9 in x 9 in 22.9 cm x 22.9 cm	APRIL 29, 1978	1:12,000 1"=1000'	15.3 sq mi 39.7 sq km
NATIONAL AERONAUTIC AND SPACE ADMINISTRATION (NASA) EROS DATA CENTER, SIOUX FALLS, SD	COLOR INFRARED	FILM BASE POSITIVE TRANSPARENCY	9 in x 9 in 22.9 cm x 22.9 cm	NOVEMBER 10, 1973	1:36,000 11"=3000'	7.4 sq mi 19.2 sq km

*speculative
**not available

Signature, as applied to imagery, refers to those visual characteristics of a subject which identify and separate it from other similar objects. Interpretation of the elements observed on the photographs in this project was enhanced by the many different types of imagery available which resulted in variations of the signatures between the same elements or features on contrasting photographs.

Scale of the imagery determines the resolution with which a feature can be observed. Small scale (low resolution) had the advantage in the mapping of larger fracture traces and lineaments such as straight valley and topographic alignments. Large scale (high resolution) imagery, however, was more advantageous in distinguishing soil tonal linears and short, straight stream segments.

The time of year imagery acquired is an important factor in the types and amounts of information that can be obtained. Most black and white panchromatic imagery was acquired during winter, the dormant season for decisuous plants, while Multispectral Scanner (MSS) and false color infrared was taken in early spring just as several plants were beginning to bloom. Bedrock data can be best observed on imagery acquired during winter and fall when foilage is less dense; however, the relationship between foilage and water can be best observed in spring which can be an asset when making hydrologic studies.

The amount of useful information that can be obtained from an area is also dependent on those energy wavelengths which are being recorded. The contrasting light and dark tones (gray scale values) of black and white panchromatic imagery proved invaluable in detecting soil tonal linears across the watershed.

Although WBW was not included in the color set of photographs, they were helpful in the delineation of fracture traces in other areas of Chestnut Ridge and Copper Ridge.

Nonphotographic imagery including Color Infrared and Multispectral Scanner data are available for WBW and parts of Chestnut Ridge and Copper Ridge. This imagery, particularly the thermal (8.00 to 14.00μ) infrared which detects relative temperature differences, was most useful in the detection of flowing water in stream channels, thereby enhancing the straight stream segment analysis.

CHAPTER V

ANALYSES OF OBSERVED ORIENTED FEATURES

I. FIELD MEASURED JOINT ORIENTATIONS

Two hundred and ten joint and bedrock fracture orientations were recorded from outcrops within the watershed and along Walker Branch below the confluence of the East and West Forks. The location and most prevalent bedrock fracture orientations of each individual data acquisition site are shown in Appendix B.

Figure 30 is a directional histogram based upon 210 observations of bedrock fracture orientations compiled for the whole watershed. The bedrock fracture principal maxima are N20°-25°W and N30°-35°W. Secondary maxima occur at

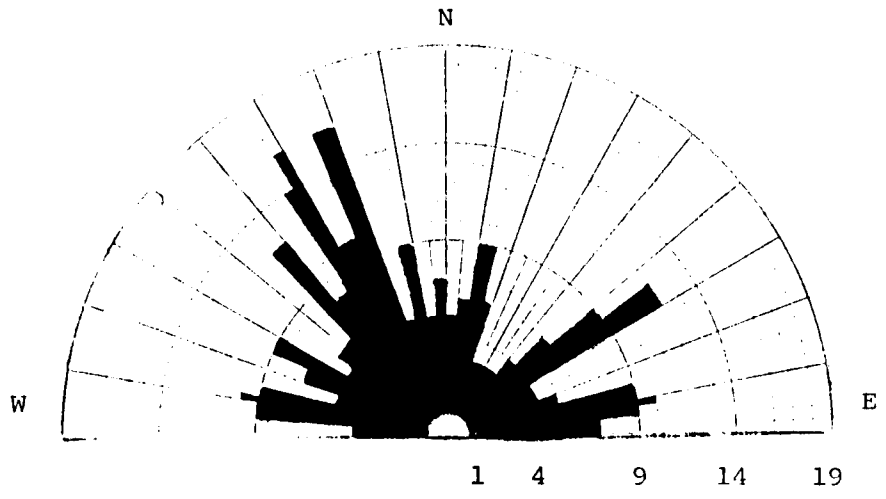


Figure 30. Histogram of bedrock fracture orientations based upon 210 observations within Walker Branch Watershed.

N55°-60°E, N40°-45°W, and N25°-30°W, and tertiary maxima occur at N10°-15°E, N50°-55°E, N75°-85°E, N10°-15°W, N60°-65°W and N75°-85°W.

II. ORIENTATIONS DERIVED FROM IMAGERY

The purpose of this phase of the research is:

1. To determine the extent and directions fracture zones (as determined from fracture traces) have on groundwater movement in the Knox dolostone of WBW, and

2. Compare and contrast results of fracture trace analyses performed on surrounding areas underlain by the Knox with those observed for WBW.

For the conterminous watershed, three analyses were conducted with delineations based on the nature of the fracture trace. These analyses were: (1) topographic alignments, (2) straight stream segments, and (3) soil tonal and tree alignments (Appendix C, Figures C.4, C.3, and C.1, respectively). This was done to establish any relationship between the particular feature(s) producing the fracture trace with corresponding preferred orientations from the joint analysis of the watershed.

Fracture trace and lineament studies were also conducted for those areas of Chestnut Ridge and Copper Ridge encompassed in Tennessee Valley Authority's Elverton, Bethel Valley, and Lovell 7-1/2' topographic quadrangle maps. These ridges

were selected as study areas because of their proximity to WBW and the large amount of imagery covering the areas and available for analysis. Three areas were delineated on the basis of apparent paired groups and greater density of fracture traces observed on imagery covering the areas described above. Appendix D (Figures D.1 and D.2) and Appendix E (Figures E.1, E.2, and E.3) show the location of the areas selected for study, along with plotted fracture traces and histograms showing main orientations.

III. GEOHYDROLOGIC FEATURE ALIGNMENT AND SINKHOLE MORPHOMETRY ANALYSES

Two different analyses were performed using:

1. Azimuths aligning concentrations of important geohydrologic features within WBW, and

2. Orientations of elongations and alignments of sinkholes, to establish preferred directions of groundwater movement in Knox dolostone terrane.

Alignment of Geohydrologic Features

Purpose and procedure. This study was initiated to test a hypothesis that if alignments of geohydrologic features can be established for an area, the positioning and development of those individual features may be the result of concentrated groundwater movement along possible fracture zones.

The procedural steps used in conducting this analysis follows:

1. Geohydrologic features were mapped in the field and plotted on a topographic base map of the Walker Branch Watershed (Appendix F, Figure F.1).

2. Concentration of geohydrologic features (group of springs, adjacent sinkholes) were delineated as a data group. This data group implies one or a combination of factors such as groundwater, structure, stratigraphy, geomorphology, etc., is exerting the same control over the formation and positioning of every feature within that data group.

3. If by visual inspection of the map, these units appeared aligned in an elongated direction, a best-fit ellipse was drawn around them.

4. The ellipse was symmetrically bisected by a line along its elongated axis on which a bearing was recorded.

5. Data groups with no elongation were encircled to designate the area.

6. The bearings of lines intersecting several designated data groups and important isolated features across the watershed were recorded to hypothesize preferred groundwater movement directions.

Sinkhole (Doline) Elongation and Alignment Analysis

Purpose and procedure. The purpose of this investigation was to compare results with the more valid aerial fracture trace and joint orientation analysis and to determine its applicability in hypothesizing groundwater movement directions in Knox dolostone terrane.

Walker Branch Watershed (Appendix C, Figure C.2, and Appendix F, Figures F.1, F.2, and F.3) and a small area of Copper Ridge located east of Whiteoak Lake (Appendix D, Figure D.2) were selected as the study areas on the basis of greater sinkhole (doline) density. The procedures used in this analysis were the same for both areas. For each area, all elongated sinkholes were symmetrically divided (in map view) by visual inspection from the topographic maps. Those sinkholes with two elongation directions were bisected by two lines along two greatest axes. Subtle irregularities in outline of sinks were ignored. The azimuth of each bisecting line was then recorded.

Proximity of the sinkholes to each other was the control factor in the alignment analysis. Where two or more sinkholes were adjacent to each other, an imaginary ellipsoid was drawn or envisioned around the group. The ellipsoid shape was then symmetrically divided by a line on which an orientation to North was recorded. No sinkholes

separated by more than 125 meters were determined to be aligned in this analysis. Most of the aligned sinkholes were separated by less than 80 meters.

IV. COMPARISON OF ORIENTATION ANALYSES

Procedure

Data in all directional histograms were divided into three maxima on the basis of relative lengths of the projections for each five degree interval. The projection length is determined by the number of observations in each five degree interval. Principal maxima contained the most observations and secondary maxima contained some lesser amount, in between principal and tertiary maxima. Tertiary maxima were not recorded in the absence of intermediate projection lengths between background scatter (very few number of observations) and secondary maxima.

Figure 31 shows the principal, secondary, and tertiary maxima for:

1. Joint orientation, fracture trace, alignment of geohydrologic features and sinkhole alignment and elongation analyses for WBW.

2. Fracture trace analysis for areas two and three in Chestnut Ridge and total Chestnut Ridge.

3. Fracture trace and sinkhole alignment and elongation analyses for Area 1 in Copper Ridge and total fracture trace analysis for Copper Ridge.

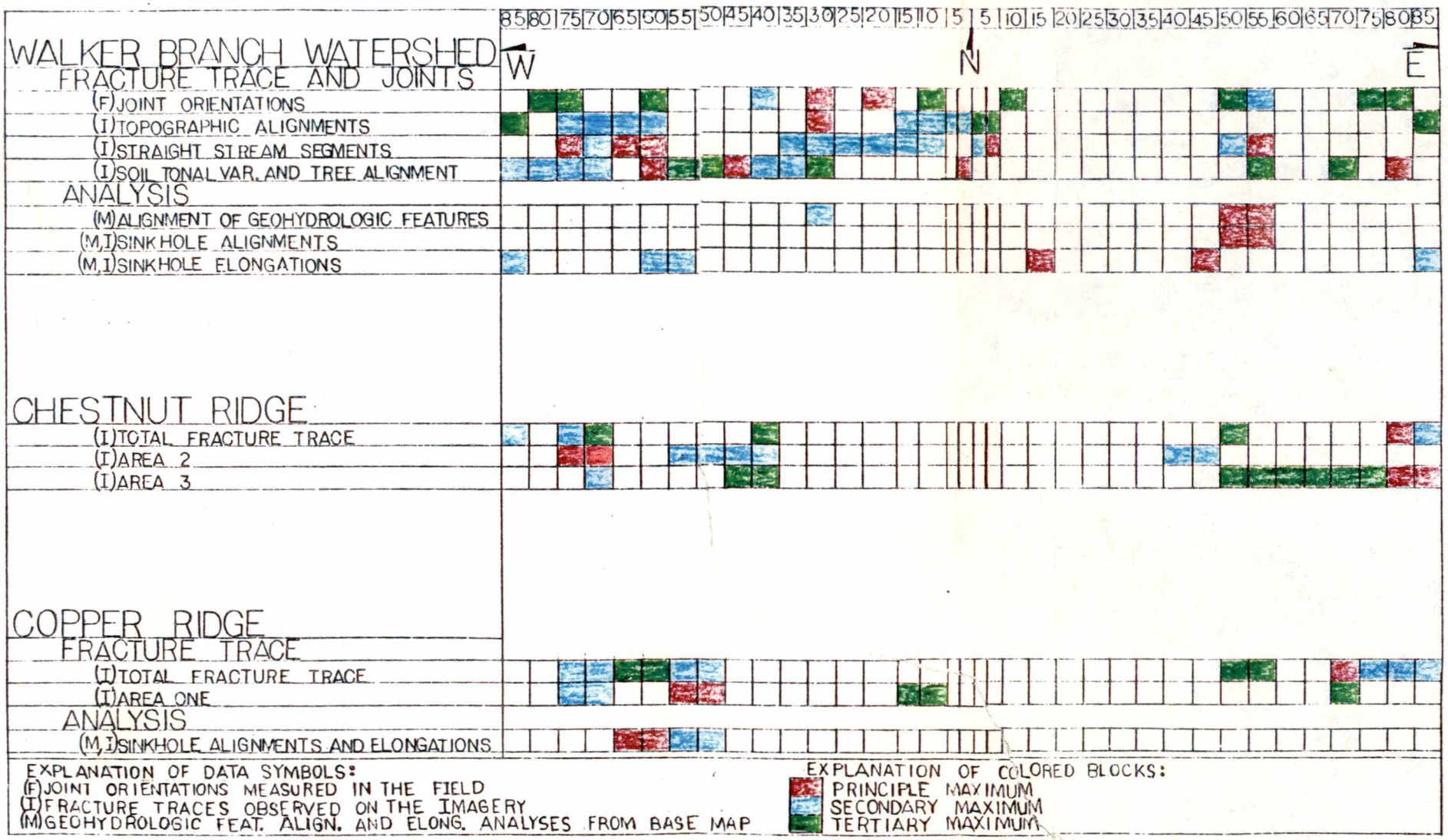


Figure 31. Joint, fracture trace, and alignment of geohydrologic features for WBW, Chestnut Ridge, and Copper Ridge (based on 799 observations).

All the data for the tabulation were taken from directional histograms prepared for each analysis (Figure 30, and Figures C.1, C.3, C.4, D.1, D.2, E.1, E.2, E.3, F.2, F.3, and F.4 in the Appendices).

Figures 32 and 33 are histograms showing the principal, secondary, and tertiary bedrock fracture, fracture trace, and alignment of geohydrologic features maxima for WBW and WBW, Chestnut Ridge, and Copper Ridge (General Knox Terrane), respectively. They were derived from combined orientation analyses data in Figure 31. The procedure used in the construction of these two histograms follows:

1. For Figure 31, each maximum orientation (red) was arbitrarily assigned three quality (level of importance) points, each secondary maximum (blue) was assigned two quality points and each tertiary maximum (green) was assigned one quality point.

2. The total quality points under each five degree interval from Due West clockwise to Due East was calculated for (1) Walker Branch Watershed and (2) General Knox Terrane.

3. For WBW, a range of 1 to 12 quality points was observed. Divided into three intervals of four (1-4, 5-8, 9-12), each range was assigned as a tertiary, secondary, or principal maximum with respect to increasing range intervals.

4. The same procedure was used for the General Knox Terrane analysis except the range was one to seventeen

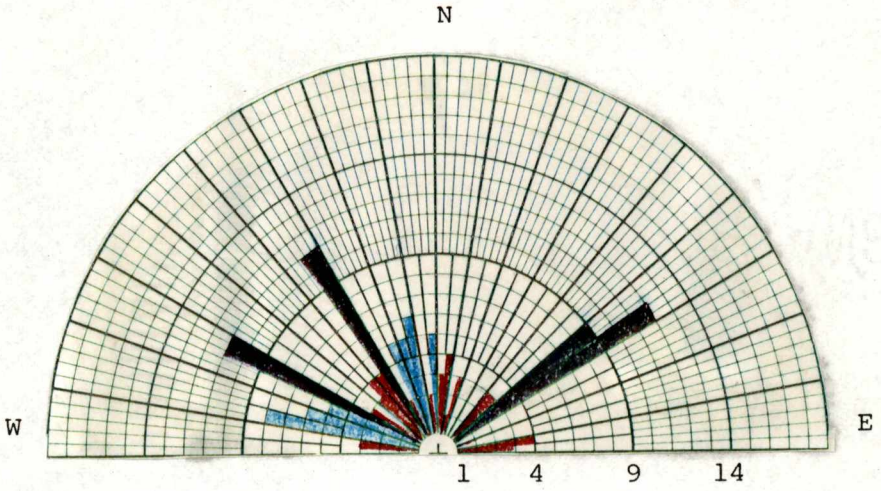


Figure 32. Preferred groundwater movement histogram for WBW derived from analyses in Figure 31 and based on 124 quality points. Scale: 1-4, each half square equals one quality point; 5-9, each square equals one quality point; 9-14, every two and one-half squares equal one quality point.

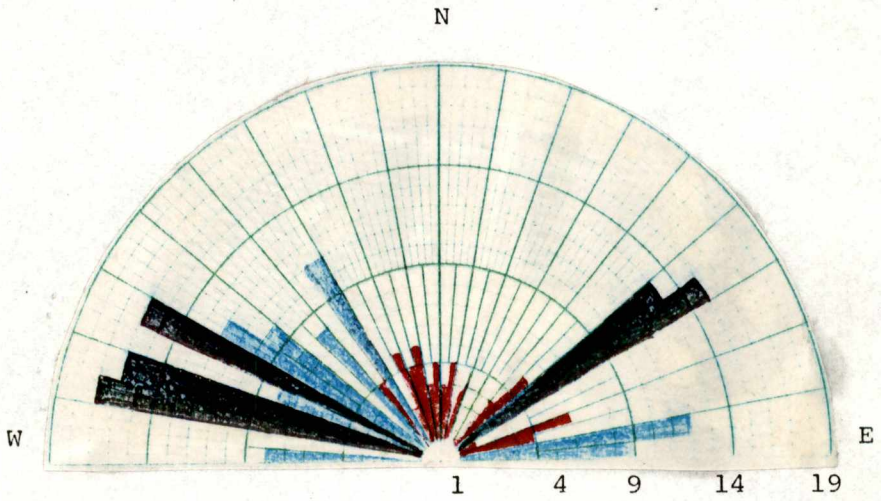


Figure 33. Preferred groundwater movement histogram for General Knox Terrane derived from analyses in Figure 31 and based on 220 quality points. Same scale as Figure 32.

quality points and the maximum orientation was assigned to a range having five quality points as opposed to six each for the other maximums.

5. In the preparation of the histograms, all principal maximum orientations were designated by black, secondary maxima by a blue color, and tertiary maxima by a red color. The length of each projection was determined by the number of quality points for each five degree interval.

The structural, stratigraphic, and geomorphologic data presented in Figure 31 are interpreted to be related to the groundwater movement in Knox dolostone terrane. Therefore, the histogram projections can also be referred to as preferred groundwater movement maxima.

To the writer's knowledge, this method for hypothesizing groundwater movement for an area has not been used elsewhere. Therefore, no previous statistics exist on the validity of such an analysis; however, detailed groundwater tracing experiments at WBW would help to prove or disprove its merit at least in Knox dolostone terrane.

A statistical analysis (Appendix G) was conducted to quantitatively determine the degree of anisotropy represented by the data in each histogram and to determine if there is justification for dividing the orientations into three maxima on the basis of relative projection lengths.

General Results

An overall pattern is developed in Figure 31 in which data for the WBW analysis is concentrated in the northwest quadrant and data for the Chestnut Ridge and Copper Ridge areas is concentrated in the N40°-80°W and N40°E to due East ranges.

The histogram of preferred groundwater movement at WBW shows principal maxima at N50°-60°E, N30°-35°W, and N60°-65°W. Secondary and tertiary maxima occur at Due N-N5°W, N10°-25°W, and N65°-80°W and at Due N-N10°E, N80°-90°E, N35°-50°W, N55°-60°W, N80°-85°W, and N40°-50°E, respectively.

The histogram of preferred groundwater movement for General Knox Terrane shows principal maxima at N50°-60°E, N60°-65°W, and N70°-80°W. Secondary and tertiary maxima occur at N30°-35°W, N40°-45°W, N50°-60°W, N65°-70°W, N85°-90°W, and N80°-90°E and at N25°W-N20°E, N35°-40°W, N40°-50°E and N70°-80°E, respectively.

It should also be noted that the principal orientation maxima are of prime importance since they reflect the most developed fracture zones (fractures are more abundant, solutionally enlarged, and vertically and laterally continuous) as well as stratigraphic control and hence greater volume of groundwater flow. This decrease in importance as one compares principal to secondary maxima and secondary to tertiary maxima is apparent in the Percentage Analysis of Appendix G.

Comparison of WBW Analysis with General Knox Terrane Analysis

The patterns between the two histograms coincide with three exceptions:

1. The N10°E-N35°W orientation maxima present in WBW but almost completely absent in the General Knox Terrane.

2. Changes in maxima degree along particular orientations between the two histograms (example: N35°W principal maximum of WBW is secondary maximum on General Knox Terrane), and

3. The secondary maxima N50°-60°W and tertiary maxima N70°-80°E of the General Knox Terrane not present on the WBW histogram.

Examples of the second exception are:

1. Principle maximum N30°-35°W and secondary maxima Due N-N5°W and N10°-25°W on the WBW histogram are lowered to secondary and tertiary maxima respectively on the General Knox Terrane.

2. Secondary maximum N70°-80°W and tertiary maximum approximately due East-West on WBW histogram are increased to principal and secondary maxima on General Knox Terrane.

However, these exceptions may be accounted for. By adding the Chestnut Ridge and Copper Ridge data to the WBW data in the total histogram, groundwater movements for Knox dolostone in general were highlighted over those for the watershed area specifically.

The conclusion that can be drawn from these results is that individual fracture zones and weaker stratigraphic intervals in various localities of Knox terrane are situated along essentially the same orientations but differ in the intensity of their respective development between areas.

Applicability of Alignment of Geohydrologic Features and Sinkhole Morphometry Analyses to the Prediction of Groundwater Movement in Knox Dolostone Terrane

The N50°-60°E direction is the principal maximum, and N30°-35°W is the secondary maximum in the Alignment of Geohydrologic Features analysis. These orientations are two of the three principal maxima observed on the preferred groundwater movement histogram for WBW. Also the N50°-60°E is a principal maximum and the N35°W is a secondary maximum on the groundwater histogram for the General Knox Terrane. The conclusion here is that this analysis is a valid method in predicting groundwater movement at WBW and may be for the Knox dolostone terrane in general.

The Sinkhole Morphometry analysis of WBW showed that for this area the orientation of sinkhole alignments (N50°-60°E) were in close agreement with major fracture trace and joint orientations but the sinkhole elongations were not. However, the same analysis conducted for an area on Copper Ridge (Appendix D, Figure D.2, and Figure 31, page 108) revealed similar bearings for the sinkhole alignments and

elongations and main fracture trace orientations in that area. There does appear to be structural control in sinkhole development at WBW if only the most concentrated area of sinkholes there is considered. This area is located directly northwest of Rain Gage One (Appendix F, Figure F.1, SHA6, and SHA7). Here the sinkholes are aligned in a N40°E and N69°W direction and elongated along preferred directions of N60°W, N43°-45°E, and N80°-90°W (Appendix F, Figure F.1, Sinkholes K, J, I, N, M). The sinkhole alignment N40°E which is parallel to the elongations of N43°-45°E may be accounted for if an approximate N45°E oriented fracture zone exists in this area. The N69°W sinkhole alignment which lies within the N60°W to N80°-Due E-W range of elongated sinkholes, is probably the result of sinkholes developing along the intersection of two possible fracture zones oriented in the latter directions.

From these analyses, it may be concluded that the validity of a sinkhole morphometry analysis in predicting structural control and therefore groundwater movement increases proportionally with the concentration, elongation, and alignment of the sinkholes.

Significance of the Geohydrologic Fracture Trace and Feature Alignment Analyses

Both types of analyses were found to be valid methods of predicting preferred groundwater movement directions in Knox dolostone terrane.

Fracture traces are phenomena that can be directly observed on aerial imagery. Also many of the features or combination of features forming the fracture trace may be directly observed in the field.

However, analyses such as the Sinkhole Morphometry and Alignment of Geohydrologic Features are based on a hypothetical consideration that the aligned forms and positioning of geohydrologic features are dependent on the orientations and areas of preferred groundwater movement.

By combining the direct observations of bedrock fractures, fracture trace, and geohydrologic features in the field with the more indirect method of the Sinkhole Morphometry and Alignment of Geohydrologic Features analyses, a stronger prediction of preferred directions of groundwater movement for the Knox dolostone terrane could be obtained than by direct observation methods alone.

CHAPTER VI

EVALUATION OF THE KNOX DOLOSTONE TERRANE FOR WASTE STORAGE/DISPOSAL

I. KNOX GROUP IN GENERAL

The Knox Group, because of the features and processes which result from the relatively higher solubility of carbonate rocks over that of other rock types, would not be ordinarily considered favorable for storage/disposal of waste materials that may contain quantities of potential contaminants. This study substantiates this consideration, although the upper Mascot Dolomite does possess some favorable characteristics for waste storage/disposal (discussed later in this section). Listed below are some features and characteristics of the Knox Group observed and measured in WBW which might present a precarious situation if wastes were stored or buried there or in similar Knox terranes.

1. Sinkholes, especially concentrated areas of sinkholes and alluvial dolines.

2. Variations in conduit and cavern development (hence, groundwater movement) with respect to space and time.

3. Areas of vast groundwater discharge such as saturated zone and seeps, concentration of springs, etc.

4. Mass movement features: Rockslides, rockfall, creep, slump, etc.

5. Gully erosion and headward sapping at spring outlets.

6. Formation of midslope springs by possible clogging of karst channels by fine clays and silts.

A favorable factor in the consideration of the utility of the Knox Group for waste/disposal is the high average depth to the top of the maximum groundwater table as measured from the summit of Knox ridges. An important criterion for the safe disposal of any wastes is to isolate the wastes as completely as possible from water, since water is the main transporting medium of contaminates to the biosphere.

In two observation wells located on the ridgetops in the West Fork Subbasin of WBW, a depth of 30 meters was drilled before reaching the groundwater table. Two observation wells do not provide sufficient data to extrapolate this depth measurement for the entire watershed; however, it does demonstrate along with the midslope seeps that the watertable in that Knox terrane does not conform to topography as might be anticipated in most areas having a temperate climate. Ordinarily, a much higher groundwater table at the center of the ridge crest would be expected.

II. POTENTIAL OF THE UPPER MASCOT DOLOMITE FORMATION OF THE KNOX GROUP AS A REPOSITORY FOR WASTES

The Upper Mascot Formation appears to possess many of the ideal conditions needed for the safe disposal of potentially hazardous wastes. At WBW, characteristics of these strata and terrain formed from it are:

1. No observed sinkholes.

2. Creep is relatively minor and no evidence of rockslides, slump, etc., were observed.

3. Although residuum is relatively thin as opposed to the other Knox formations (except the Kingsport Fm.) no bedrock pinnacles were observed on the Upper Mascot ridgetops.

4. Comparatively less fractured outcrops with only minor solutional enlargement of joints.

5. No major groundwater discharge outlets.

6. No midslope seeps or springs giving evidence for the presence of clay aquicludes.

7. No major gully erosion development.

These characteristics imply that the terrain here seems to be more stable with respect to slope processes and vertical subsidence. Also due to the comparatively less densely fractured and solutionally enlarged outcrops along with minor fracture trace development, it appears that

relatively less groundwater movement is occurring through these strata.

However, before any valid determination for the disposal of waste in this area can be made, observation drillholes and seismic surveys need to be completed to determine configuration of the soil-bedrock interface, depth to groundwater table, etc. Also groundwater movement directions and velocities must be determined by tracer experiments.

CHAPTER VII

CONCLUSIONS

Data collected during this investigation indicate that structure and stratigraphy have a pronounced effect on geomorphology and on directions of preferred groundwater movement in Knox dolomite terrane.

Comparison of the bedrock fracture, fracture trace, alignment of geohydrologic features and sinkhole morphometry analyses performed on terrain underlain by the Knox Group in WBW and surrounding areas revealed a close parallelism between hypothesized preferred direction of groundwater movement maxima. However, although orientations remained essentially constant, the relative importance of each orientation in individual areas varied between localities.

In the evaluation of Knox dolomite terrane for storage/disposal of potentially hazardous waste, the terrain associated with all formations of the Knox Group with the possible exception of the Upper Mascot Formation were determined unsafe for storage/disposal of wastes. Favorable conditions for waste storage/disposal may exist in the terrain underlain by Upper Mascot Dolomite, but these characteristics should be verified by coring and well log data, tracer studies, and possibly seismic surveys.

Thus, in an area such as WBW where drillhole and tracer data are limited, structural and geomorphological analyses can be used to determine preferred directions of groundwater movement.

BIBLIOGRAPHY

BIBLIOGRAPHY

Allum, J. A. E., 1966, Photogeology and Regional Mapping: Pergamon Press, New York, 107 pp.

_____, 1968, Manual of Color Aerial Photography (First ed.): American Society of Photogrammetry, Falls Church, Va.

_____, 1975, Manual of Remote Sensing--Volume II, Interpretation and Applications (First ed.): American Society of Photogrammetry, Falls Church, Va.

Avery, T. E., 1962, Interpretation of Aerial Photographs: Burgess Publishing Company, Minneapolis, 192 pp.

Blanchet, P. D., 1957, Development of Fracture Analysis as Exploration Method: Bull. AAPG, V. 41, No. 8, pp. 1748-1759.

Bögli, A., 1964, Corrosion par melange des eaux: Internat. J. of Speleo. 1 (1-2), pp. 61-70.

Bonner, 1968, A Table Comparing Chemical Constituents of Springs S1E and S3W; In Some Relationships between Constituents and Stream Flow Rates of the East and West Forks of the Walker Branch Watershed, Oak Ridge National Laboratory, Oak Ridge, Tennessee.

Bridge, J. and Rogers, J., 1956, Stratigraphy of Mascot Formation: U.S.G.S. Professional Paper, Number 277, 76 pp.

Brown, R. H., Konoplyantsex, A. A., Kneson, J., and Kovalevsky, V. S., 1975, Groundwater Studies: Unesco, Paris.

Butts, Charles, 1926, The Paleozoic Rocks, in Geology of Alabama: Alabama Geol. Survey Spec. Rept. 14, 312 pp.

Carson, M. A., and Kirkby, M., 1972, Hillslope Form and Process: Cambridge Univ. Press, London.

Cramer, H., 1941, Die Systematik der Karstdolinen: Nenes Jb. Miner. Geol. Paläont, v. 85, pp. 293-382.

Cummings, David, 1960, The Basal Chepultepec Sandstone (Cambrian-Ordovician Boundary) in the Ridge and Valley Province of East Tennessee, in Marble Deposits of East Tennessee: Tenn. Div. Geology Bull. 28, pp. 87-162.

Curlin, J. W. and Nelson, D. J., 1968, Walker Branch Watershed Project: Objectives, Facilities and Ecological Characteristics. ORNL/TM-2271, Oak Ridge National Laboratory, Oak Ridge, Tennessee.

Davies, W. E., 1949, Features of Cave Breakdown: Bull. Natn. Speleol. Soc., v. 11, pp. 34-35.

Davies, W. E., 1960, Origin of Caves in Folded Limestone: Bull. Natn. Speleol. Soc., v. 22, pp. 5-18.

Davis, Stanley N., and DeWiest, Roger J. M., 1966, Hydrogeology: John Wiley and Sons, Inc., New York.

Douglas, Ian, 1977, Humid Landforms: MIT Press; Cambridge, Massachusetts, 238 pp.

Elwood, J. W. and Henderson, G. S., 1973, Hydrologic and Chemical Budgets at Oak Ridge, Tennessee. IN: A. D. Hasler (ed.), Coupling at Land and Water Systems, pp. 31-51. Springer-Verlag Ecological Study Series, Springer-Verlag, New York.

Ford, D. C., 1965, Stream Potholes as Indicators of Erosion Phases in Limestone Caves: Bull. Natn. Speleol. Soc. v. 27, pp. 27-32.

Ford, T. D. and Cullingford, C. H. D., 1976, The Science of Speleology: Academic Press, London, 574 pp.

Gams, I., 1965, Types of Accelerated Karst Corrosion: Problems of the Speleological Research, edited by O. Stelcl, pp. 133-39. Prague.

Gilbert, G. K., 1914, The Transportation of Debris by Running Water: U.S. Geol. Surv. Prof. Paper 86.

Gregory, K. J., and Walling, D. E., 1974, Fluvial Processes in Instrumented Watersheds: Institute of British Geographers, London, 194 pp.

Hall, G. M. and H. C. Amick, 1934, The Section on the West Side of Clinch Mountain, Tennessee. Tennessee Academy of Science, vol. 9, pp. 157-220.

Haney, Donald, 1966, Structural Geology along a Segment of the Saltville Fault, Hawkins County, Tennessee, unpublished dissertation.

Harris, Leonard D., 1969, Kingsport Fm. and Mascot Dolomite (Lower Ordovician) of East Tennessee in Papers on the Stratigraphy and Mine Geology of the Kingsport and Mascot Fms. (Lower Ordovician of East Tennessee) Tennessee Division of Geology.

Henderson, G. S., D. D. Huff and T. Grizzard, 1977, Hydrologic Characteristics of Walker Branch Watershed. IN: Correll, D. L. (ed.), Watershed Research in Eastern North America, Proc. Workshop, Smithsonian Institution, Edgewater, Md., pp. 307-320.

Herak, M., and Stringfield, V. T., 1972, Karst. Important Karst Regions of the Northern Hemisphere: Elsevier Publishing Co., Amsterdam.

Hobbs, W. H., 1911, Repeating Patterns in the Relief and in the Structure of the Land: Geol. Soc. of Amer. Bull., v. 22, pp. 123-176.

Holz, R. K. (editor), 1973, The Surveillant Science—Remote Sensing of the Environment: Houghton Mifflin Company, Boston, 309 pp.

Jacobson, Roger L. and Langmuir, Donald, 1970, The Chemical History of Some Spring Waters in Carbonate Rocks. IN: Ground Water, Volume 8, No. 3.

Jakus, L., 1977, Morphogenetics of Karst Regions, Budapest, Hungary.

Jennings, J. N., 1971, Karst: M.I.T. Press, Cambridge, Mass.

Kaiser, E. P., 1960, Structural Significance of Lineaments (abs.), Geol. Soc. of America.

Lattman, L. H., 1958, Technique of Mapping Geologic Fracture Traces and Lineaments on Aerial Photographs: Photogram. Eng., v. 24, No. 4, pp. 568-576.

Lattman, L. H., and Ray, R. G., 1965, Aerial Photographs in Field Geology: Holt, Rinehart, and Winston, New York, 221 pp.

LaValle, P., 1967, Some Aspects of Linear Karst Depression Development in South Central Kentucky: Ann. Assoc. Am. Geog., Vol. 57, pp. 49-71.

Legrand, Harry E., and Stringfield, V. T., 1971, Water Levels in Carbonate Rock Terranes. IN: Ground Water, Vol. 9 No. 3.

Legrand, Harry E., Stringfield, V. T., and LaMoreaux, P. E., 1976, Hydrologic Features of United States Karst Regions; in Karst Hydrology and Water Resources, edited by Yevjevich, Vujica. Vol. I.

Malott, C. A., 1939, Karst Valleys: Geol. Soc. America Bull. v. 50, p. 1984.

Mandell, S., 1965, A Conceptual Model of Karstic Erosion by Groundwater, in Hydrology of Fractured Rocks, v. 2, Unesco, Paris.

McMaster, William M., 1967, Geologic Map of Oak Ridge Reservation: TEI-783, Oak Ridge National Laboratory, Oak Ridge, Tennessee.

McMaster, William M., 1971, Geology and Hydrology of Walker Branch Watershed (in a letter to James W. Curlin), Oak Ridge National Laboratory, Oak Ridge, Tennessee.

Meyer, Stuart L., 1975, Data Analysis for Scientists and Engineers: John Wiley and Sons, Inc., New York, New York.

Milici, Robert C., 1973, The Stratigraphy of Knox County, Tennessee in Geology of Knox County, Tennessee: Tennessee Div. of Geology, Bulletin 70.

Miller, V. C., and Miller, C. F., 1961, Photogeology: McGraw-Hill, New York, 248 pp.

Morisawa, Marie, 1968, Streams, Their Dynamics and Morphology: McGraw-Hill Book Company, New York, 165 pp.

Oak Ridge Operations, 1975, Oak Ridge Reservation Land Use Plant: Technical Information Center, Oak Ridge, Tennessee, ORO-748.

Oak Ridge National Laboratory, 1975, Technical Progress Report on WBW: Environmental Sciences Division.

Oder, C. R. L., 1934, Preliminary Subdivision of the Knox Dolomite in East Tennessee: Jour. Geology, v. 42, pp. 469-497.

Palmer, N., 1974, Dynamics of a Sinking Stream System: Onesquethaw Cave. Albany County, New York, The Bulletin of the National Speleological Society, Volume 34, Number I.

Parizek, Richard R., 1976, On the Nature and Significance of Fracture Traces and Lineaments in Carbonate and Other Terranes: Karst Hydrology and Water Resources; Volume I: Karst Hydrology: LithoCrafters, Ann Arbor, Michigan, pp. 47-97.

Pinchemel, P., 1954, Les Plaines de Craie du Nord-ouest du Bassin Parisien et du Sud-est du Bassin de Londres et leurs Bordures, Paris.

Ritter, Dale F., 1978, Process Geomorphology: Wm. C. Brown Company Publishers, Dubuque, Iowa.

Safford, J. M., 1869, Geology of Tennessee, State of Tennessee, Nashville, p. 550.

Smith, James William, 1968, The Saltville Fault Near Mooresburg, Tennessee, an unpublished dissertation.

Shuster, E. T., and White, W. B., 1971, Seasonal Fluctuations in the Chemistry of Limestone Springs: A Possible Means for Characterizing Carbonate Aquifers. J. Hydrol. Vol. 14, pp. 93-128.

Sheppard, J. D., 1971, Some Relationship between Constituents and Stream Flow Rates of the East and West Forks of the Walker Branch Watershed, Intra-Laboratory Correspondence to G. S. Henderson, Oak Ridge National Laboratory, Oak Ridge, Tennessee.

Sheppard, J. D., 1971, Some Preliminary Observations of Chemical Discharge from Walker Branch Watershed, Intra-Laboratory Correspondence to G. S. Henderson, Oak Ridge National Laboratory, Oak Ridge, Tennessee.

Sheppard, J. D., 1972, High Stream Flow Rates on Walker Branch Watershed, Intra-Laboratory Correspondence to D. J. Nelson, Oak Ridge National Laboratory, Oak Ridge, Tennessee.

Slusarski, Mark L., 1979, Photogeologic Fracture Traces and Lineaments in the Wartburg Basin Section of the Cumberland Plateau Physiographic Subprovince, Tennessee; Thesis, University of Tennessee, Knoxville.

Spiller, Reginal W., 1979, Univariate and Multivariate Analysis of Water Well Yields as Related to Fracture Traces and Lineaments in the Martinsburg Shale in Eastern Pennsylvania: Thesis, Pennsylvania State University.

Stringfield, V. T., and LeGrand, H. E., 1969, Hydrology of Carbonate Rock Terranes—A Review: Jnl. Hydrol., v. 8, pp. 349-413.

Sweeting, Marjorie M., 1973, Karst Landforms: Columbia University Press, New York, 331 pp.

Taylor, Larry E., 1980, Fracture Traces and Water Wells, A Review.

Thrailkill, J., 1968, Chemical and Hydrologic Factors in the Excavation of Limestone Caves: Geol. Soc. America Bull., v. 79, pp. 19-45.

Ulrich, E. O., 1911, Revision of the Paleozoic Systems: Geol. Soc. America Bull., v. 22, pp. 281-680.

Vistelius, Andrew B., 1966, Structural Diagrams: Pergamon Press Ltd., London, England.

White, William B., 1969, Conceptual Models for Carbonate Aquifers. IN: Groundwater, Volume 7, No. 3.

Williams, P. W., and Jennings, J. N., 1969, Contributions to the Study of Karst: Australian Nat. Univ. Canberra.

APPENDICES

APPENDIX A

GEOHYDROLOGIC MAP OF WALKER BRANCH WATERSHED

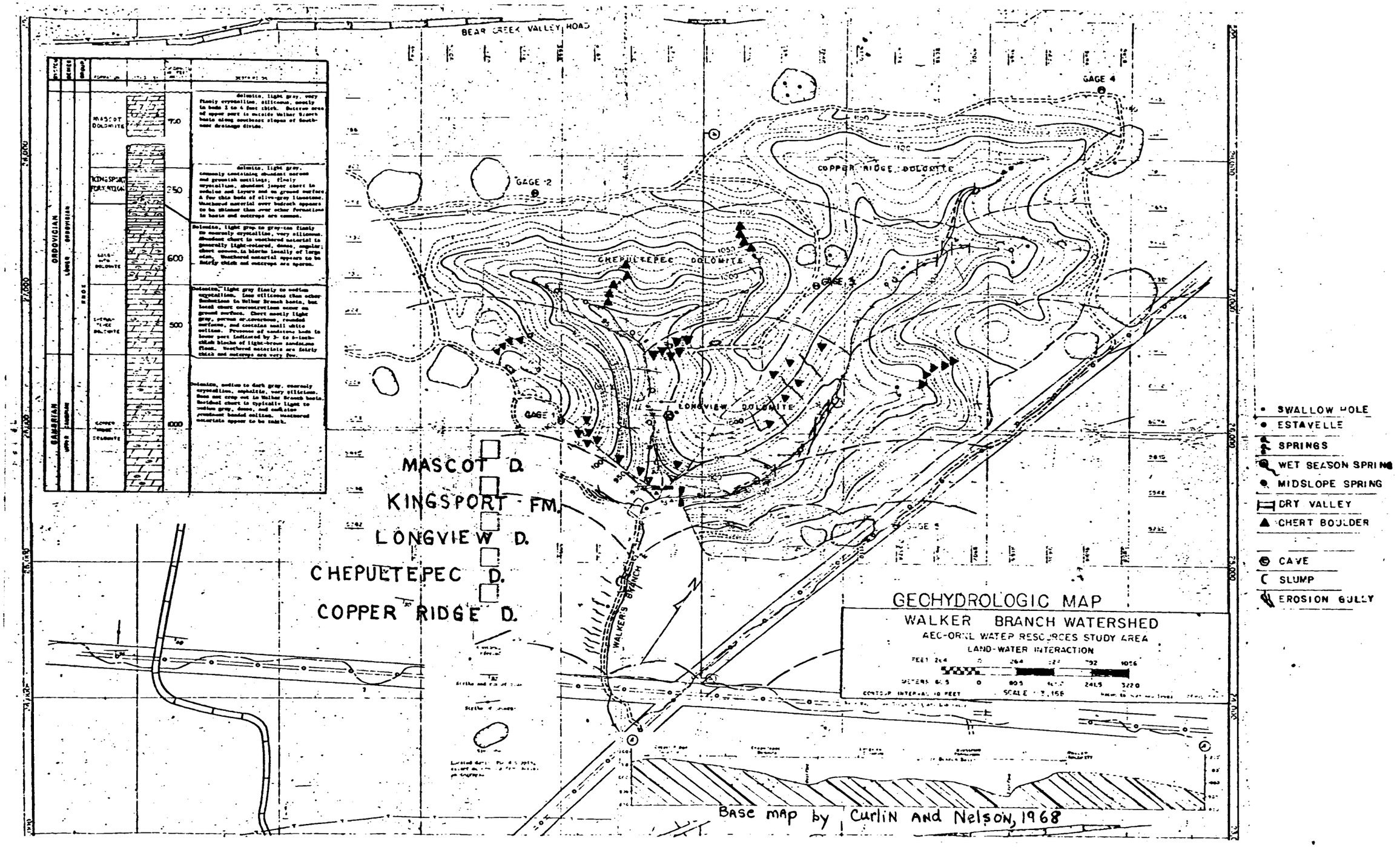


Figure A.1. Geohydrologic map of Walker Branch Watershed.

APPENDIX B

GEOHYDROLOGIC FEATURE LOCATION AND JOINT ACQUISITION SITE MAP

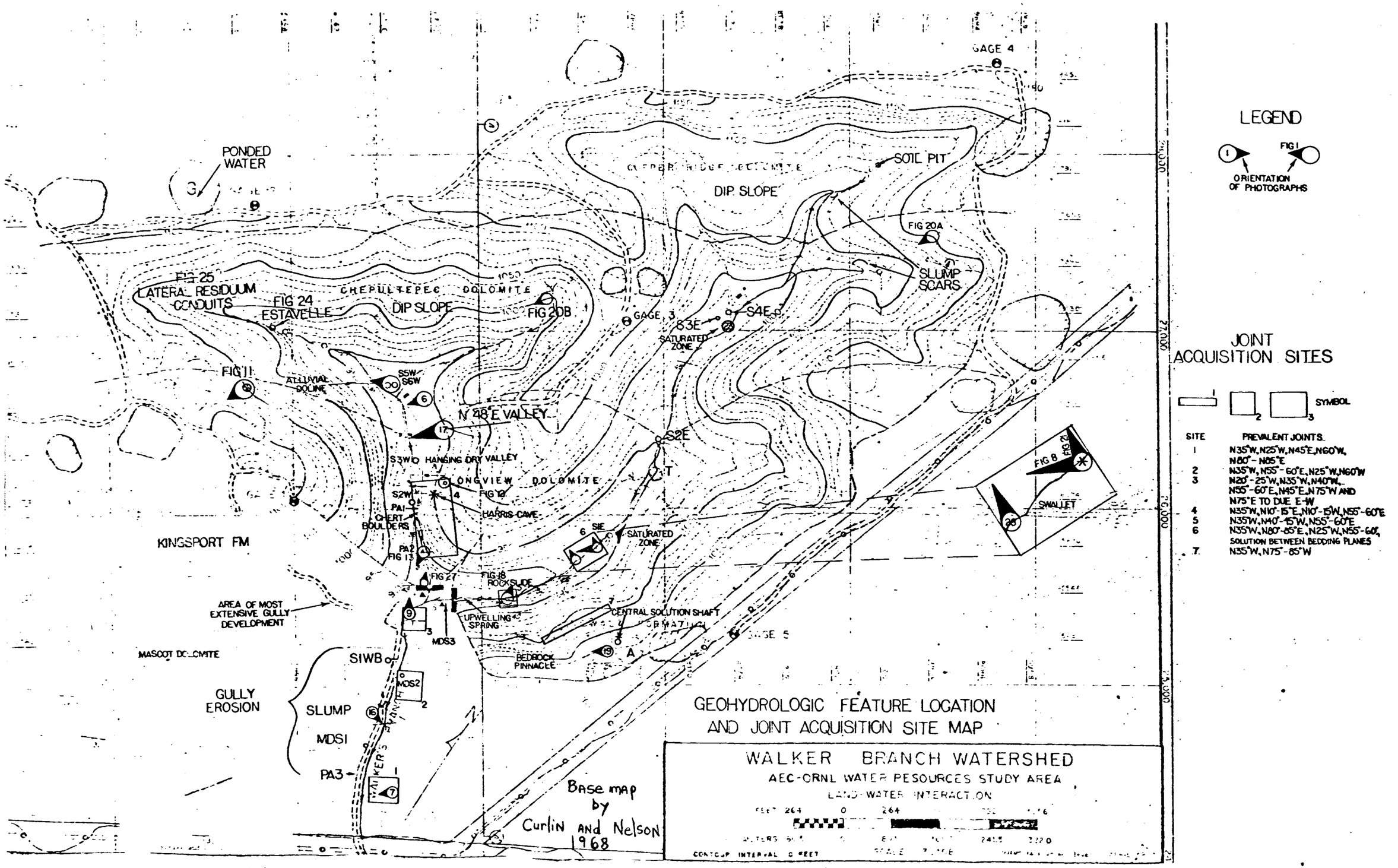


Figure B.1. Geohydrologic feature location and joint acquisition site map.

APPENDIX C

MAP AND HISTOGRAMS OF PHOTOGEOHYDROLOGIC LINEAR FEATURE ORIENTATIONS AND SINKHOLE ELONGATION OBSERVED IN WALKER BRANCH WATERSHED

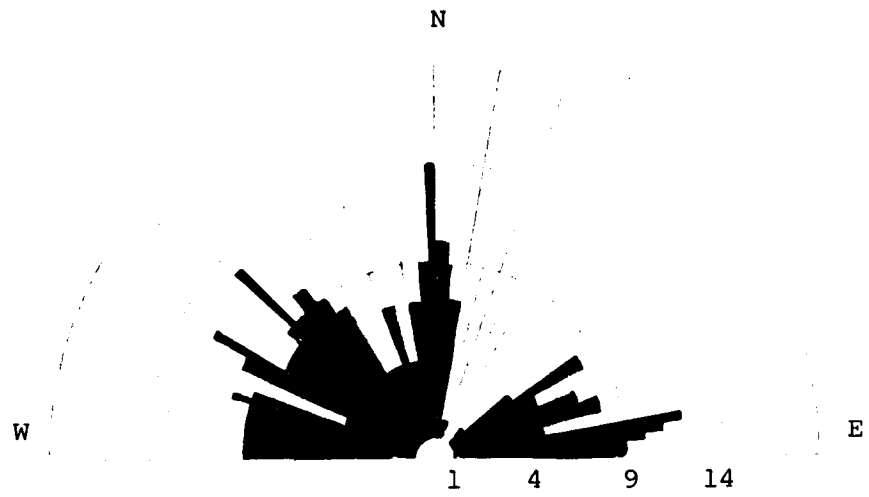


Figure C.1. Histogram of fracture traces as observed from soil tonal variations and tree alignments in WBW, based on 178 observations.

The fracture trace principal maxima occur at Due N5°W, N45°-50°W, N60°065°W, N80°-85°E. Secondary and tertiary maxima occur at N35°-45°W, N70°W-Due W, and at N30°-35°W, N50°-60°W, N55°-60°E and N70°-75°E, respectively.

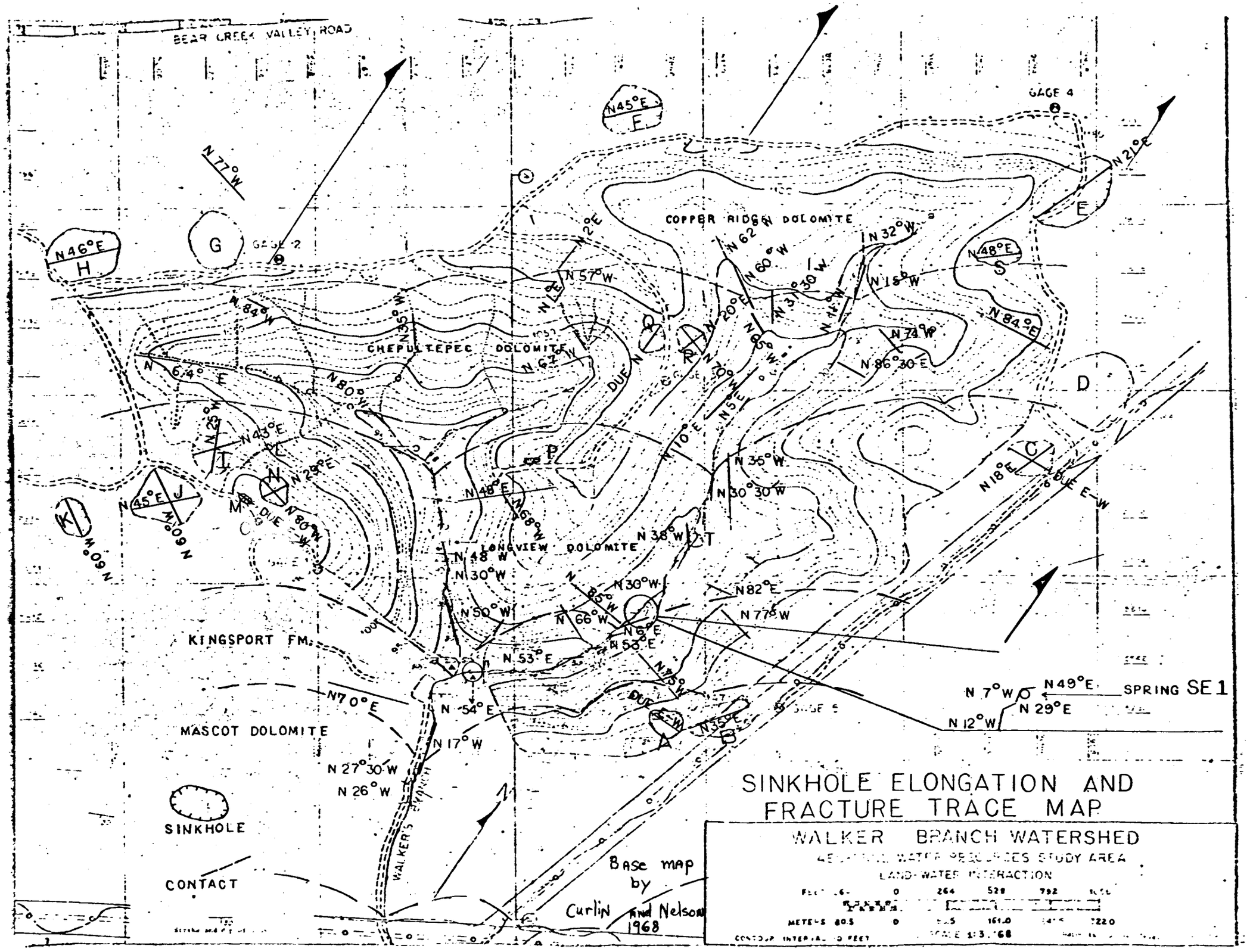


Figure C.2. Sinkhole elongation and fracture trace map.

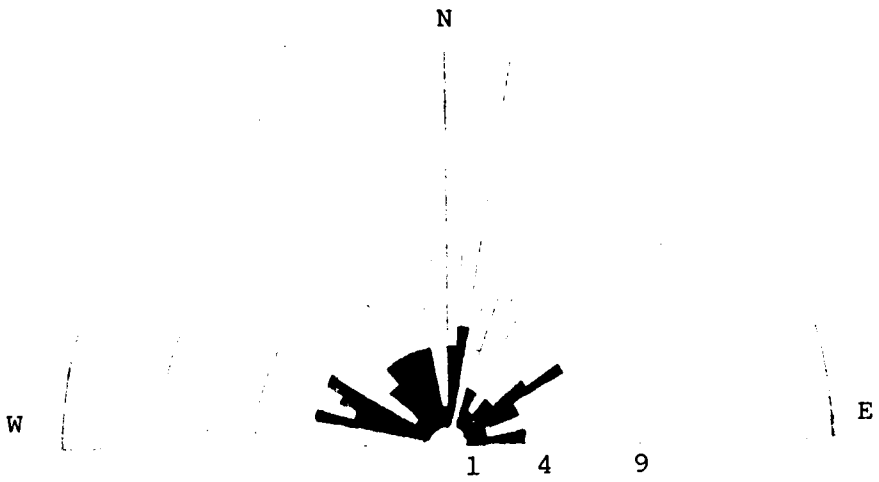


Figure C.3. Histogram of fracture traces as observed from straight stream segments in WBW based on 53 observations.

The fracture trace principal maxima are N5°-10°E, N55°-60°E, N60°-70°W, and N75°-80°W. Secondary maxima occur at Due N-5°E, N10°-40°W, N70°-75°W, and N50°-55°E.

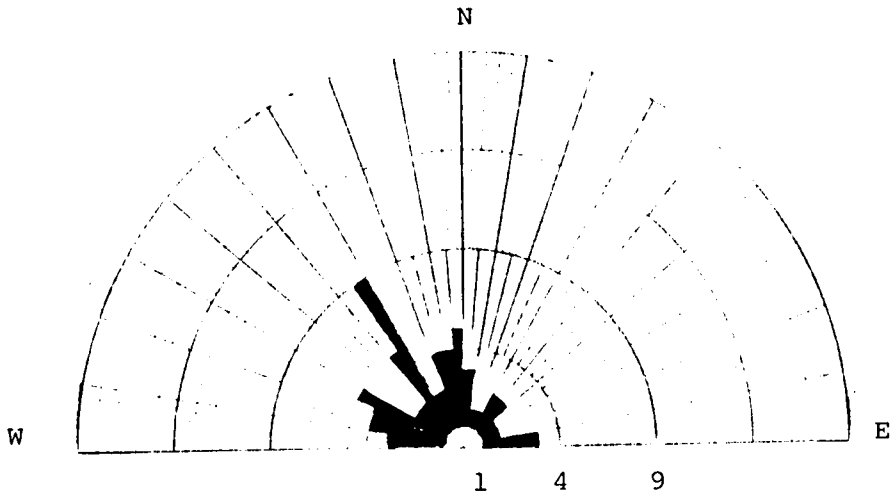


Figure C.4. Histogram of fracture traces as observed from topographic alignments in WBW and based on 51 observations.

The fracture trace maximum is N30°-35°W. Secondary maxima occur at Due N-20°W and N60°-80°W. Tertiary maxima occur at Due N-10°E and Due East-West.

APPENDIX D

MAP AND HISTOGRAMS OF PHOTOGEOHYDROLOGIC LINEAR FEATURES AND SINKHOLE ELONGATIONS AND ALIGNMENTS (FOR AREA 1) ON COPPER RIDGE

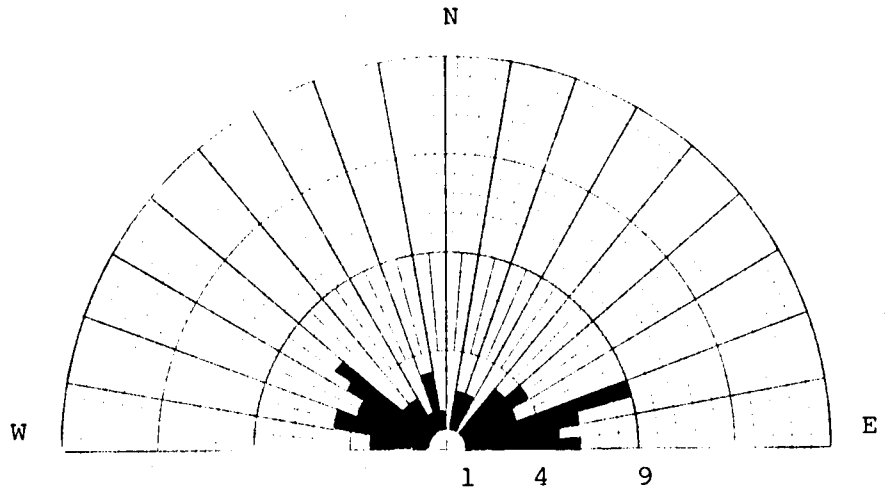
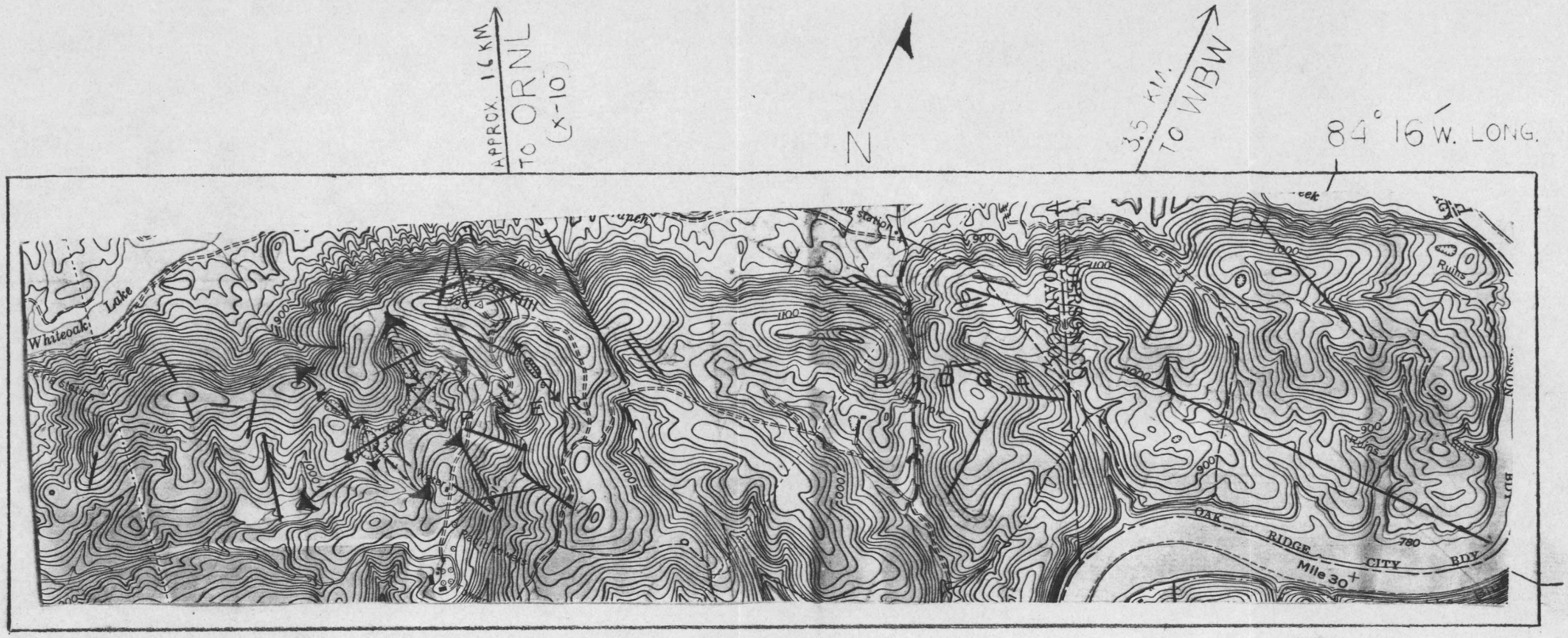
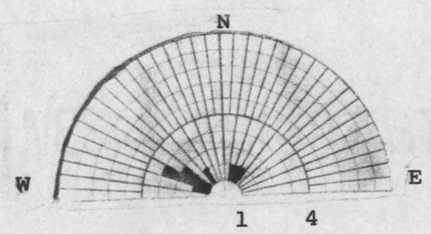


Figure D.1. Histogram of fracture traces observed for that part of Copper Ridge encompassed in TVA's Lovell, Bethel Valley, and Elverton 7.5 minute quadrangle maps based on 61 observations.

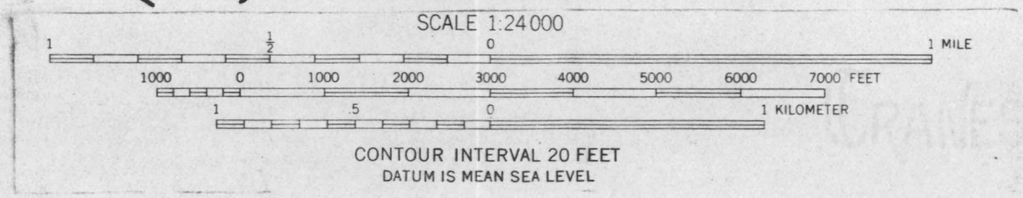
The principal maximum occurs at N70°-75°E. Secondary maxima occur at N70°-80°W, N50°-60°W, N75°-90°E, and tertiary maxima occur at N60°-70°W and N50°-60°E.

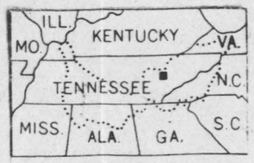


⟷ SINKHOLE ELONG. ⟨----⟩ SINKHOLE ALIGN.

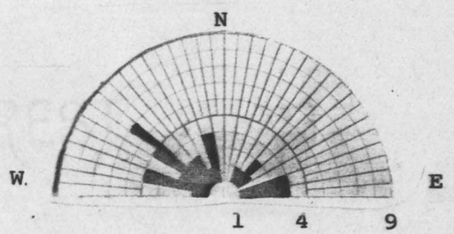


The sinkhole elongation and alignment analysis revealed a principal maximum of N60°-70°W and a secondary maximum of N50°-60°W. Number of observations is 10.





QUADRANGLE LOCATION



The fracture trace maximum is at N50°-60°W. The secondary maximum is at N70°-80°W and the tertiary maxima are at N10°-20°W and N70°-75°E. Number of observations is 32.

Figure D.2. Map and histograms of fracture traces and sinkhole elongations and alignments observed in Area 1 on Copper Ridge located northeast of Whiteoak Lake on Bethel Valley quadrangle.

APPENDIX E

MAP AND HISTOGRAMS OF PHOTOGEOHYDROLOGIC LINEAR FEATURE ORIENTATIONS OBSERVED FOR CHESTNUT RIDGE

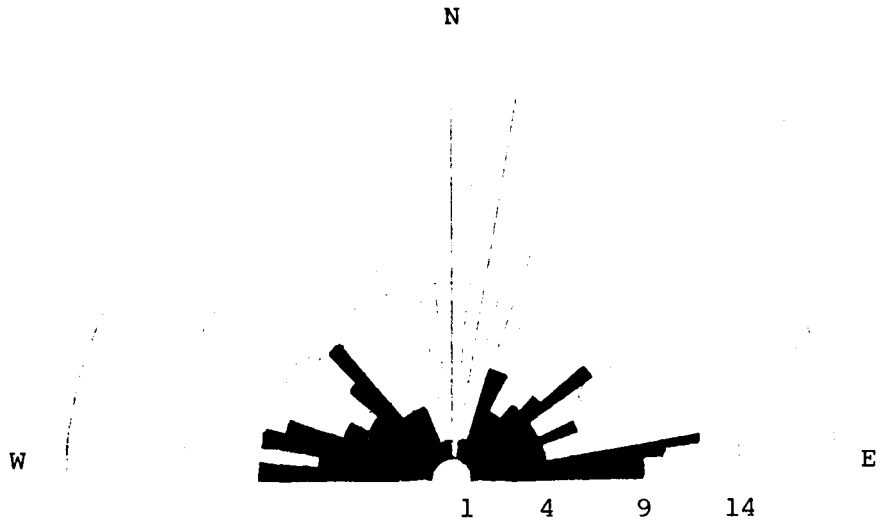
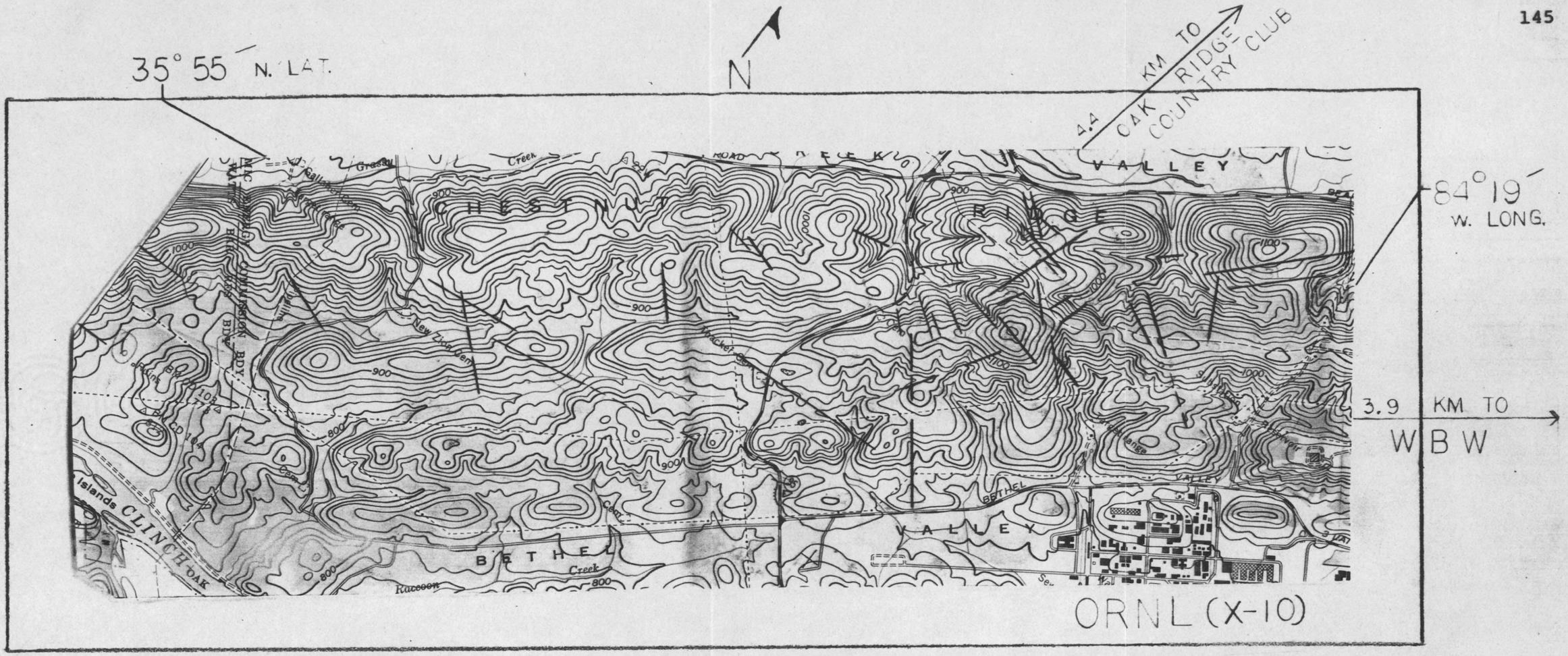
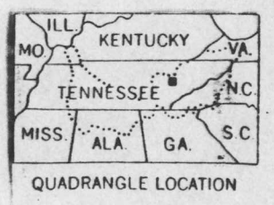
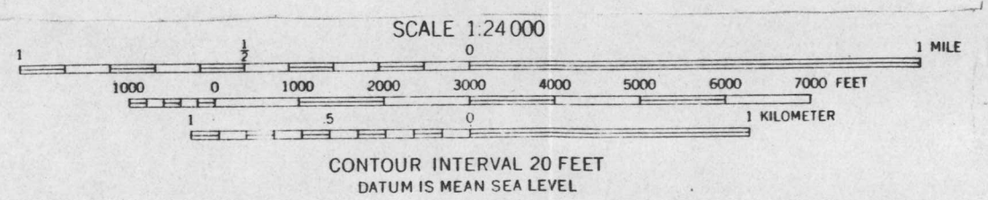


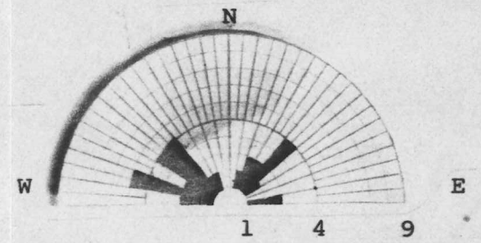
Figure E.1. Histogram of fracture traces observed for that part of Chestnut Ridge encompassed in TVA's Lovell, Bethel Valley, and Elverton 7.5 minute quadrangle maps, based on 103 observations.

The fracture trace maximum is N80°-85°E. Secondary maxima and tertiary maxima occur at Due East-West, and N75°-80°W and at N50°-55°E, N40°-45°W, and N70°-75°W, respectively.



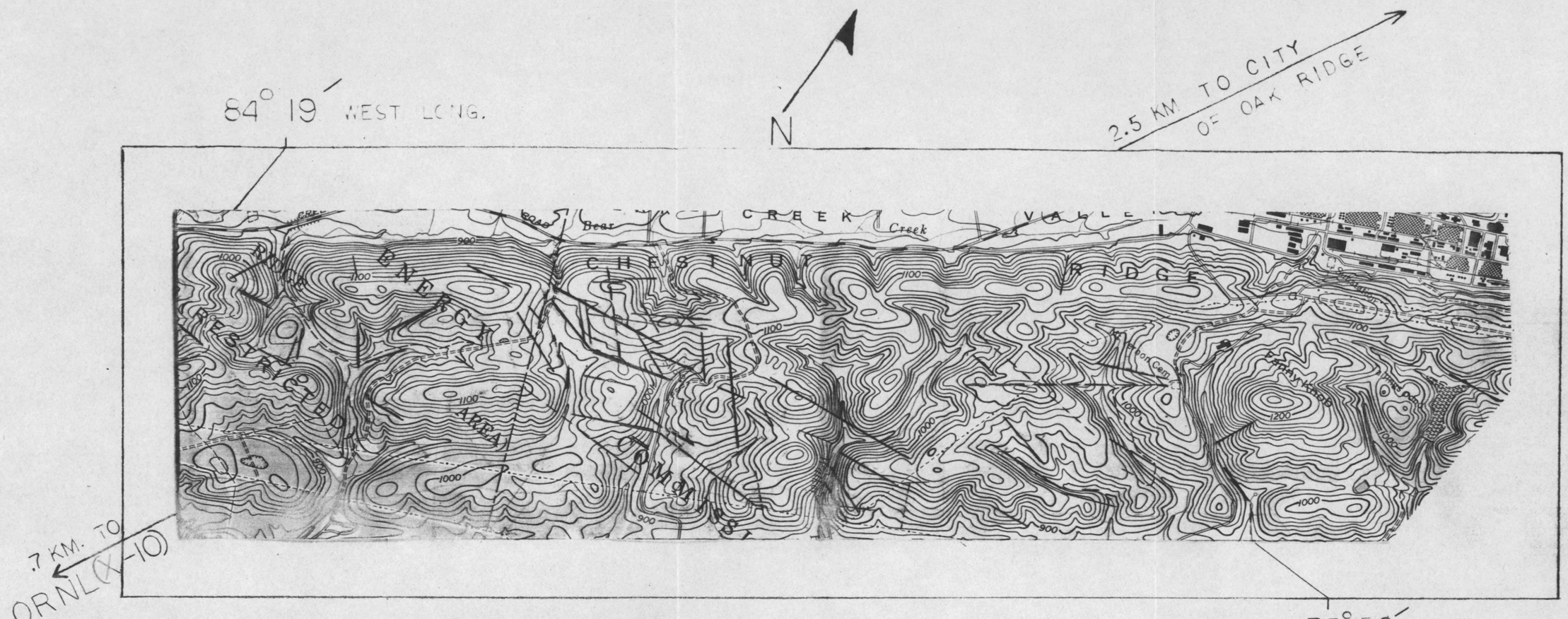






The fracture trace maximum is at N70°-80°W and the secondary maxima are at N40°-60°W and N40°-50°E. Number of observations equals 32.

Figure E.2. Map and histogram of fracture traces observed for Area 2 on Chestnut Ridge located northwest of ORNL Plant X-10 on Bethel Valley quadrangle.



The principle maximum is at N80°-90°E. Secondary maximum is at N70°-75°W and tertiary maxima occur at N40°-50°W and N50°-80°E. Histogram is based on 44 observations.

Figure E.3. Map and histogram of fracture traces observed for Area 3 in Chestnut Ridge encompassing WBW and the immediate area Northeast and Southwest on Bethel Valley quadrangle.

APPENDIX F

MAPS AND HISTOGRAMS OF ALIGNMENT OF GEOHYDROLOGIC FEATURES AND SINKHOLE ALIGNMENTS IN WBW

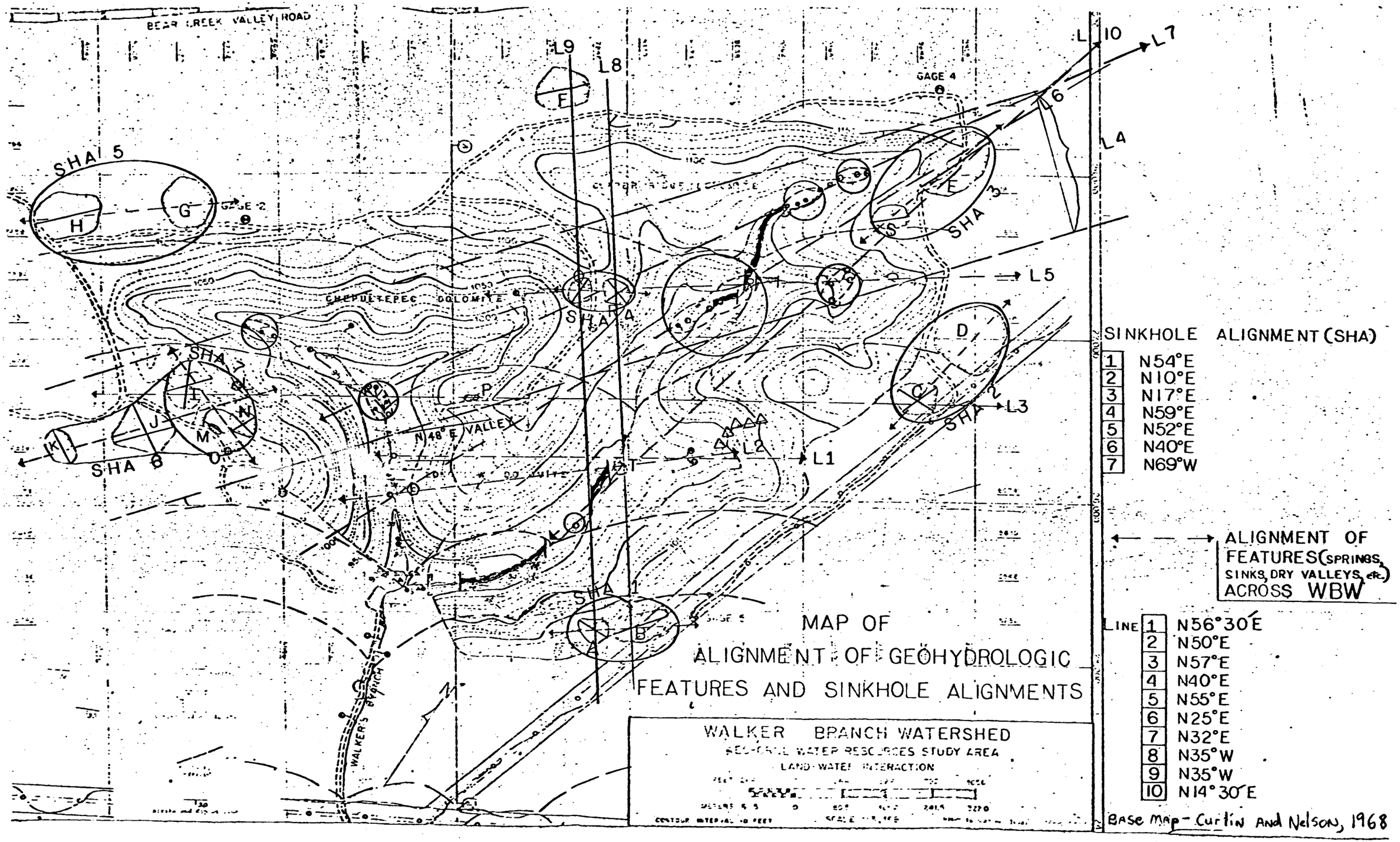


Figure F.1. Map of alignment of geohydrologic features and sinkhole alignments.

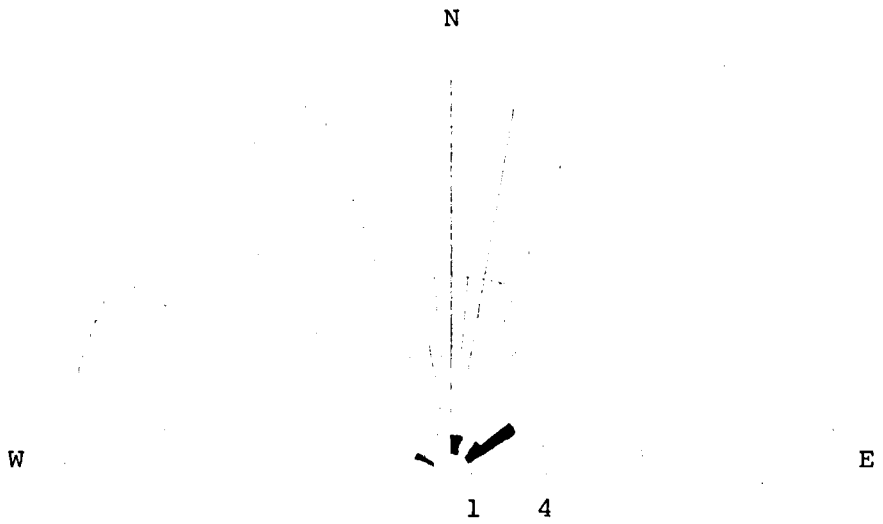


Figure F.2. Histogram of orientation of hypothetical lines adjoining aligned sinkholes in WBW based on 7 observations.

The maximum of this analysis is at N50°-60°E.

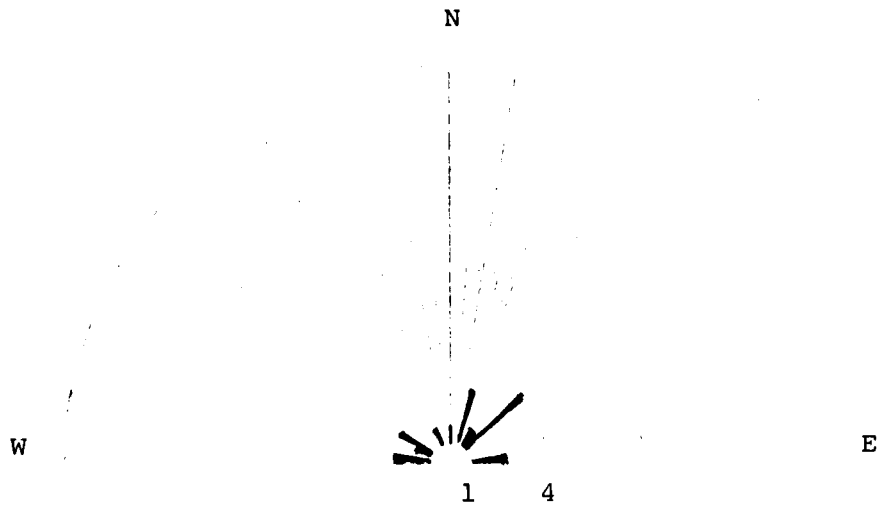


Figure F.3. Histogram of orientations of sinkhole elongations observed for WBW and based on 18 observations (see Appendix C, Figure C.2). The principal maxima are N15°-20°E and N45°-50°E. Secondary maxima are N55°-65°W and Due East-West.

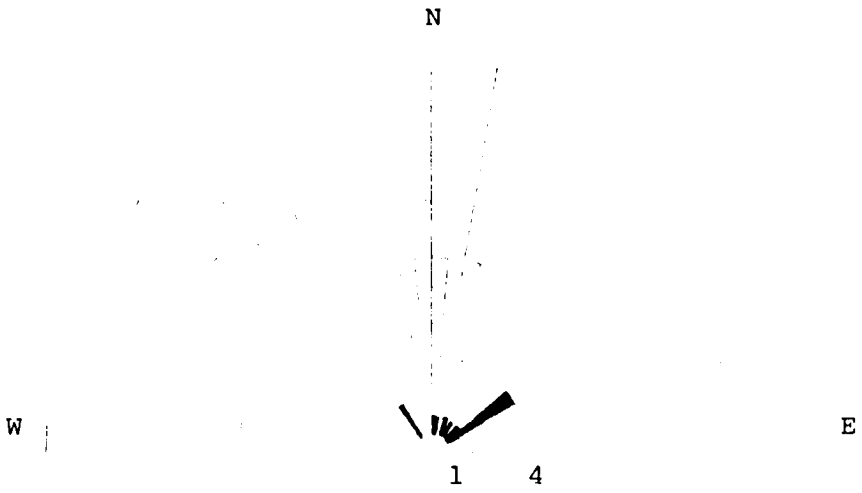


Figure F.4. Histogram of orientations of hypothetical lines adjoining concentrations of geohydrologic features across WBW based on 10 observations.

The maximum for this analysis is at N50°-60°E and the secondary maximum is at N30°-35°W.

APPENDIX G

STATISTICAL EVALUATION OF ORIENTATION DATA

STATISTICAL EVALUATION OF ORIENTATION DATA

I. CHI-SQUARE (χ^2) TEST

Purpose and Procedure

A chi-square (χ^2) statistical test was conducted for each directional histogram to test the null hypothesis that the orientations are uniformly distributed and therefore no preferred orientations exist in the data. The chi-square formula is:

$$\chi^2 = \frac{(O - E)^2}{E}$$

This formula requires taking each observed frequency (O), subtracting from it the corresponding expected frequency (E), squaring the difference, and dividing the result by the expected frequency. The sum of these equal the chi-square.

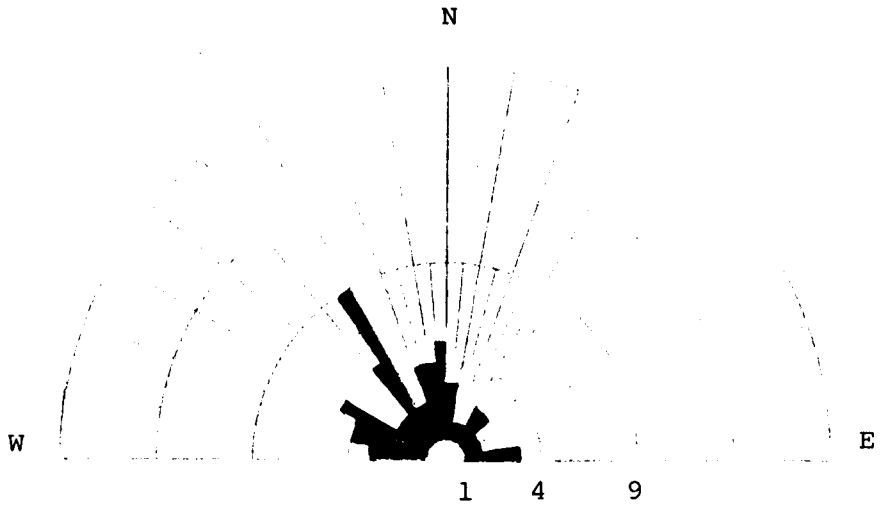
The histograms are divided into eighteen, ten degree intervals or classes which gives seventeen degrees of freedom (number of classes minus one) in the chi-square test. The writer has arbitrarily chosen a confidence coefficient equal to 0.1 (10% level of significance) as the boundary between the isotropic and anistropic distribution of orientations. For any χ^2 values equal to or greater than the χ^2 value determined for seventeen degrees of freedom at the 10% level of significance, the null hypothesis will be rejected. The

minimum value that χ^2 can be for the null hypothesis to be rejected is 24.8.

Results

Figure G.1 is an example of a chi-square test conducted on fracture trace orientation data. Table III is the chi-square value and corresponding level of significance determined for each directional histogram.

Vistelius (1966) states strong preferred orientations are denoted by large values of χ^2 and distributions which differ only slightly from the uniform are denoted by small values of χ^2 (both relative to 24.8). All the value for χ^2 in the histograms were relatively large therefore suggesting a preferred orientation in each diagram. The null hypothesis is rejected in all cases except Figures C.3 and D.2 (pp. 138 and 142). However, if the limit on the level of significance for the null hypothesis is extended only 5% more (15%), then the chi-square test suggests a preferred orientation in all the histograms. The anomalously large χ^2 values in the WBW and General Knox Terrane result from the absence of considering background scatter (tendency to parallel the normal distribution and lower the chi-square value) since these analyses are a compilation of only the principal, secondary, and tertiary maxima from the other analyses.



Example. Statistical Chi-Square (χ^2) Test

$$\text{Formula} = \chi^2 = \frac{(O-E)^2}{E}$$

Observed (O) frequencies noted around histogram

$$\text{Expected (E) frequencies} = \frac{\text{sum of observed}}{\text{no. of classes}} = \frac{51}{18} = 2.83$$

$$\chi^2 = \frac{.03+1.37+4.71+.79+.69+38.06+.69+1.37+}{2.83}$$

$$\frac{+4.71+.03+3.35+3.35+.69+.69+3.35+3.35+}{2.83}$$

$$\frac{3.35+.03}{2.83} = \frac{70.51}{2.83} = 24.92$$

Figure G.1. Histogram of fracture traces as observed from topographic alignments in WBW and based on 51 observations.

The fracture trace maximum is N30°-35°W. Secondary maxima occur at Due N-20°W and N60°80°W. Tertiary maxima occur at Due N-10°E and Due East-West.

TABLE III

CALCULATED χ^2 AND CORRESPONDING LEVEL OF SIGNIFICANCE VALUES FOR ORIENTATION DATA

Histogram	χ^2 Value	Level of Significance
Figure 30 and G.2	28.0	5%
Figure C.1	31.8	2.5%
Figure C.3	24.1	13%
Figure C.4 and G.1	24.9	10%
Figure D.1	25.9	10%
Figure D.2	24.4	11.5%
Figure E.1	38.9	Less than .5%
Figure E.2	26.5	10%
Figure E.3	33.5	1%
Figure F.2	26.5	10%
Figure F.3	25.0	10%
Figure F.4	32.0	2.5%
WBW (total)	54.2	Less than .5%
General Knox Terrane	67.1	Less than .5%

II. PERCENT ANALYSIS

Purpose and Procedure

A percent analysis was performed for each histogram to quantitatively determine if there is adequate amounts of separation in the orientations to divide the data into three maxima (principal, secondary, and tertiary) on the basis of relative projection lengths (function of the number of observations per maxima interval).

Figure G.2 is an example of the calculations performed on orientation data in all the histograms, the procedure of which is outlined in detail below.

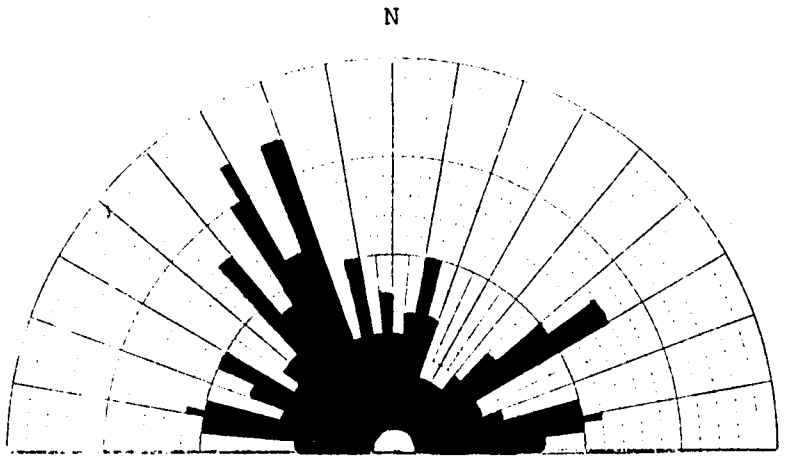
1. For each histogram, the number of total observations was divided by 36 (number of five-degree intervals in 180°) to determine the number of observations per five-degree interval which would result in an isotropic distribution.

2. The average number of observations for the principal, secondary, tertiary maxima and background scatter was recorded.*

3. Each average was divided by the number of observations calculated for the isotropic distribution and

---

*In the Percent Analysis, each of the first four observations (from the center half circle) is equal to one-half of an observation since the data is plotted in ten degree intervals in this portion of the diagram, but the analysis is divided into five degree intervals. All other squares are equal to one observation.



Scale: For Total Observations 1 4 9 14 19
For Percent Analysis 1 2 7 12 17

Example. Percent Analysis of the Separation between Principal (P), Secondary (S), Tertiary (T), and Background Scatter (BS) Orientation Data

Step 1. $\frac{\text{Number of observations}}{\text{Number of five degree intervals}} = \frac{210}{36} = 5.83$ (Isotropic distribution)

Step 2. Average number of observations per P, S, T, and BS orientations.

P maxima	No. of Obs.
N20°-25°W	21
N30°-35°W	19
	20 = Average P

S maxima	No. of Obs.
N55°-60°E	16
N40°-45°W	13
N25°-30°W	10
	13 = Average S

T maxima	No. of Obs.
N10°-15°E	7
N50°-55°E	7
N75°-80°E	7
N80°-85°E	8
N10°-15°W	7
N60°-65°W	7
N75°-80°W	8
N80°-85°W	7
	7.25 = Average T

BS (calculation of average)

Number of obs. in five degree intervals from a Due E to Due W direction: 5, 3, 2, 2, 4, 2, 1.5, 1.5, 1.5, 1.5, 4, 4, 3, 5, 3, 3, 6, 4, 4, 3, 5, 3, 2

Average BS = 3.17

P percentage = $\frac{\text{Average P}}{\text{Isotropic distribution}} = \frac{20}{5.83} = 3.43 \times 100 = 343\%$

S percentage = $\frac{13}{5.83} \times 100 = 223\%$

BS percentage = $\frac{3.17}{5.83} \times 100 = 54\%$

T percentage = $\frac{7.25}{5.83} \times 100 = 124\%$

Figure G.2. Histogram of bedrock fracture orientations based upon 210 observations within Walker Branch Watershed.

multiplied by 100 to determine the percent of each maxima length and the background scatter as compared to the isotropic distribution.

4. The separation in percent values between principal and secondary maxima, secondary and tertiary maxima, and tertiary and background scatter was then analyzed.

Results

Table IV contains the results of the percent analysis performed on the orientation data. Both the "average number of observations" and the "percent compared to isotropic distribution" calculations clearly indicate good separation between principal and secondary maxima, secondary and tertiary maxima, and tertiary and background scatter. The following is a summary of the important findings in this analysis:

1. There is greater separation between principal and secondary maxima than between secondary and tertiary maxima. This indicates the overall greater importance of the principal maxima over secondary and tertiary maxima as discussed previously.

2. With the exception of Figures F.2 and F.3 (pp. 149 and 150), the background scatter average is 100% or less of the value calculated for the isotropic distribution.

TABLE IV

RESULTS OF THE PERCENT ANALYSIS CONDUCTED ON ORIENTATION MAXIMA AND BACKGROUND SCATTER WITH COMPARISON TO THE ISOTROPIC DISTRIBUTION

Histogram	Total No. of Obs.	Isotropic Distribution	Average No. of Obs.				% Compared to Isotropic Distribution			
			P	S	T	BS	P	S	T	BS
Figure 30 and G.2	210	5.83	20.0	13.0	7.25	3.17	343	223	124	54
Figure C.1	178	4.94	11.75	7.63	6.0	3.29	238	155	122	67
Figure C.3	53	1.47	3.6	2.0	x	.94	245	136	x	64
Figure C.4 and G.1	51	1.42	7.0	2.25	1.50	.81	493	159	106	57
Figure D.1	61	1.69	5.50	3.67	2.0	1.1	325	217	118	65
Figure D.2	32	.89	3.0	2.0	1.5	.80	337	225	169	90
Figure E.1	103	2.86	10.0	7.0	6.0	1.0	350	245	210	35
Figure E.2	32	.89	3.0	2.0	x	.75	337	225	x	84
Figure E.3	44	1.22	4.5	3.0	2.0	.83	369	246	164	68
Figure F.2	7	.19	1.5	x	x	.5	789	x	x	263
Figure F.3	18	.50	1.75	1.0	x	.5	350	200	x	100
Figure F.4	10	.28	2.0	1.0	x	.5	714	357	x	179
WBW (Total)	124	3.44	10.75	5.71	3.0	x	313	165	87	x
General Knox Terrane	220	6.11	14.8	9.88	3.82	x	242	162	63	x

Note: x = No observations.

3. The average of the percent values calculated for the background scatter in all the histograms (except F.2 and F.4, pp. 149 and 151) is 68.4% which is over two-thirds the value expected if the data were isotropically distributed. This indicates background scatter and isotropic distribution are closely related.

In the background scatter versus isotropic distribution test, the discrepancy between the results obtained for Figures F.2 and F.4 with those results obtained from the remaining data is a function of the total number of observations and the equation used for deriving these values. The relatively few total observations in Figures F.2 and F.4 (7 observations and 10 observations, respectively) give a low isotropic distribution value as compared to the average number of background scatter observations. Therefore the ratio of the two values gives percentages two to three times higher than the histograms with eighteen or more observations.

VITA

Donald V. Crider was born in Nashville, Tennessee, on March 1, 1955. He attended Hillsboro High School, graduating in June 1973. That summer he attended Middle Tennessee State University for one semester and the following September he entered The University of Tennessee, Knoxville. After graduating with a Bachelor of Arts degree in Geology in June 1977, he began work toward a Master's degree in September of that year.

The author is a member of the American Society of Photogrammetry and Sigma Gamma Epsilon. Mr. Crider will be employed with Natural Resources Group, Exploration Staff, Phillips Petroleum Company, after graduation.